

THESIS

HEAT TRANSFER EFFICIENCY OF BIOMASS COOKSTOVES

Submitted by

Daniel Joseph Zube

Department of Mechanical Engineering

In partial fulfillment of the requirements

For the Degree of Master of Science

Colorado State University

Fort Collins, Colorado

Summer 2010

COLORADO STATE UNIVERSITY

July 5, 2010

WE HEREBY RECOMMEND THAT THE THESIS PREPARED UNDER OUR SUPERVISION BY DANIEL JOSEPH ZUBE ENTITLED HEAT TRANSFER EFFICIENCY OF BIOMASS COOKSTOVES BE ACCEPTED AS FULFILLING IN PART REQUIREMENTS FOR THE DEGREE OF MASTER OF SCIENCE.

Committee on Graduate Work

Bryan D. Willson

Eric D. Maloney

Advisor: Morgan Defoort

Department Head: Allan T. Kirkpatrick

ABSTRACT OF THESIS

HEAT TRANSFER EFFICIENCY OF BIOMASS COOKSTOVES

Nearly half of the world's human population burns biomass fuel to meet home energy needs for heating and cooking. Biomass combustion often releases harmful chemical compounds, greenhouse gases, and particulate matter into the air which all have a detrimental effect on both human health and global climate and ecology. In order to mitigate the harmful effects of biomass combustion, thermal efficiency of the combustion process must be improved. Thermal efficiency is influenced equally by combustion efficiency and heat transfer efficiency, but the emphasis of this research is on heat transfer efficiency since it offers the most room for improvement.

A theoretical approach is taken to understand the fundamental physics underpinning the three modes of heat transfer: conduction, convection, and radiation. A strong theoretical understanding of each mode as it applies to cookstoves is established and used as a tool to evaluate potential design enhancements. Based on these evaluations, certain design modifications are suggested as a practical means to boost heat transfer efficiency. Future

research topics are suggested which will further increase the accuracy of theoretical predictions surrounding stove performance.

Daniel Joseph Zube
Department of Mechanical Engineering
Colorado State University
Fort Collins, CO 80523
Summer 2010

ACKNOWLEDGMENTS

I would like to express my gratitude to everybody who has provided me with their expertise, advice, knowledge and moral support through these past couple of years. Special thanks to Dr. Morgan DeFoort and Dr. Bryan Willson for guiding me through such an interesting, challenging and meaningful project. I have benefitted immensely from this experience and consider it a privilege to contribute to such an effort. I would also like to recognize and sincerely thank other members of the stoves team for sharing their expertise including Cory Kreutzer, Christian L'Orange, Dan Lionberg, Josh Agenbroad, Melanie Sloan, and Sean Babbs. Other members of the faculty and staff at Colorado State University who have been invaluable resources for advice and knowledge include Phillip Bacon, Dr. Steven Schaeffer, Kirk Evans, and Dr. Eric Maloney. This research effort has been supported by the Colorado State University Engines and Energy Conversion Laboratory, Envirofit International, and the Shell Foundation. I would like to thank these organizations for the opportunity to join them in their pursuit of providing improved cookstoves to the developing world.

TABLE OF CONTENTS

Abstract of Thesis.....	iii
Acknowledgments.....	v
List of Abbreviations.....	ix
1. Motivation – The Importance of Heat Transfer in Biomass Cookstoves.....	1
1.1. Human Health Effects.....	3
1.2. Global Climate Impact.....	3
1.3. Summary.....	5
2. Cooking with Biomass – Past, Present and Future.....	6
2.1. Traditional Cooking.....	6
2.2. Improved Stoves.....	8
2.3. Focus of Future Development.....	12
3. Fundamental Physics Governing Heat Transfer in Biomass Cookstoves.....	18
3.1. The First Law of Thermodynamics.....	18
3.2. Contributing Roles of Conduction, Convection, and Radiation.....	22
3.2.1. Conduction.....	22
3.2.2. Convection.....	23
3.2.3. Radiation.....	26
3.2.4. Summary.....	28
3.3. Effects of Gas Path Geometry on Flow Characteristics.....	29

3.4. Mass Flow Rate, Temperature, and Their Effects on Heat Transfer.....	34
3.5. The influence of Firepower on Convection Efficiency.....	39
3.6. Summary.....	43
4. Practical Applications to Improving Heat Transfer Efficiency of Cookstoves.....	46
4.1. Case Study #1 – Effect of Pot Gap Adjustment on Heat Transfer.....	46
4.1.1. Fundamental Concepts and Underlying Theory.....	46
4.1.2. Effects on Flow Characteristics.....	49
4.1.3. Impact on Heat Transfer Efficiency.....	51
4.1.4. Experimental Validation.....	53
4.2. Case Study #2 – Hot Gas Path Geometry and Flow Characteristics.....	54
4.2.1. Pot Skirt.....	55
4.2.1.1. Theory and Practice.....	55
4.2.1.2. Optimizations.....	55
4.2.2. Double-pot attachment.....	58
4.3. Case Study #3 – Extended Surface Heat Transfer Experimentation.....	61
4.3.1. First Approach – Heat Exchanger Plate.....	61
4.3.1.1. Design Objective and Development Strategy.....	61
4.3.1.2. Fundamental Physics.....	62
4.3.1.2.1. Contact Resistance.....	63
4.3.1.2.2. Thermal Capacitance.....	64
4.3.1.2.3. Surface Area.....	65
4.3.1.3. Theoretical Model.....	66
4.3.1.4. Contact Resistance Experimentation.....	68
4.3.1.5. Testing.....	71

4.3.2. Second Approach – Commercially Available Finned Pot.....	73
4.3.2.1. Testing.....	74
4.3.3. Summary – Extended Surface Heat Transfer.....	75
4.4. Case Study #4 – Radiation Heat Transfer: Diffusion vs. Premixed Flames.....	76
4.4.1. Experimental Set-up and Results.....	77
5. Conclusions and Future Work.....	80
Works Cited.....	82
Appendix.....	85
Appendix A – Theoretical Convection Coefficient using MathCAD.....	86
Appendix B – Semi-empirical Convection Coefficient using MathCAD.....	89
Appendix C – Single-pot Stove Energy Balance using MathCAD.....	92
Appendix D – Mass Flow Rate, Temperature, Firepower, and Heat Transfer using Microsoft Excel.....	116
Appendix E – Pot Gap Calculations using MathCAD.....	117
Appendix F – Pot Gap Calculations using Microsoft Excel.....	122
Appendix G – Pot Skirt Calculations using MathCAD.....	123
Appendix H – Pot Skirt Calculations using Microsoft Excel.....	130
Appendix J – Double-pot calculations using MathCAD.....	132
Appendix K – Heat Plate Time-to-Boil Calculation using MathCAD.....	143
Appendix L – Contact Resistance Experiment Calculations using MathCAD.....	151
Appendix M – Contact Resistance Experiment Results using Microsoft Excel.....	155

LIST OF ABBREVIATIONS

AFR – Air Fuel Ratio

BC – Black Carbon

CO – Carbon Monoxide

CS – Cold Start

CSU – Colorado State University

EAR – Excess Air Ratio

EECL – Engines and Energy Conversion Laboratory

GHGs – Greenhouse Gases

HTE – Heat Transfer Efficiency

IAP – Indoor Air Pollution

LC – Loss Coefficient

NMVOCs – Non-methane Volatile Organic Compounds

NO₂ – Nitrogen Dioxide

OC – Organic Carbon

PGC – Pot Gap Coefficient

PICs – Products of Incomplete Combustion

PM – Particulate Matter

SO₂ – Sulfur Dioxide

TTB – Time to Boil

WBT – Water Boil Test

1. Motivation – The Importance of Heat Transfer in Biomass Cookstoves

Half of the world's human population cooks their food on an open fire inside their homes by burning various forms of biomass such as wood, charcoal, dung and crop residues. Burning each of these biomass fuels emits harmful chemicals and large amounts of particulates, each of which have adverse effects on human health, global climate and regional ecosystems from which the fuel is extracted. In the year 2000, it was estimated that the combustion of biomass fuels was responsible for 13 % of global energy consumption. A large majority of this consumption occurs in developing countries where 90% of rural households rely upon biomass as a means to provide for their heating and cooking needs (1). Unfortunately, most of these people use very inefficient traditional cooking methods that cause excessive air pollution and use more fuel than necessary.

For approximately 40 years, many international organizations have been striving to provide people with clean burning efficient cookstoves as an alternative to traditional cooking methods. Over the years great strides have been made in improving cookstove technology. Examples of such improvements include reducing fuel usage of the stove by increasing heat transfer efficiency, dramatically reducing air pollution by increasing the combustion efficiency of the fuel and establishing a standard test protocol by which stoves can be evaluated fairly. All these improvements have allowed stove designers to more effectively provide improved cookstoves to people who need them. As improved cookstoves have been distributed throughout the developing world, the quality of air people breathe has improved and environmental damage has been reduced. Despite these considerable improvements in

cookstove performance many households in developing countries still rely on inefficient stoves and procedures to cook their food because they cannot afford an improved stove.

An effective way to provide people with better cooking options is to seek out opportunities for improvement and transform them into valuable assets. Heat transfer is currently underutilized as a means of increasing stove thermal efficiency and opportunities exist that could change this. Hence, this is the area of research offering the greatest potential to enhance performance and provide more people with improved cooking procedures.

Heat transfer efficiency (HTE) is defined as the percentage of heat contained in the combustion gases that gets transferred to the substance being cooked (e.g. water). Improved cookstoves are constructed of materials that reduce the amount of heat drawn away from combustion gases giving rise to higher flow temperatures and higher heat transfer efficiencies than traditional methods. Gains in HTE realized through increased flow temperatures can be better utilized if the focus shifts to the interface between the pot and hot reacting flow. The interaction between the pot and hot gases is dependent on the relative geometry between the pot and stove. The manner in which the pot and stove fit together highly influences how much each of the three modes of heat transfer (i.e. conduction, convection and radiation) contribute to the overall cooking process. Research is needed to determine how different stove/pot configurations affect performance through the impact they have on HTE. If heat transfer between the pot surface and hot gases from the fire is optimized, then overall thermal efficiency of the cooking operation is improved dramatically. Achieving this through cost effective means allows more people in developing countries to improve their health and reduce environmental impact.

1.1. Human Health Effects

Individuals in developing countries who cook their food indoors by inefficiently burning biomass fuel often produce a significant amount of indoor air pollution (IAP). IAP is a broad term associated with the emission of several indoor air pollutants that include particulate matter (PM), carbon monoxide (CO), nitrogen dioxide (NO₂), sulfur dioxide (SO₂) and other products of incomplete combustion (PICs). Prolonged exposure to these pollutants has proven to be harmful to human health and is believed to be responsible for an estimated 1.6 million deaths each year (2). Studies have indicated that people who frequently cook with biomass indoors are likely to suffer from various health ailments including chronic obstructive lung disease, adverse pregnancy outcomes, pneumonia, lung cancer, bronchitis and acute respiratory infection (3). Most of the health risks associated with IAP fall disproportionately upon women and children since they spend the most time in the kitchen. A study by Reid found that rural Nepali women spent up to 5 hours a day breathing polluted air in their kitchen where they cook using biomass fuels (4). Research from the World Health Organization suggests that IAP exposure increases the risk of acute lower respiratory infections in children under the age of five. The same source believes it to be the leading cause of death globally for this age group (2).

1.2. Global Climate Impact

Negative impacts from burning biomass fuel indoors extend beyond the immediate surroundings. Most PICs given off as a result of biomass combustion such as methane (CH₄) and other non-methane volatile organic compounds (NMVOCs) are potent greenhouse gases (GHGs). PIC emissions alone from biomass cookstoves may contribute to about 1-3% of global warming (5). Sometimes they can have a greater global warming potential on a mass basis than the most well-known GHG, carbon dioxide (CO₂). Carbon dioxide emissions become problematic when the collection of wood for cooking causes deforestation at a rate which exceeds that of

forest re-growth. This is the case on a globally averaged scale; in fact the inefficient use of biomass for cooking is the cause of about one-eighth of global deforestation which threatens ecosystems by decreasing biodiversity and destroying wildlife habitat (6) (7). Deforestation by itself contributes to roughly 18.2% of global warming, which means the collection of wood for cookstove fuel is responsible for 2.3% of global warming due to the imbalance of CO₂ in the atmosphere (6). If this data is coupled to PIC emission data from above, then the total global warming contribution from biomass cookstoves is approximated to be 3.3-5.3% (6) (5).

Most climate researchers suggest these types of human activities that emit GHGs play a significant role in disrupting the natural climate cycle of our planet (8). Over approximately the last 150 years scientists have measured an increase in average global surface temperature of 0.76 degrees Celsius and a sea level rise of 0.17m due to melting land and sea ice (8). An increase in average global surface temperature leads to more intense precipitation and severe drought distributed unevenly throughout the globe. These patterns of climate change threaten the livelihoods of a growing number of ecosystems on the planet (9).

Considerable uncertainty is associated with quantifying PIC emissions and their interaction with the climate system. Carbonaceous aerosols of Black Carbon (BC) and Organic Carbon (OC) are two PICs that present some of the largest uncertainty. Even still, some studies estimate BC imposes a radiative climate forcing equivalent in magnitude to 60% of CO₂ (10). A study by Aunan estimated the burning of household fuel for cooking may account for about one quarter of global BC emissions (11). OC aerosol emissions increase the surface albedo of the planet, causing a net cooling effect on the climate which can sometimes partially cancel the effects of BC emissions. Thus, the BC:OC emission ratio along with other GHG emissions are of concern to the stove designer trying to limit global impact.

1.3. Summary

Inefficient biomass cookstoves used in developing countries emit toxic levels of IAP which claims millions of human lives each year. The global climate impacts from biomass combustion are relatively small compared to that of large scale fossil fuel emission; however, the causes and effects of anthropogenic climate change pervade the entire socioeconomic spectrum requiring that all activities be included in the mitigation plan. Therefore, further enhancements to biomass cookstoves are necessary to help curb the effects of global warming in addition to improving the human condition for individuals who use them.

Advancements in cookstove technology to present day demonstrate efficiency gains in combustion and heat transfer leading to reductions in both fuel usage and air pollution. HTE holds the greatest potential to further enhance stove performance since it is much lower than combustion efficiency. Previous advancements in HTE allow the pot to be exposed to gases with higher flow temperatures. This provides a building block from which additional heat transfer improvements can be made by modifying the pot/gas interface. Relative geometries between the stove and pot are critical since their positioning affects the flow characteristics of the stove and consequent HTE to the pot. Improving the HTE of cookstoves is the primary focus of this research since it provides the most direct route to further reduce fuel usage and air pollution.

2. Cooking with Biomass – Past, Present and Future

2.1. Traditional Cooking

The inefficient traditional cooking methods previously mentioned can be separated into two basic categories. The most common method – the “three-stone fire” – involves building a fire directly on the ground, and placing a pot or pan atop three stones that surround the fire. Another common method – the “built-in stove” – is a slight modification of the three-stone fire in that a more permanent structure is built around the fire using local earthen materials. Examples of each of these cooking methods are illustrated in Figure 2.1.

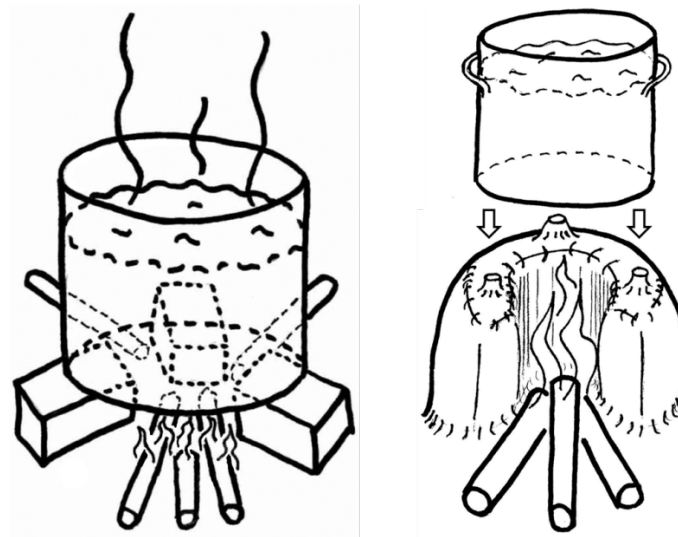


Figure 2.1. Three-stone fire (left) and built-in stove (right).

The three-stone fire and the built-in stove share some common advantages and disadvantages. Some advantages include very low capital cost and the familiarity the user has with its operation. A common disadvantage is they often involve placing the fire directly on the ground. This causes two major problems; heat from the fire is lost to the ground through

conduction and the surface area of fuel exposed to primary air is reduced. Reducing the amount of primary air available to react with the fuel can lead to incomplete combustion, resulting in an increase in IAP. In addition to these similarities, each cooking method has its own unique set of benefits and drawbacks.

The three-stone fire is known for its disadvantages but can be surprisingly efficient if operated carefully. Nonetheless its reputation for being inefficient is due mostly in part to a handful of design flaws. One such flaw stems from the radiative losses from the fire and coal bed to the surroundings. Another flaw is the lack of a confined flow path for the hot combustion gases which causes too much entrainment of cooler ambient air. Finally, the three-stone fire is notorious for using too much fuel; however, this can be highly user dependent. Studies have shown that people generally use more fuel than necessary when supplies are abundant, but can reduce their fuel usage when supplies are scarce (12). One advantage of the three-stone fire is the possibility to place the pot very close to the fire to maximize radiation heat transfer. Also, the absence of any surrounding material prevents the absorption of heat that could otherwise be directed to the pot. Considering these drawbacks and benefits to three-stone fires, studies have shown average thermal efficiency values to be roughly 14% (13).

Built-in stoves provide some advantages over three-stone fires, though they can sometimes offer worse performance if they are designed improperly. By constructing a wall that surrounds the fire, it restricts the amount of fuel that can be fed into the fire at any one time, thereby limiting fuel use. A secondary benefit to the built-in stove is the more enclosed gas path created by the walls which controls the entrainment of ambient air. This allows the user to operate the stove at a more optimal air-fuel ratio while increasing flow temperatures and improving convection heat transfer to the pot. The walls of the built-in stove also prevent the radiative losses experienced by the three-stone fire.

Despite the potential benefits described above, constructing walls around the fire can hinder performance if they absorb more energy from the fire than they redirect to the pot. This phenomenon is commonly observed during the “start-up” phase of cooking when a lot of the thermal energy from the fire can be transferred to the stove body. At the beginning of the start-up phase, the inner wall temperatures are cold relative to the elevated gas temperatures required to achieve complete combustion. As the fuel is ignited, stove performance suffers since the cold walls drastically reduce the temperature of the gases released from the fire. During this time, the lowered gas temperatures cause the fuel to undergo incomplete combustion which is characterized by high soot (PM) production and elevated CO emissions. The stove will continue to operate poorly in this fashion until the inner walls of the stove body reach a temperature close to that of the fire. Once this occurs, complete combustion is more likely and emissions are reduced. If the walls are large and massive, then it will take a long time for this to happen; consequently, emissions are increased to a point where the cost of having walls can outweigh the potential benefit of using less fuel. Striking the right balance between emissions reduction and fuel savings is the main objective of any person or organization seeking to improve upon traditional cooking methods.

2.2. Improved Stoves

The basic performance metrics used to evaluate a stove include the time to boil (TTB), fuel usage, thermal efficiency, and emissions in the form of CO and PM. The goal of a cookstove is to improve upon the inadequacies of the three-stone fire and traditional built-in stove described above while maintaining affordability for the user. Conventional improved cookstoves currently on the market achieve this goal by incorporating a few common design strategies found to boost performance.

Similar to a built-in stove, a typical family sized improved cookstove is cylindrical in shape (~23cm outer diameter), about 30cm tall and is constructed of low density walls that surround the fire. Also, the stove design depends upon whether the user continuously feeds fuel into the stove during operation or if a batch-fed process is used. A batch-fed stove performs a cooking operation for a prescribed duration depending on the batch-size of fuel supplied at a single time. In contrast, a continuously fed stove allows the user to adjust fuel input throughout the cooking process until additional fuel is not needed. One example of a continuously fed improved cookstove is shown in Figure 2.2 with a corresponding cross-sectional view and typical flow path shown in Figure 2.3. This particular model, the G3300, is a product from Envirofit International – a company specializing in biomass cookstove design and production.



Figure 2.2. Envirofit's G3300 model improved cookstove.

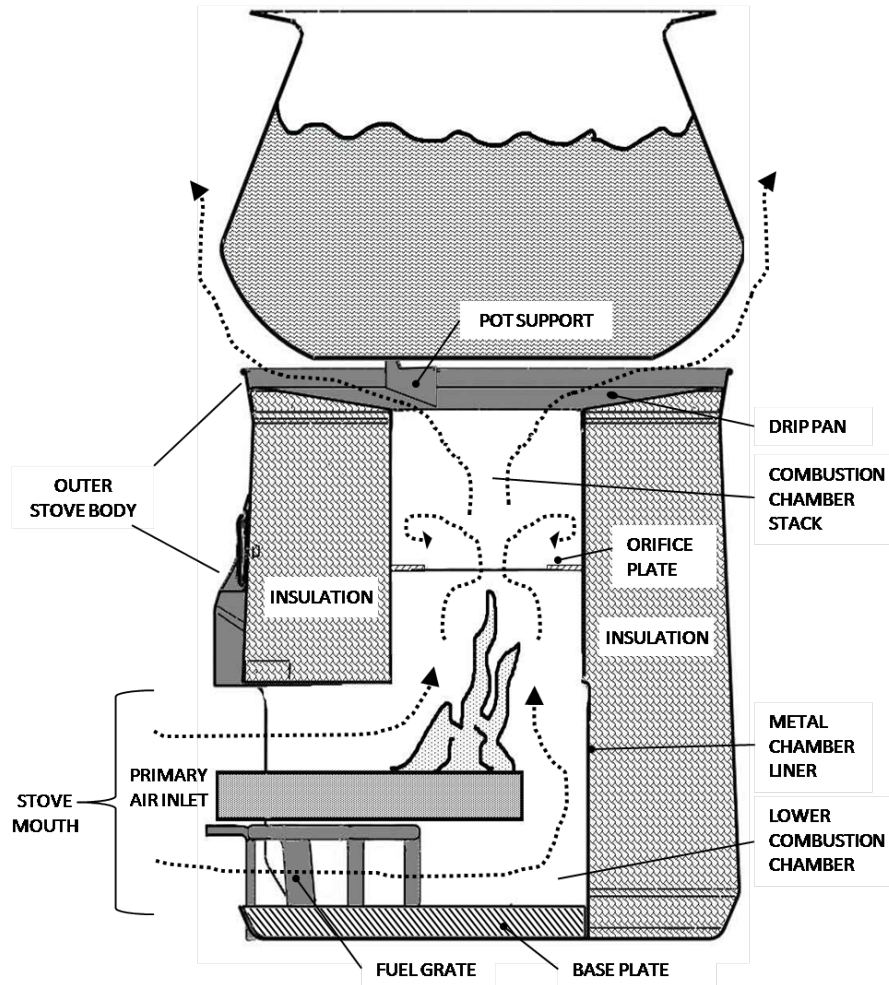


Figure 2.3. Cross-sectional view of improved cookstove with typical flow path.

Improved cookstoves exhibit many of the same advantages offered by traditional methods but with many additional benefits. For example, the walls are made of a low density, low specific heat (i.e. low thermal capacitance) material so they quickly reach the elevated temperatures desired to maximize combustion and heat transfer efficiencies. Conduction losses to the ground are mitigated by placing a metal fuel grate on top of a low mass, low thermal conductivity base plate. The metal grate raises fuel off the base plate which allows air to surround it on all sides, enabling more complete combustion through the chamber stack. The flow path as illustrated in Figure 2.3 is very typical for many improved stoves and is responsible for the “rocket elbow” name often associated with this type of cookstove. The rocket elbow

design results in a more controlled and better utilized fire with increased heat transfer and consistently higher overall efficiencies. Unlike built-in stoves, cookstoves are portable – allowing users to cook their food indoors, outdoors, or with neighbors. Stoves with combustion chambers made from thin sheet metal (e.g. Envirofit’s G3300) enable manufacturers to attain high production volumes; thus, increasing the number of people who have access to improved cookstoves.

The positive attributes described above prove to make a real difference in field tests comparing a conventional improved rocket elbow stove to traditional methods. Test results from the Approvecho Research Center showed the rocket elbow stove performing favorably by reducing fuel 41%, CO 46% and PM 56% as compared to a three-stone fire. Comparisons of the rocket elbow stove to a traditional built-in stove also yielded positive results by reducing fuel 18%, CO 41% and PM 46% (14). These test results are consistent with laboratory tests conducted at the Engines and Energy Conversion Laboratory (EECL) at Colorado State University (CSU).

Improved stoves can reduce time and money people spend collecting and/or purchasing fuel for cooking. A study by Barnes estimated that in the hill areas of rural Nepal women spent 2.5 – 3.6 hours per day collecting fuelwood to burn using inefficient traditional cooking methods. The same study focused on urban Sub-Saharan Africa where money saved through reduced fuel consumption of improved charcoal stoves represented 5% - 22% of a family’s income (15).

As more people acquire improved cookstoves, overall human health is promoted and fewer pollutants are emitted into the atmosphere. Nevertheless, there is still opportunity for improved cookstoves to use less fuel, become more affordable, and pollute less than products currently on the market. An effective way to target each of these goals is to focus on improving

thermal efficiency through HTE gains. Existing improved cookstoves have boosted HTE by increasing combustion gas temperatures. Further progress is possible by focusing on how the stove and pot fit together to create an optimal environment for the gases and pot to interact. Optimizing heat transfer of this interaction is dependent upon how various stove/pot geometries change the relative contributions of conduction, convection, and radiation.

2.3. Focus of Future Development

Previous cookstove research has improved overall thermal efficiency through parallel gains in combustion and HTE. Overall thermal efficiency (η_t) is influenced equally by combustion efficiency (η_c) and HTE (η_h) as indicated by equation 1 from Kirk R. Smith (5).

$$\eta_t = \eta_c \times \eta_h \quad [1]$$

Combustion efficiency is defined as the percentage of chemical energy stored in the fuel that is converted into thermal energy, or heat. According to the Aprovecho Research Center, typical combustion efficiencies for cookstoves and even sometimes three-stone fires can be above 90%. Contrasting this behavior, typical heat transfer efficiencies for cookstoves frequently fall within 10% to 40% (12). Therefore, it is apparent that HTE emerges as the most influential parameter to further improve stove performance. If HTE increases, then it can potentially have a positive impact on all other stove performance metrics including TTB, overall thermal efficiency, and total emissions. This is not always the case however, since increasing HTE can sometimes be at the expense of combustion efficiency. A study cited by Kirk Smith monitored this tradeoff by comparing the performance of an improved cookstove against a traditional stove. Overall thermal efficiency improved from 15% to 37% but combustion efficiency dropped from 97% to 92%, which caused PIC emissions to increase by 8% (5). Even if total fuel consumption is reduced through HTE gains, the human health and global climate impact of total stove emissions may increase, depending upon the type and quantity of PICs

produced from decreased combustion efficiency. Combustion and heat transfer efficiencies are strongly interdependent and this relationship must be recognized as modifications to stove and pot geometries are considered. HTE gains often accompany combustion efficiency losses because combustion is most efficient when gases are hot, and optimal heat transfer requires a maximum extraction of heat from the gases into the water. These conflicting interests make it challenging to arrive at design improvements that satisfy one aspect without compromising the other.

Research from Edwards relating PIC emissions to combustion efficiencies in cookstoves provides a way to quantify PIC emissions for any particular combustion efficiency (16). This relationship helps to compare the decrease in PICs from heat transfer gains and subsequent fuel savings to potential increases in PICs from combustion efficiency losses. HTE gains predicted or measured by modifying various stove and/or pot parameters must be compared to consequent combustion efficiency losses to accurately evaluate overall stove performance.

The focus of this paper is to develop a thorough scientific understanding of heat transfer as it relates to biomass cookstoves. This requires examining all parts of the stove and pot with a thermal perspective to allow the most relevant governing principles to emerge. Such fundamental underpinnings include conduction, convection, radiation, the first law of thermodynamics, surface boundary layer behavior, impinging jet flow, and all inherent interrelationships. From these governing principles, temperature, mass flow rate and firepower all emerge as being the most influential variables for HTE. Firepower is defined as the lower heating value of the fuel multiplied by the mass of the fuel used, all divided by the amount of time taken to burn it. Firepower, temperature and mass flow rate are strongly interrelated with respect to one another, and so a framework must be established that dictates the degree of influence each of them have on each other.

The first step in developing this framework is to address the competing effects of gas temperature and mass flow rate on convective heat transfer for impinging jet flow. Firepower from the stove is fixed, but ambient air flow rate through the stove is variable. As the flow rate of cooler ambient air increases, gas temperatures reduce while pot surface boundary layer thickness reduces due to higher velocities. The trends are reversed as the flow rate of cooler ambient air decreases. Reducing boundary layer thickness increases convective heat transfer since the gases are closer to the surface of the pot. In contrast, cooler gas temperatures reduce heat transfer to the pot due to a smaller temperature difference. The degree to which each of these phenomena occurs with respect to one another determines the effect of ambient air entrainment on convective heat transfer.

The second step in developing this framework is to vary the firepower of a stove and measure how mass flow rate and temperature change with it. Combining the first and second steps together provides a fundamental understanding of stove performance based on the three critical parameters that have the most impact on HTE: temperature, mass flow rate, and firepower.

The fundamental framework described above provides a strong theoretical understanding which is applied to evaluating how various stove design modifications affect HTE. Each potential design modification serves as a case study with an intended purpose to isolate the three heat transfer modes of conduction, convection and radiation. The objective is to study each mode individually based on its respective case study, and determine its influence in improving overall thermal efficiency of the stove. A descriptive summary of all case studies is necessary to highlight the relevant design parameters each one addresses.

The first case study investigates the influence of pot gap cross-sectional area on convection heat transfer, and ultimately on stove thermal efficiency. Pot gap is the minimum

distance between the bottom of the pot and the drip pan (see Figure 2.3); adjusting this distance controls ambient air entrainment and the resulting flow rate through a stove for a given firepower. Flow rate magnitude is directly related to pot gap adjustment relative to the nominal position (i.e. increased pot gap leads to increased flow rate and vice versa). Not only does pot gap adjustment affect entrainment of ambient air, it alters flow path geometry which affects frictional losses and subsequent exit pressure. Compounding effects like this illustrate why it is important to first determine how entrainment of ambient air alone influences heat transfer prior to measuring the effect of pot gap. Conventional wisdom suggests that maintaining a constant cross-sectional area throughout the flow path of the stove produces the best thermal efficiency. The validity of this claim is investigated along with determining the pot gap that gives the optimal efficiency for a given firepower.

Shifting the focus away from altering flow characteristics, the second case study explores how convection is improved by increasing the surface area of the pot(s) exposed to the combustion gases. This is accomplished by adapting the stove geometry to either direct gases to the sides of the pot or to accommodate multiple pots. Directing gases to pass along the sides of a pot after impinging upon the bottom surface is achieved by employing the use of a pot skirt. This is a proven technology used on many existing cookstoves, but it is important to identify its limitations of heat transfer improvement. Using a second or third pot to recapture the remaining hot flue gases that are not utilized by the first pot is another common practice, but efficiencies are often in the same range as a standard single pot cookstove. It is necessary to discover why multiple pot stoves do not have higher efficiencies despite the seemingly large surface area exposed to the hot gases.

Building upon lessons learned from studying convection heat transfer in the previous case studies, the third case study investigates the applicability of conduction heat transfer to

stoves. Instead of absorbing heat directly from the combustion gases, the pot absorbs heat by conduction through a plate with a flat top and finned bottom. The plate is placed on top of the stove with the intent to capture more heat from the combustion gases than a flat bottom pot normally would and transfer this heat through conduction to its flat surface. The objective is to determine whether the extended surfaces (i.e. fins) on the plate will transfer more thermal energy to the pot via convection than is lost through conduction resistance and absorbed by the plate itself. A comparative study is conducted with a commercially available finned pot to eliminate conduction resistance and significantly reduce thermal absorption of the heat plate.

The fourth and final case study explores the effect of radiation heat transfer from flames on stove thermal efficiency. Combustion of biomass fuel is best characterized by the presence of diffusion flames which are commonly recognized as having a visible yellow/orange glow. The visible glow from a typical diffusion flame is due to the collective incandescent radiation emitted by soot particles and PICs as they are exposed to very high combustion temperatures. When fuel undergoes incomplete combustion, the diffusion flames can be larger and more radiant compared to when the combustion is more complete. Thus, a stove with high combustion efficiencies may potentially be associated with flames that transfer less radiative energy to the pot as compared to a stove with lower combustion efficiencies. A controlled experiment is conducted to evaluate the degree to which this phenomenon influences biomass cookstove performance. A pot of water is heated first by a clean burning premixed flame and then by a sooty diffusion flame – both created using a Bunsen burner. Observations from this experiment hope to indicate the importance of flame radiation to overall thermal efficiency.

The results from each of these case studies contribute to the expanding knowledge base that further improves the way people design and manufacture biomass cookstoves. The ideal

stove design is not the fruit of this labor, but a deep investigation into the effects of heat transfer certainly adds value to ongoing research in this field.

3. Fundamental Physics Governing Heat Transfer in Biomass Cookstoves

The physics that govern the behavior of cookstoves are rooted in thermodynamics, further explained using principles of heat transfer, and influenced by various stove geometries. To begin understanding the principles of heat transfer, a simple schematic in Figure 3.1 is used to represent the modes of heat transfer that play a role in stove performance.

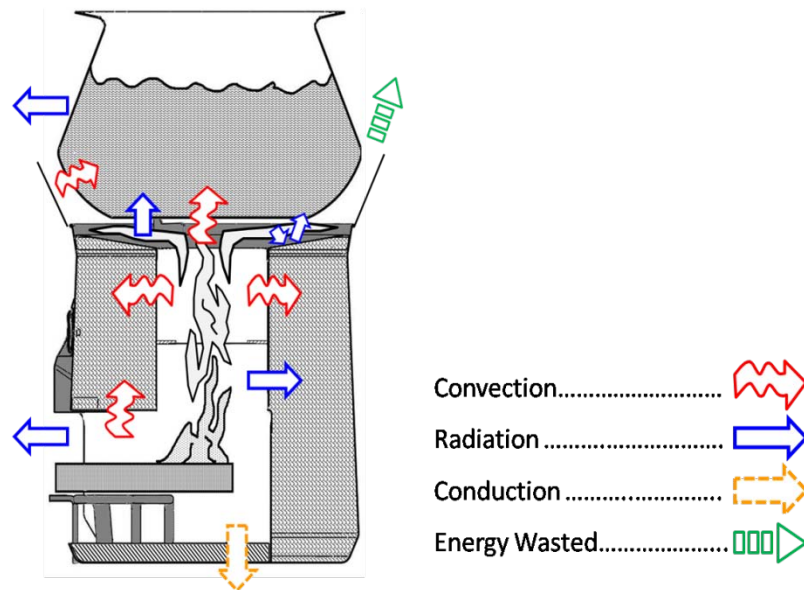


Figure 3.1. Schematic of stove cross-section with heat transfer modes.

3.1. The First Law of Thermodynamics

If HTE of existing cookstoves is to be accurately assessed and improved upon, then all energy involved in the combustion process must be accounted for. The first law of thermodynamics plays an instrumental role in this assessment, as it provides a tool that allows a thorough energy balance to be performed on the cookstove. Deriving an accurate energy balance is vital in determining the most effective way to improve HTE. The first law of thermodynamics requires all energy within a system to be conserved, even if it changes forms.

In the interest of cookstoves, combustion transforms stored chemical energy of the fuel into thermal energy. Part of this thermal energy takes on the form of flow energy which is responsible for the buoyant flow of hot combustion gases through the stove and past the surface of the pot.

Properly applying the first law to a cookstove leads to a better understanding of the principles governing its operation. The first law is used to perform a mass and energy balance on either a closed or open system. A cookstove represents an open system since it is characterized by fluid flowing across the boundary of a fixed volume, referred to as a control volume. The control volume in this case is bounded by the walls of the combustion chamber with the mouth of the stove acting as the inlet and the annulus formed by the pot and stove interface acting as the outlet, as shown in Figure 3.2. A control volume establishes a finite system boundary to analyze the balance of energy transferred between heat, work, and mass flow.

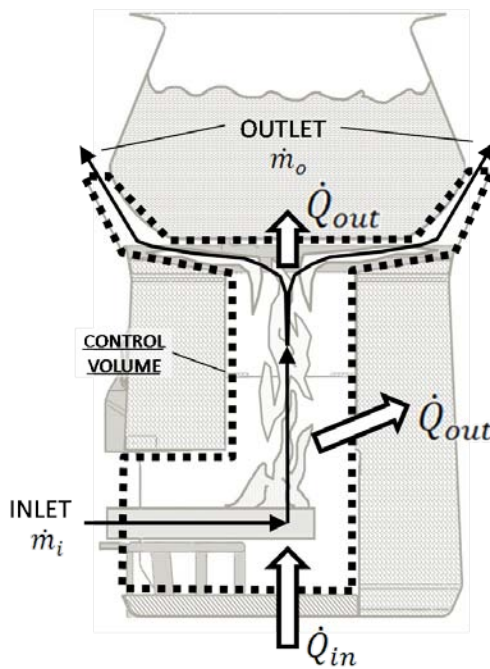


Figure 3.2. Cookstove control volume schematic.

The rate of mass flow energy transfer to or from a system is represented by equation 2.

$$\text{rate of energy flow} = \dot{m} \times \theta \quad [2]$$

Where:

\dot{m} – bulk mass flow rate of fluid

θ – total energy of a flowing fluid per unit mass

The total energy of a flowing fluid per unit mass can be broken down further into its fundamental components as in equation 3.

$$\theta = Pv + e$$

$$\theta = Pv + (u + ke + pe)$$

$$\theta = h + ke + pe \quad [3]$$

Where:

Pv – flow energy of moving fluid

P – pressure difference between inlet and outlet

v – specific volume of the fluid

u – internal energy

ke – kinetic energy

pe – potential energy

h – enthalpy

A cookstove is evaluated assuming isobaric steady-flow conditions where bulk mass flow rate remains constant. These assumptions ignore transient effects since these add significant complexity to the energy balance calculations with minimal gains in accuracy. Additionally, most of the time users spend cooking is typically when the stove is past the “warm up” stage and steady state assumptions are valid. Other simplifying assumptions include constant kinetic

and potential energy between the inlet and outlet of the control volume, zero mechanical work, and ideal gas behavior. Based on these assumptions, the energy balance of a cookstove is evaluated through the following relationships to arrive at equation 4.

$$\begin{aligned} \dot{E}_i &= \dot{E}_o \\ \dot{Q}_i + \dot{W}_i + \sum_i \dot{m} \theta &= \dot{Q}_o + \dot{W}_o + \sum_o \dot{m} \theta \\ \dot{Q}_i - \dot{Q}_o &= \dot{m}(\theta_o - \theta_i) \\ \dot{Q}_i - \dot{Q}_o &= \dot{m}(h_o - h_i) \\ \dot{Q}_i - \dot{Q}_o &= \dot{m}C_{p,avg}(T_o - T_i) \end{aligned} \quad [4]$$

Where:

Subscripts *i* and *o* – inlet and outlet variables, respectively.

\dot{Q} – rate of heat energy transfer

\dot{W} – rate of work energy transfer

$C_{p,avg}$ – average constant pressure specific heat of air between T_i and T_o

T – gas temperature

Equation 4 is a fundamental equation that demonstrates the interdependency between mass flow rate, temperature and heat transfer in and out of the stove. Research conducted at the EECL allows overall stove mass flow rate and combustion gas temperature to be determined from a range of heat transfer inputs, or firepowers (17). These calculations assume perfectly insulated stove walls and do not include any heat transfer to a pot ($\dot{Q}_o = 0$). Therefore both gas temperature and induced mass flow rate remain constant through the system and are entirely influenced by \dot{Q}_i , or firepower input. In contrast, heat transfer out of the control volume (\dot{Q}_o) must be considered when analyzing the overall energy balance of the stove. Nonetheless,

neglecting \dot{Q}_o contributions to arrive at approximate \dot{m} and temperature values provides a foundation from which an energy balance of the stove can be quantified.

An accurate energy balance assessment cannot uphold the assumption of constant gas temperature through the system. In fact the temperature of the combustion gases must decrease along the path length of the control volume as heat is transferred into the stove and pot. Determining the amount of heat transferred into the pot and stove from the hot gases requires careful consideration of the different modes of heat transfer involved. Relative contributions of conduction, convection, and radiation to the overall stove energy balance must be evaluated and understood before any HTE improvements are considered.

3.2. Contributing Roles of Conduction, Convection, and Radiation

Each heat transfer mode is split into two categories: losses and gains. The losses are associated with heat that is transferred into the stove body or out to ambient while the gains are associated with heat that is transferred to the pot. A cross sectional view of the stove is provided for each heat transfer mode in Figures 3.3 – 3.5. Arrows drawn in each figure indicate the direction of heat transfer, noting that they are all pointing out of the control volume (\dot{Q}_o). The percentage values given represent the fraction of chemical energy contained in the fuel converted to heat that is either lost or gained. A closer look into each heat transfer mode will provide further insight into how they apply to HTE of the stove. Detailed calculations for each heat transfer mode described here are provided in Appendix C.

3.2.1. Conduction

Conductive heat transfer occurs through the floor of the stove to the ground, through the body of the stove to the surroundings, and through the thickness of the pot. There is zero energy gains associated with conduction heat transfer to the pot. The rate of steady state

conduction heat transfer is defined by equation 5, where k = thermal conductivity, A = cross sectional area of object, ΔT = temperature difference, L = object thickness.

$$Q_{conduction} = \frac{k * A * \Delta T}{L} \quad [5]$$

Conduction through the stove floor to the ground is the only instance where the heat from the fuel is transferred to the stove via a stationary medium – the charcoal bed.

Consequently, this represents the sole conduction loss contribution to the overall energy balance as shown in Figure 3.3.

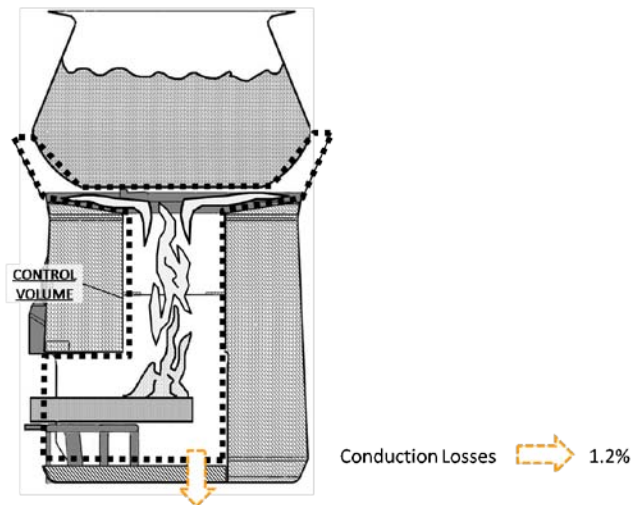


Figure 3.3. Conduction contribution to energy balance.

Conduction through the stove walls does not directly contribute to the energy balance since it affects contributions from radiation and convection as discussed later. Conduction resistance through the metal pot is neglected due to high thermal conductivities and small wall thickness.

3.2.2. Convection

Hot combustion gases interact with two separate surfaces: the inner surface of the stove (losses) and the outer surface of the pot (gains). The rate of steady state convection heat

transfer is defined by equation 6, where h = convection coefficient (W/m^2K), A = exposed surface area, ΔT = temperature difference.

$$Q_{convection} = h * A * \Delta T \quad [6]$$

A summary of convection contributions to the overall energy balance is shown in Figure 3.4.

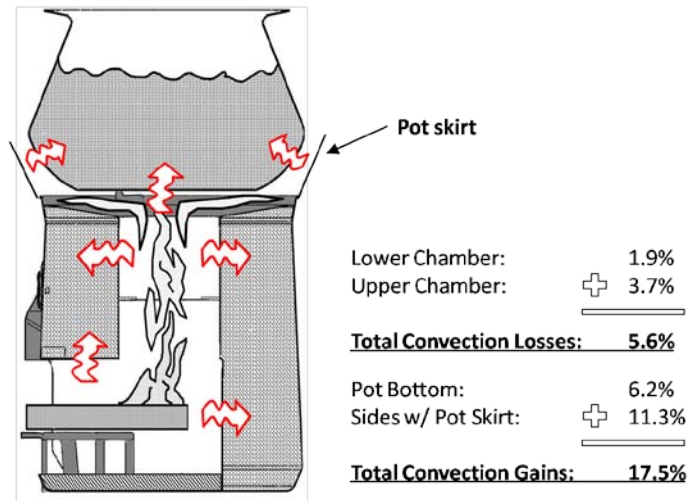


Figure 3.4. Convection contributions to energy balance.

The magnitude of convective heat transfer is influenced by the velocity of the gases flowing through the stove, the exposed surface area contacting the gases, and the temperature difference between the gases and the exposed surface. Higher flow velocities and increased temperature differences through the stove increase convective heat transfer. Convective heat transfer improves by increasing the exposed surface area of the pot and/or decreasing the inner surface area of the stove. Since the latter is not practical, focus is often placed on increasing the surface area of the pot exposed to combustion gases.

Total convection losses are represented by the lower and upper combustion chamber portions of the stove. Both portions are treated as two independent cylindrical tubes with fully developed internal flow characteristics based on constant specified mass flow rate and gas temperature (17). Surface temperatures were obtained experimentally using several

thermocouples mounted to the inner walls of the stove. The flow through each portion is calculated to be in the transition zone between laminar and turbulent, which allows for a rough approximation of the convection coefficient and related heat transfer for each portion. The overall convective heat transfer contribution from the lower chamber is less than that from the upper chamber.

Total convection gains come from two sources: impinging combustion gases upon the bottom surface of the pot, and scraping of the same gases along the sides of the pot. Both of these sources are analyzed independently aside from outside influences on gas temperature. For impinging flow, the temperature depends on how much heat is drawn away from the gas flow upstream through the upper chamber via radiation and convection losses. Similarly, the gas temperature along the pot sides depends on how much heat is drawn away from the impinging flow.

Heat transfer to the pot bottom is analyzed by first deriving the convection coefficient for isothermal, non-reacting, impinging jet flow. Details of these calculations are provided in Appendices A and B, and this topic is covered more thoroughly in sections 3.3 and 3.4. The gas temperature exposed to the pot bottom is calculated by using equation 4 to solve for T_o while $\dot{Q}_i = 0$, T_i equals the initial gas temperature and \dot{Q}_o equals the sum of heat lost by both radiation and convection to the inner walls of the upper combustion chamber. The exposed surface area only accounts for the bottom of the pot, which causes the estimated contribution to be lower than expected. In reality, hot gases are buoyantly driven up the sides of the pot which increases the exposed area, but this effect is addressed separately with the provision of a pot skirt.

As shown in Figure 3.4, a pot skirt reduces the cross sectional flow area which forces the gases to more closely follow the contours of the pot and also reduces the surface boundary

layer thickness. Surface boundary layer thickness is reduced because the gas velocity increases as it travels through the flow restriction, thereby increasing the convection coefficient. The flow around the pot is assumed to behave similarly to a fully developed laminar flow through a cylindrical annulus. Outer walls of the skirt are also assumed to be perfectly insulated while the inner wall temperature of the pot is held constant. The contribution to the overall energy balance from using a pot skirt is slightly higher than expected since gases would still travel along the sides of the pot without a skirt.

This overestimated pot skirt contribution is balanced by the underestimated contribution from pot bottom impingement. When assessing total convection gains, the accuracy of the lumped sum contribution from both sources is more important than the accuracy of individual portions. If the accuracy of the individual sources was improved, then the impingement flow contribution percentage would increase but pot skirt percentage would decrease by the same amount. Thus, total percentage of the energy balance attributed to convection gains would remain the same. This is why the simplified calculations outlined above are sufficiently accurate to understand overall HTE.

3.2.3. Radiation

Radiant energy originating from either the coal bed or flames is transferred to the stove body, pot, or ambient surroundings. The rate of blackbody radiation heat transfer between two surfaces is described by equation 7, where T_2 and T_1 are the respective temperatures of each surface.

$$Q_{radiation} = A * \sigma * (T_2^4 - T_1^4) \quad [7]$$

A summary of individual radiation contributions to the overall energy balance is shown in Figure 3.5.

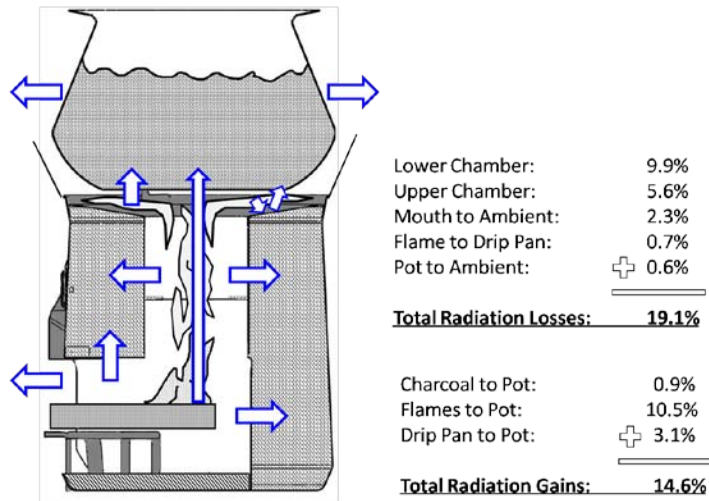


Figure 3.5. Total radiation contributions to energy balance.

The magnitude of radiation being emitted as either a loss or a gain is strongly dependent on the temperature difference between the two objects, the area of the emitting surfaces, emissivity of both surfaces, and the associated view factor. As each of these variables grows larger, radiation heat transfer increases. The view factor is a dimensionless number used in surface-to-surface radiation calculations which accounts for the relative areas of each surface along with the distance between them.

In regard to radiation losses to the stove body, the upper and lower chambers are analyzed separately; each being treated as fully enclosed infinitely long concentric cylinders with the charcoal/flame sheet representing the inner geometry as shown in Figure 3.6. Emissivity values of typical biomass flames, charcoal surface, and stove body surfaces are estimated from literature (18) (19) (20) (21). Radiation from the flames to the drip pan is calculated assuming the flames are represented by a flat plate beneath the pot with a specified view factor between the two surfaces. Radiation losses to the ambient environment from both the outer sides of the pot and out the stove mouth are estimated based on the relevant geometry and assuming negligible irradiation from the surroundings.

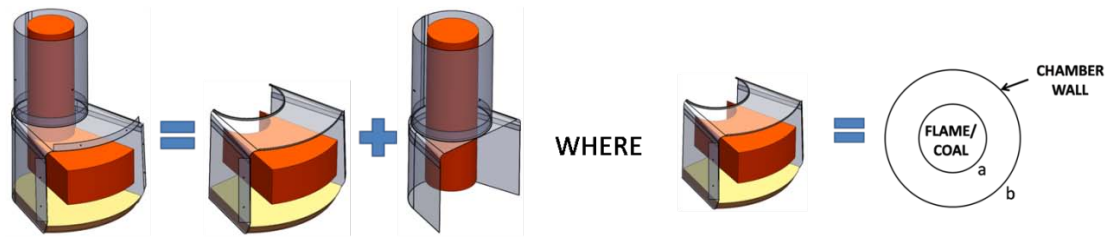


Figure3.6. Simplified radiation schematic for stove losses.

Radiation gains to the pot originate from three areas: charcoal bed, flames, and reflected flame radiation from drip pan. Emissivity values for all objects of concern are used along with transmissivity and reflectivity values of the flame and drip pan, respectively, based on a flame reflectivity of zero and assuming the pan is a gray surface. View factors are used to correct for relative areas of the respective surfaces and also the distance between them. The pot surface is assumed to behave as a black body since it absorbs all incident radiation; however, irradiation from the pot surface to the hotter object is ignored.

3.2.4. Summary

Summarizing the steady state energy balance provides a necessary perspective to begin evaluating each mode of energy transfer. A schematic of the cookstove cross-section along with relative heat transfer contributions is provided below in Figure 3.7. Combustion losses are due to incomplete combustion of the fuel and a certain amount of heat is unaccounted for due to errors associated with the calculations. Overall theoretical stove thermal efficiency is calculated by simply adding together convection and radiation gains ($17.5\% + 14.6\% = 32.1\%$). Comparing this theoretically derived value to a typical experimental value of 29.0% instills confidence in the theoretical model. A typical experimental thermal efficiency of a three-stone fire is $\approx 15.9\%$, which reinforces the notion that further heat transfer efficiency improvements to existing cookstoves are worthwhile.

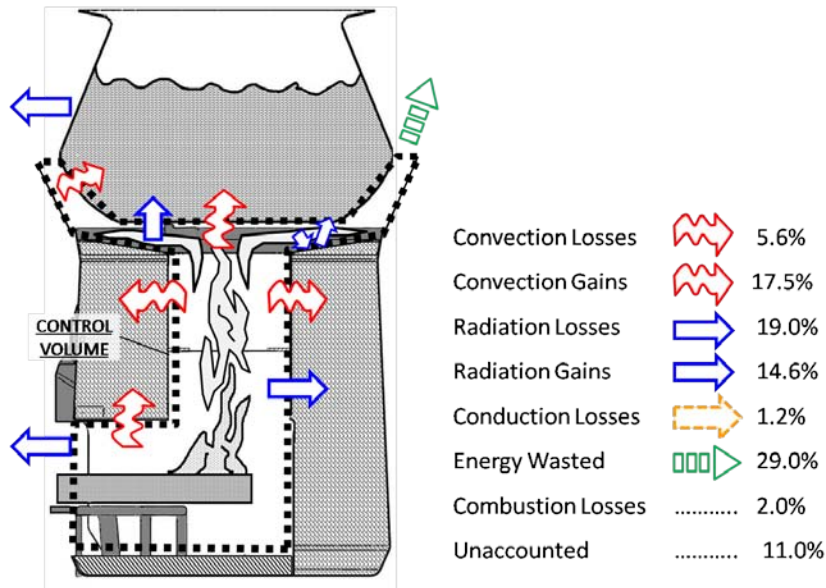


Figure 3.7. Steady state energy balance with heat transfer contributions.

3.3. Effects of Gas Path Geometry on Flow Characteristics

All heat transfer modes described above are influenced by the flow characteristics of the combustion gases as they are buoyantly driven through the geometry of the stove. The two properties that most predominantly characterize the flow are mass flow rate and temperature. Along with examining the effects of gas temperature and mass flow on heat transfer, it is important to understand how they are controlled by gas path geometry which changes based on stove geometry and the interface between the stove and pot(s).

Chimney height (h_{chim}) is one of the primary geometrical parameters of the stove which refers to the vertical distance from the heat source to where the hot gases escape to ambient. For a single pot stove, chimney height equals the distance from the base plate to either the bottom of the pot or the top edge of the pot skirt if applicable. The chimney height for a double pot stove is represented more literally since a tall vertical chimney is usually provided as shown in Figure 3.8.

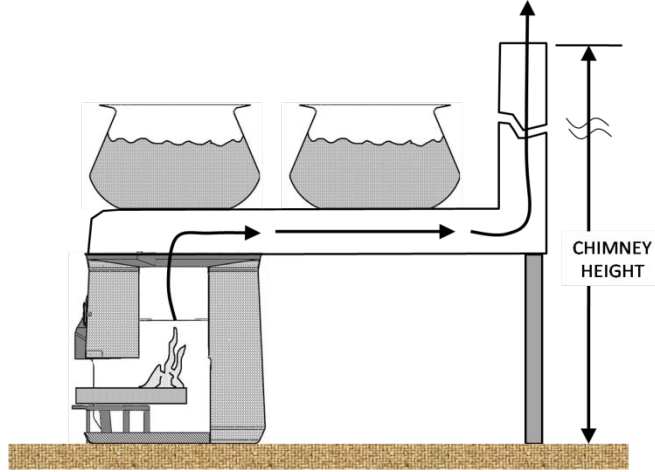


Figure 3.8. Double pot stove cross-section schematic.

When a fire burns inside of a stove as pictured above, it produces high temperature gases with lower densities (ρ_{hot}) than ambient air located just outside of the stove mouth ($\rho_{ambient}$). This density gradient across the entrance induces a pressure differential ($\Delta P_{induced}$) from buoyancy effects in accordance with Archimedes' Principle represented by equation 8, where g is the gravitational acceleration.

$$\Delta P_{induced} = gh_{chim}(\rho_{ambient} - \rho_{hot}) = gh_{chim}\rho_{ambient} \left(1 - \frac{T_{ambient}}{T_{hot}}\right) \quad [8]$$

The pressure gradient described by equation 8 translates into a mass flow rate (\dot{m}) through the stove which is dependent upon the chimney height, chimney cross sectional area (A), loss coefficient (LC), and temperature of both combustion gases (T_{hot} or T_o) and ambient surroundings ($T_{ambient}$ or T_i). This relationship is described by equation 9.

$$\dot{m} = LC * A \left(\frac{\Delta P_{induced}}{R_s T_{hot}}\right) \sqrt{2gh_{chim} \left(\frac{T_{hot} - T_{ambient}}{T_{ambient}}\right)} \quad [9]$$

The loss coefficient (LC) in this equation accounts for efficiency losses associated with frictional and viscous losses of the fluid due to stove geometry, heat lost to chimney walls, and

the unrealistic single point heat addition at the very base of the stove. Research at the EECL has shown $LC \approx 0.5$ without a pot placed on the stove, and $LC \approx 0.35$ with a pot (17).

It is apparent from equation 8 that if all other variables are held constant, increasing chimney height increases the induced pressure through the stove. According to equation 8, this rise in induced pressure also increases the total mass flow rate (\dot{m}), as defined by equation 10.

$$\dot{m} = \dot{m}_{fuel} + \dot{m}_{air} \quad [10]$$

A rise in mass flow rate leads to increasing firepower potential, meaning the actual firepower increase depends on the relative contributions of ambient air entrainment (\dot{m}_{air}) vs. fuel input (\dot{m}_{fuel}). Either way, raising chimney height increases mass flow rate through the stove, but the effect on flow temperature depends on whether the actual firepower input matches the newfound potential. The relationship between mass flow rate, temperature, and velocity is examined more closely in Section 3.4. These relationships are then correlated with firepower for a fixed geometry in Section 3.5.

Increasing the flow velocity often leads to more turbulence which improves HTE compared against laminar flow behavior. As hot gases flow over a solid surface, a very thin boundary layer of stagnant air forms against the surface. The thickness of this boundary layer is inversely proportional to the flow velocity of the gases – boundary layer thickness decreases as velocity increases. Thick boundary layers reduce convective heat transfer due to the greater distance between the surface and the free stream flow. This boundary layer effect influences the convection coefficient value through its relationship with the Nusselt and Reynolds numbers. The Reynolds number is a dimensionless variable that provides the ratio of inertial to viscous forces in a fluid, as provided by equation 11 where ρ = gas density, v = velocity, L = characteristic length (or diameter, D_h), μ = absolute viscosity.

$$Re = \frac{\rho v L}{\mu} \quad [11]$$

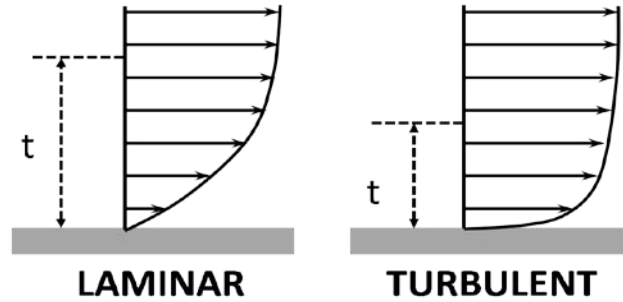


Figure 3.9. Velocity profile for laminar and turbulent flows with same free stream velocity.

High velocity (turbulent) flow has a smaller boundary layer thickness (t) and hence, a larger associated convection coefficient than low velocity (laminar) flow, as depicted in Figure 3.9. Typical flow properties through a cookstove tend to be either fully laminar or in the transition zone between laminar and turbulent. These regimes correspond to Reynolds numbers within the range of $500 < Re < 5000$ depending upon influences that include firepower, entrance effects, fuel obstruction, flame interaction and stove geometry.

Flow characteristics are most relevant to HTE in the region where the stove interfaces to the pot. If a pot is placed directly on top of a stove, then it forces the upward-traveling gases to impinge upon the flat bottom surface of the pot. The flow then quickly changes direction to travel radially outward, thereby creating a stagnation zone of low velocities around the center point of the pot bottom. Calculating the Reynolds number for this impingement flow ($Re \approx 500$) in the stove revealed laminar behavior, and this value was then used to calculate a Nusselt number assuming a fully developed free jet. A convection coefficient was calculated based on these findings and details related to this are in Appendices A and B. The maximum radial velocity for impingement flow occurs about one “jet diameter” (i.e. combustion chamber diameter) from the center point of the pot (22). This indicates an ideal location on the pot bottom to place extended surfaces (i.e. fins) which would increase surface area and improve convective heat transfer. Literature also suggests turbulent heat transfer rates for impingement

flow can be 1.4-2.2 times higher than laminar rates (22). This suggests running the stove at higher flow velocities to achieve a larger Reynolds number.

To go along with the effects of impingement heat transfer to the pot bottom, flow behavior at the stove/pot interface can be investigated further by examining the effect of pot gap thickness. Pot gap refers to the distance between the bottom of the pot and the top surface of the stove as shown in Figure 3.10.

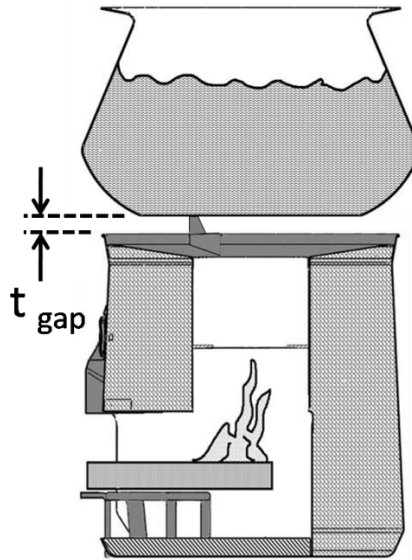


Figure 3.10. Cross-section of stove with pot gap thickness labeled.

Firepower, total mass flow rate, and flue gas temperature are all strongly interrelated through equations 4 and 9. In reality, changing one parameter like pot gap simultaneously affects all three of these variables making it difficult to evaluate how pot gap can affect mass flow rate and temperature separately. Therefore, a fixed firepower must be assumed to evaluate the heat transfer impact of pot gap in addition to other design parameters. Even with a fixed firepower, there still exists a competing relationship between temperature and mass flow rate as pot gap is varied. More is discussed about this phenomenon in Section 4.1.

Aside from altering the temperature and velocity, the flow path geometry can be modified in ways to improve HTE. This is achieved by increasing the pot surface area exposed to

the hot combustion gases by forcing them to trace along the sides of the pot, or by adding a second pot to capture the residual heat leftover from the first. One or both of these options may be used to extract the maximum amount of heat from the stream of hot gases. A pot skirt may be used to implement the first strategy; however understanding the trade-offs between surface area, pressure losses, and financial costs associated with an increasingly tall pot skirt is critical. If a stove is designed with the goal of warming two separate pots, then similar considerations must be evaluated. An added factor for a double pot stove is the requirement to provide a chimney to overcome the pressure losses that are likely to be experienced by such a stove configuration with an extended flow path. Further details in regard to the effects of increasing surface area exposure are provided in Sections 4.2 and 4.3.

3.4. Mass Flow Rate, Temperature, and Their Effects on Heat Transfer

Knowing that various geometrical parameters of the flow path influence certain flow characteristics, the next step provides a detailed look into exactly how mass flow rate and temperature modifications can affect heat transfer. A hypothetical scenario is developed focusing on how the magnitude of heat transfer changes when mass flow rate increases alongside a simultaneous decrease in temperature, and vice versa. This is performed by first choosing a nominal total mass flow rate (\dot{m}) and gas temperature (T_o) of the stove for a given firepower (Q_{in}) based on Figure 3.11 (17). From here a stove inlet temperature is assumed (T_i) along with an average constant pressure specific heat (C_p). All of these parameters are related through equation 12 which is a rearrangement of the first law derived earlier.

$$T_o(\dot{m}) = \frac{Q_{in}}{\dot{m}C_p} + T_i \quad [12]$$

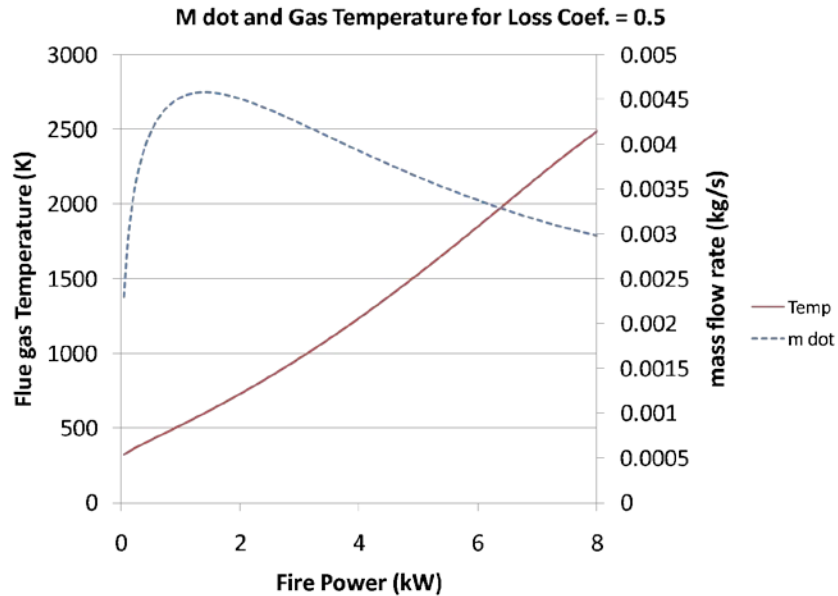


Figure 3.11. Relationship between firepower, gas temperature and mass flowrate (17).

If firepower (mass flow rate of the fuel) is held constant while the total mass flow rate increases within the boundaries of Figure 3.11, then based on the relationship given in equation 12, the outlet gas temperature must decrease. Since fuel mass flow rate is fixed, the increasing total mass flow rate can only be due to additional entrainment of ambient air, resulting in a larger excess air ratio and cooler temperatures. The opposite is also true for the case of decreasing mass flow rate leading to increasing gas temperatures. The magnitude of change for each of these flow characteristics relative to one another governs the total impact they have on heat transfer.

When evaluating contributions from the different heat transfer modes, it is more intuitive to refer to the flow rate in terms of velocity rather than mass. Flow velocity (\vec{v}) is directly tied to total mass flow rate; however, it is also influenced by temperature through density (ρ) with the ideal gas assumption as indicated in equation 13, where A is the cross sectional area of the flow path. As shown in data from the appendix, the velocity increases

along with mass flow rate but does not increase quite as sharply since this trend is reduced by the increasing gas density.

$$\vec{v} = \frac{\dot{m}}{\rho A} \quad [13]$$

Each mode of heat transfer is affected by the velocity and temperature of the combustion gases, but not all are affected equally. Conduction contributions to the overall energy balance are modest to begin with, so changing the flow characteristics has a very small effect on this heat transfer mode. Radiation contributions are not as trivial. The flame luminosity (and hence emissivity) is directly proportional to the excess air ratio (EAR) due to a larger percentage of soot particles that exist from cooler flame temperatures. The length of the flame is also greater when it exists in a higher velocity flow, providing a larger emitting area. Both of these flame effects are counteracted by a lower temperature, which partially cancels any radiation gains that may result due to increased velocities. This being said, it is assumed that the percentage contribution of radiation gains from the energy balance relative to convection gains will remain the same. Convection is the heat transfer mode most sensitive to the changing flow characteristics described above. Thus, it remains the focus of this study to analyze how the trade-offs between velocity and temperature affect convection heat transfer.

As velocity through the stove increases, the boundary layer thickness surrounding the pot becomes smaller which translates to a greater convection coefficient. To contradict this behavior, lower temperatures lead to lower thermal conductivity values of the gas, which reduces the convection coefficient. Before examining the details of this trade-off, a strong foundational understanding of the convection coefficient must be established. All derivations for both semi-empirical and theoretical convection coefficient calculations are provided in Appendices A and B. Comparing the results from each leads to a commonly agreed upon convection coefficient value of $\approx 9.0 \text{ W/m}^2\text{K}$ for the bottom of the pot on a 3.5kW firepower

stove, neglecting radiation contributions. Since both versions of the convection coefficient produce very similar values, it inspires confidence to proceed with determining how convection heat transfer changes depending on various mass flow rate and temperature inputs.

A value of 3.5kW is chosen for the firepower based on the measured quantity of biomass fuel typically consumed during a 25 minute water boil test (also shown in Appendix C, Step 5.1). An associated nominal mass flow rate is taken from Figure 3.11 and a range of flow rate values is chosen based on the boundaries set by the curve presented on the graph. A respective outlet temperature is calculated for each flow rate value using equation 12 and together they are used as inputs to calculate a convection coefficient. Finally, the rate of convection heat transfer to the pot is calculated; this procedure is repeated for several flow rate values and temperatures. The results from this study provide a fair assessment regarding which flow characteristics have the most influence on heat transfer.

Before presenting the results it is appropriate to illustrate how the convection coefficient is affected by changing the mass flow rate and temperature. Convection coefficient (h) is a function of Nusselt number (Nu), gas thermal conductivity (k_{gas}), and diameter of the upper chamber stack (d) as defined by equation 14.

$$h = \frac{Nu * k_{gas}}{d} \quad [14]$$

Nusselt number is a dimensionless temperature gradient at the surface, and is a function of Prandtl number (Pr) and Reynolds number as defined by equation 15 for a fully developed free jet impinging on a flat plate (23).

$$Nu = .565 * Pr^{0.5} Re^{0.5} \quad [15]$$

Prandtl number (ratio of momentum and thermal diffusivities, $C_p\mu/k$) remains relatively constant while Reynolds number increases linearly with mass flow rate. A basic

schematic showing these relationships and how they tie back to Nusselt number is provided in Figure 3.12. Clearly, Nusselt number increases along with increasing mass flow rate.

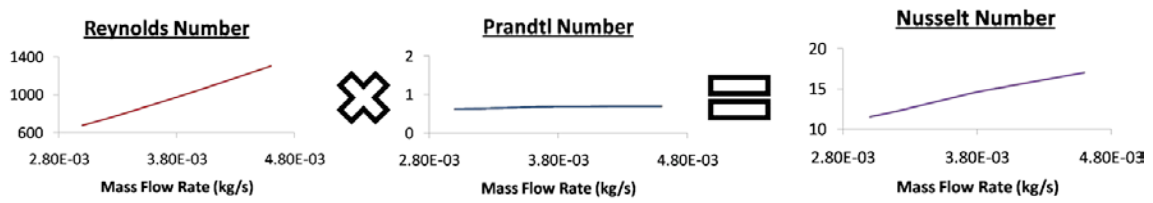


Figure 3.12. Schematic showing how Nusselt number changes with mass flow rate.

Recalling how temperature and mass flow rate are inversely related, as Nusselt number increases gas thermal conductivity decreases since it is directly proportional to temperature. The magnitude that Nusselt number increases is nearly matched by the magnitude that gas thermal conductivity decreases. Hence, as illustrated in Figure 3.13, convection coefficient is held almost constant as mass flow rate and temperature change.

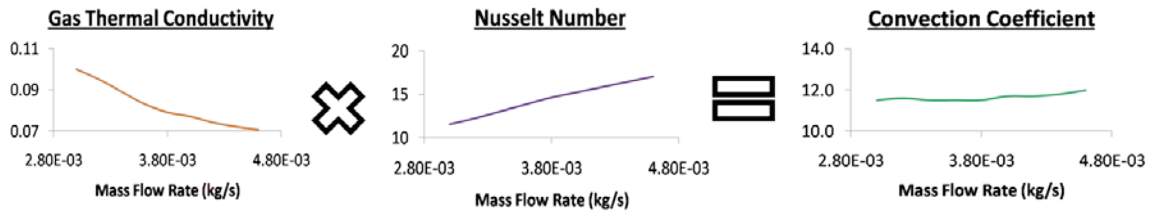


Figure 3.13. Schematic showing how convection coefficient changes with mass flow rate.

Since convection heat transfer is influenced equally by the convection coefficient and temperature (equation 6), the total convection heat transfer for this scenario is directly proportional to the change in temperature. This relationship is shown in Figure 3.14., as both heat transfer and temperature are reduced as mass flow rate increases.

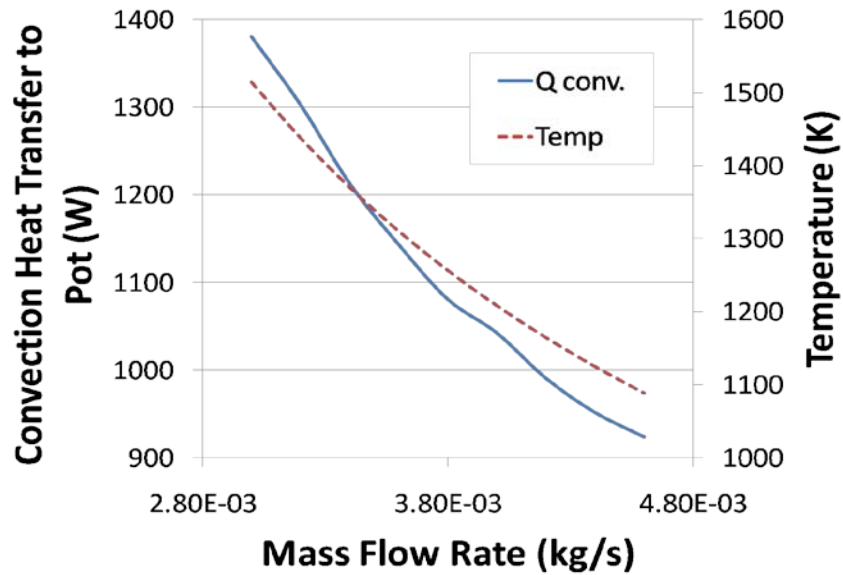


Figure 3.14. Relationship between mass flow rate, temperature, and convection heat transfer for firepower = 4kW.

3.5. The influence of Firepower on Convection Efficiency

The previous section establishes how changing values of mass flow rate and temperature can affect heat transfer if firepower is held constant. Building from this understanding, it is necessary to determine how these flow characteristics influence heat transfer if firepower is varied, but stove geometry is held constant. Combining each of these lessons together provides the ability to answer the following question: Does a large stove have better or worse HTE than a small stove, or are they the same?

For the same reasons explained in the previous section, the focus is targeted specifically on how convection heat transfer changes with firepower. Mass flow rate, temperature and firepower are all highly interdependent as expressed through equations 4 and 9. As presented before in Figure 3.11 and below in Figure 3.15, research conducted here at the EECL quantifies this relationship (17). Unlike Figure 3.11, Figure 3.15 is generated with a smaller loss coefficient

(LC = 0.35) due to the placement of a pot above the stove which increases the viscous and frictional pressure losses throughout the flow, and acts as an additional heat sink.

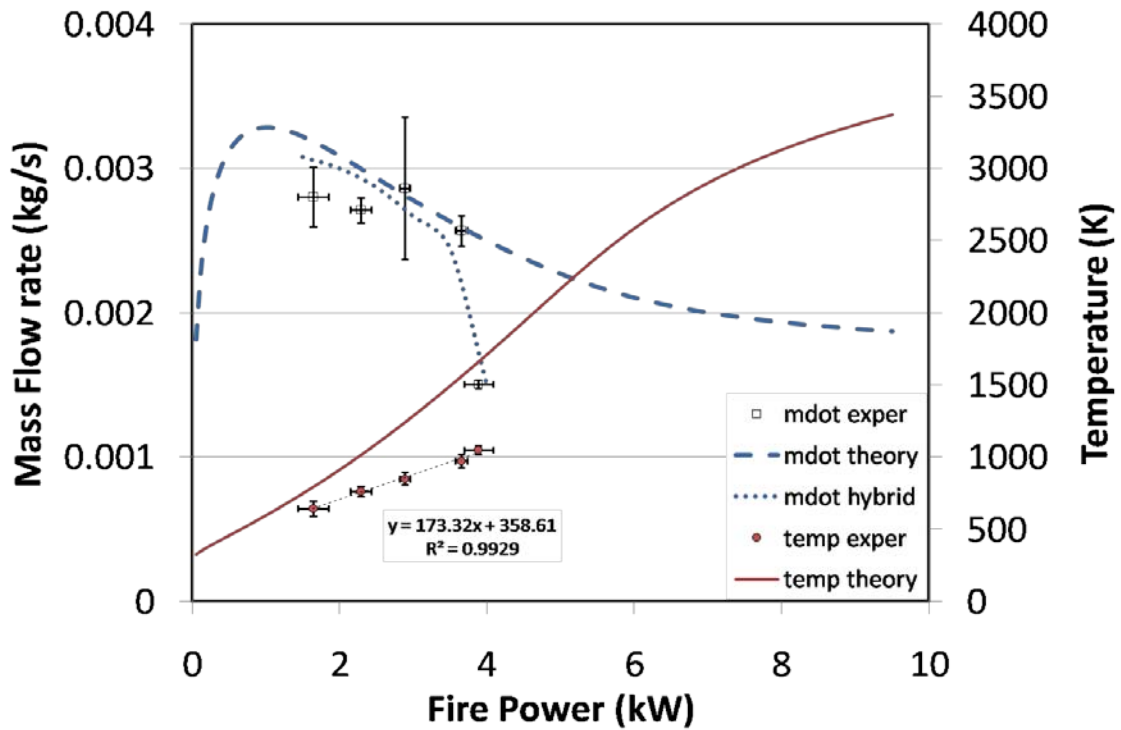


Figure 3.15. Mass flow rate and temperature vs. firepower with LC = 0.35 (17).

Data from both experimental testing and theoretical predictions are presented together in this figure, highlighting both the validity of each as well as where the experimental data strays from predicted behavior. Specific details regarding the theoretical and experimental procedures involved in collecting this data is available from the thesis paper written by Agenbrood (17). The curve labeled as “mdot hybrid” approximates the mass flow rate by considering the experimental trends compared against the theoretical predictions. This is a separate addition to the raw data provided by Agenbrood and is not included in his research. In the interest of heat transfer, firepower variations that affect mass flow rate and temperature reference the “mdot hybrid” and “temp exper” (experimental temperature) curves, respectively from Figure 3.15. This allows for a more realistic heat transfer assessment to be made from this data.

The particular stove used in the test is a typical rocket elbow stove similar in size to the stove shown previously in Figure 2.3. The sharp drop-off of mass flow rate around 3.5 kW illustrates the location along the power spectrum where the fuel feed rate exceeds the amount of air that is required to oxidize the fuel for efficient combustion. Essentially, the air fuel ratio (AFR) which is limited by the stove geometry and fuel feed rate becomes too small to maintain optimal performance. Firepower cannot be increased any further than 3.5 kW for this particular stove unless its geometry is expanded to accommodate the additional entrainment of air required to meet the demands of a higher fuel feed rate. Despite this upper limitation that stove geometry places on firepower, monitoring the flow characteristics for the intermediate firepowers provides the necessary information to determine the effect firepower has on convection heat transfer.

The relationships between flow velocity, temperature and convection heat transfer outlined in the section 3.4 are intrinsically tied to firepower. The most effective way to determine the impact of firepower on convection heat transfer is to relate them through the convection coefficient. As before, this begins with noticing how the Reynolds number and Prandtl number change with firepower and hence, influence the Nusselt number value. This relationship is portrayed nicely in Figure 3.16. Notice the slight knee present in the Reynolds number plot which is due to the sharp decline in mass flow rate mentioned earlier around 3.5 kW. A similar shape is also present in the Nusselt number graph since Prandtl number remains relatively constant throughout the firepower range.

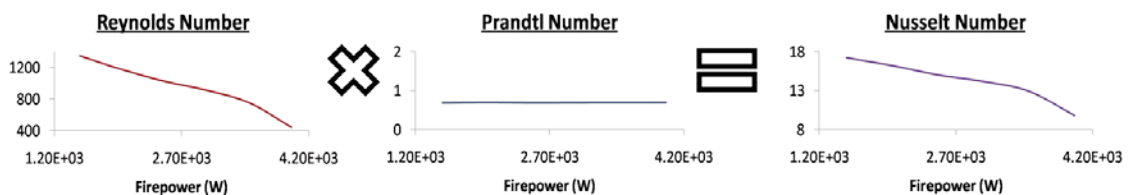


Figure 3.16. Schematic showing how Nusselt number changes with firepower.

This Nusselt number behavior is combined with the relevant influence of firepower on gas thermal conductivity to determine the effect on the convection coefficient, as shown in Figure 3.17. Similar to the previous section, gas thermal conductivity and Nusselt number nearly cancel each other which results in a relatively constant convection coefficient throughout the range of firepowers presented. The only exception occurring as the stove approaches its firepower limit. Here, the non-linearity in the flow rate (represented by the knee on the Nusselt number curve) begins to dominate the linear rise in temperature and consequent gas thermal conductivity. Convection coefficient is compromised due to this effect and is projected to worsen further as AFR continues to diminish.

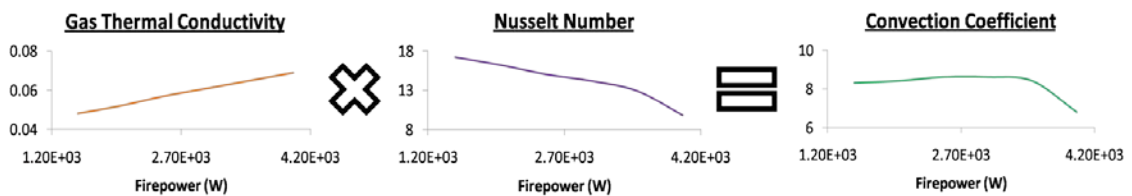


Figure 3.17. Schematic showing how convection coefficient changes with firepower.

Convection coefficient by itself does not determine the total influence of firepower on heat transfer. From equation 6, it is apparent that the temperature difference between the combustion gases and pot also play an important role since the exposed area does not change. The temperature of the gases increase approximately linearly with firepower, and this relationship causes a similar rise in convection heat transfer as indicated by the plot from Figure 3.18 entitled “Conv. to Pot”.

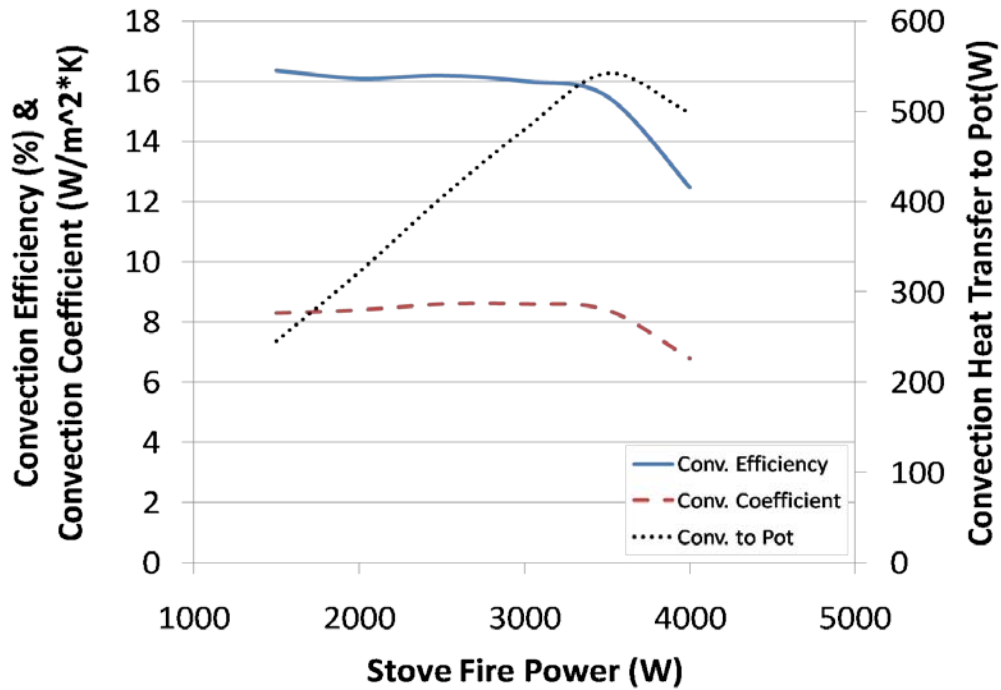


Figure 3.18. The effect of firepower on various convection parameters.

Despite this rise in total convection heat transfer, the equivalent rise in firepower causes the convection efficiency (defined as convection heat transfer divided by firepower) to remain constant while firepower is increased within the intermediate firepower values. All three plots in Figure 3.18 indicate the firepower quantity (~3.5kW) where AFR becomes too small and stove performance suffers. Convection heat transfer reaches a peak around this point and then declines along with convection efficiency and convection coefficient. Comparing convection coefficient results between sections 3.4 and 3.5 presents a lower value in section 3.5. This reduced convection coefficient is due to more realistic (lower) values for temperature and mass flow used in section 3.5.

3.6. Summary

Data from the preceding sections is summarized pictorially in Figures 3.19-21 and raw data from the calculations is available in Appendix D. Figure 3.19 is an illustration of the same size fire (equal firepower) being burned in two separate stoves. Stove A is depicted as being

smaller since it represents a stove with a reduced mass flow rate compared with Stove B. Based on data derived in section 3.4, increased entrainment of ambient air mixing with the combustion gases lowers the overall gas temperature. The only way to achieve this in practice is to increase the opening of the stove mouth or increase chimney height; thereby increasing the overall stove size (Stove B). This leads to a reduction in total (convective) HTE as indicated by the direction of the inequality.

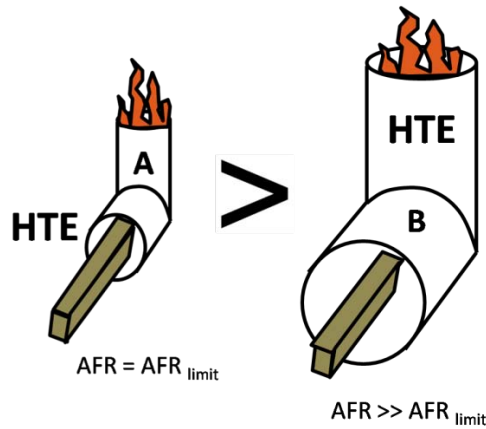


Figure 3.19. Effect of stove geometry on heat transfer for fixed firepower.

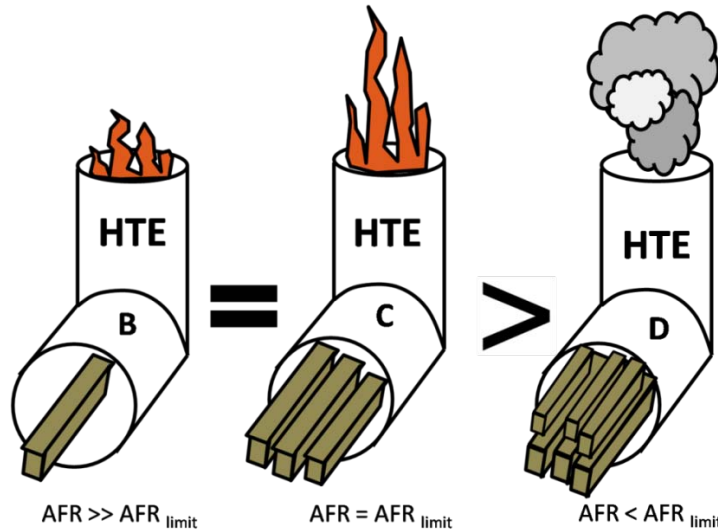


Figure 3.20. Effect of firepower on heat transfer for fixed stove geometry.

Figure 3.20 illustrates how HTE of a stove with fixed geometry is affected as firepower is increased through its regular operating range and past its AFR limit. Evidence in section 3.5

shows how constant efficiency is maintained through the normal operating range (Stoves B and C) as firepower increases, but drops off dramatically once AFR is less than its practical limit and the fire is “choked” (stove D).

Figure 3.21 combines the results presented in Figures 3.19 and 3.20 so by definition, Stove A must have higher HTE than Stove C. This means that assuming equal AFR, a smaller stove has higher HTE than a larger stove, but only if the pot used for each has the same diameter. This is likely due to a larger percentage of wasted energy that would occur when the larger stove is used. Another practical consideration is the reduction in TTB that would result due to using a smaller stove with a reduced firepower. The special case outlined here assumes each stove configuration is at maximum firepower ($AFR = AFR_{limit}$) but the relationship should hold true throughout the operating range of each stove so long as the respective AFR values remain equivalent.

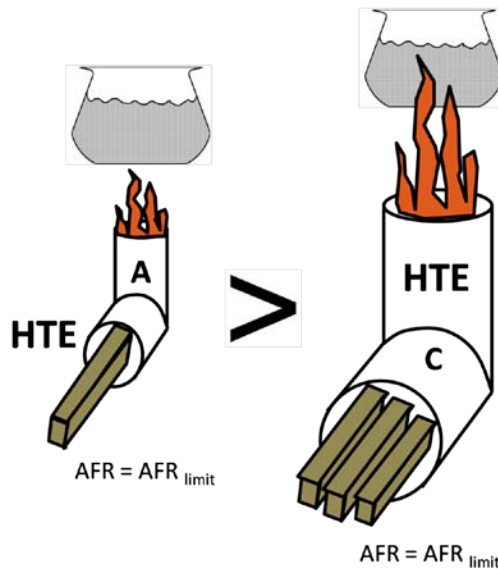


Figure 3.21. Schematic showing how HTE varies if firepower is increased proportionally with stove size.

4. Practical Applications to Improving Heat Transfer Efficiency of Cookstoves

4.1. Case Study #1 – Effect of Pot Gap Adjustment on Heat Transfer

This case study illustrates a relationship between pot gap, convection heat transfer, and stove thermal efficiency. As previously shown in Figure 3.10, pot gap refers to the distance between the bottom of the pot and the top surface of the stove. A theoretical approach shows that reducing pot gap from a nominal distance of 18mm reduces the associated nominal loss coefficient value and consequently reduces flow rate and increases gas temperature. The nominal $LC = 0.35$ is used as a reference point from which lower LC values are calculated for smaller pot gaps. Convection heat transfer effects are limited by a minimum LC value determined from a specified Excess Air Ratio (EAR). Convection heat transfer effects are used to determine the potential impact of pot gap adjustments on thermal efficiency. To validate the data, theoretical temperatures and associated theoretical LC values are compared to experimental temperatures that are related to LC values through EAR.

4.1.1. Fundamental Concepts and Underlying Theory

In order to fully understand how pot gap affects thermal efficiency, it is necessary to describe how the important variables that contribute to this relationship are derived. The loss coefficient (LC) has been previously defined to account for several pressure losses inherent to the flow through the stove and non-ideal heat addition. Experimental research conducted at the EECL suggests that $LC = 0.35$ for a stove with a pot gap = 18mm, and pot diameter = 8.75 inches (17). Starting with a nominal LC ($LC_{nominal}$), an equivalent LC can be calculated for smaller pot gap distances less than 18mm, due to the increase in pressure losses caused by a

narrower opening for the gases to pass through. As pressure losses from a smaller pot gap (ΔP_{loss}) increase, this magnitude relative to the induced chimney pressure ($\Delta P_{induced}$) defines an associated LC by equation 16.

$$LC = (LC_{nominal} + .012) \frac{\Delta P_{induced} - \Delta P_{loss}}{\Delta P_{induced}} \quad [16]$$

The LC provides a convenient dimensionless parameter to represent pot gap distance, thus the minimum possible pot gap distance is represented in terms of LC . Specific details associated with the derivation of various LC values are available in Appendices E and F, where calculations from *MathCAD* and *Microsoft Excel* are found. A brief explanation as to how each of these numerical analysis tools were used together is necessary to understand how different LC values are calculated.

Assuming firepower = 2.5kW, mass flow rate and temperature values are taken from Figure 3.15 and assumed to be fixed to calculate preliminary LC values. The flow rates and temperatures are input into the *MathCAD* worksheet (Appendix E) along with several pot gap distances and other parameters that are dependent on both temperature and flow. These calculations provide preliminary values for induced chimney pressure and pressure losses for each pot gap distance. These pressure calculations assume the flow through the pot gap is represented by a laminar, fully developed channel flow with dimensions analogous to the pot gap. Preliminary LC values are calculated in section A of Appendix F using equation 16 for each pot gap, without accounting for feedbacks from temperature and mass flow rate. These preliminary LC values are then provided along with the specified firepower (2.5kW) as inputs to code developed by Agenbroad to obtain more realistic temperatures and flow rates. The above procedure is then repeated (*MathCAD* worksheet combined with section B of *Excel* sheet), enabling a relationship between LC , pot gap, and pot gap coefficient (PGC) to be established, as presented in Figure 4.1.

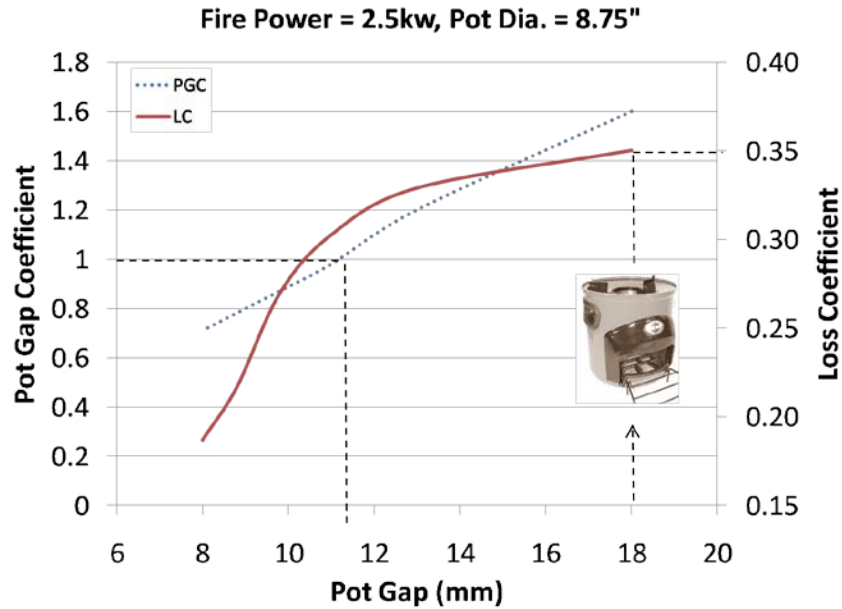


Figure 4.1. Loss coefficient and pot gap coefficient plotted against pot gap.

The PGC is defined as the cross sectional area of the pot gap opening divided by the cross sectional area of the chimney. Conventional wisdom suggests a value of $PGC = 1$ is optimal for most biomass stove applications, and one goal is to determine the validity of this guideline. This figure shows an image of Envirofit's G3300 stove with dotted lines indicating its pot gap distance and respective LC and PGC values. Also extractable from this plot is the pot gap distance and associated LC value that would satisfy a $PGC = 1$ for this particular stove. Now that a relationship between LC, PGC, and pot gap has been established, this information is used to illustrate how pot gap affects pertinent flow characteristics such as temperature and flow rate, as discussed in the next section and shown in Figure 4.2.

4.1.2. Effects on Flow Characteristics

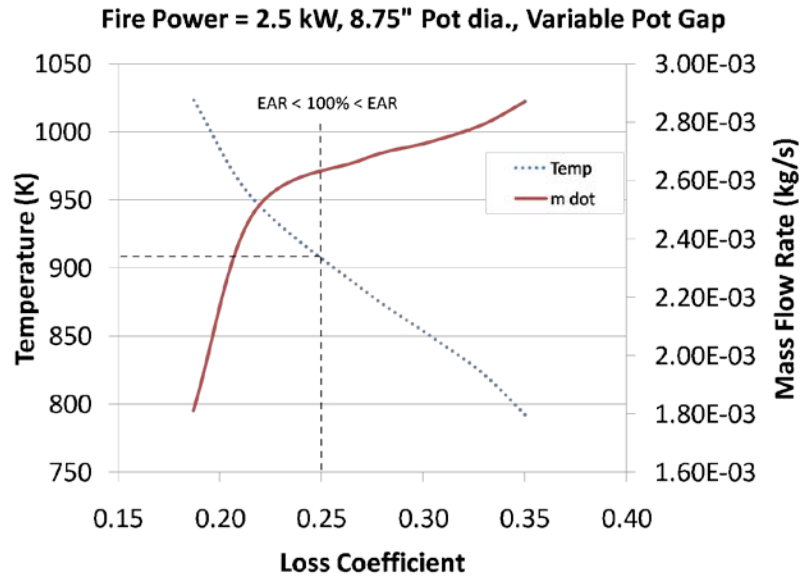


Figure 4.2. Temperature and mass flow rate vs. loss coefficient for specified firepower and pot gap.

Comparing Figure 4.2 against Figure 3.15 reveals an interesting similarity. Reducing LC (i.e. reducing pot gap) has the same relative effect on temperature and mass flow rate as increasing the firepower, except firepower in this case study is held constant at 2.5kW. It may be helpful to think of a LC reduction as an effective firepower increase. The sharp decline in mass flow rate around $LC \approx 0.22$ occurs for the same reason it experiences a sharp decline around 3.5kW in Figure 3.15: The AFR is too small which causes incomplete combustion of the fuel and reduced performance. The general relationship between temperature and mass flow rate in Figure 4.2 is also consistent with results presented in Figure 3.14.

When focusing on convection heat transfer, it is appropriate to examine how temperature is related to velocity instead of mass flow rate. As LC is initially reduced, both temperature and velocity increase. Both of these trends are expected to contribute to an increasing convective heat transfer, but their relative contributions are not equivalent or equally

consistent. This is evident by comparing the temperature results from Figure 4.2 with the velocity profile shown in Figure 4.3.

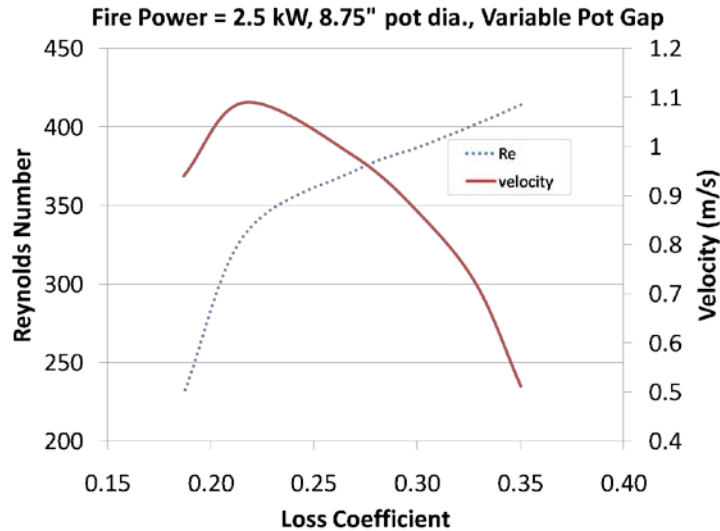


Figure 4.1. Reynolds number and Velocity plotted against loss coefficient.

Velocity rises steadily but then sharply falls around $LC \approx 0.22$ when mass flow rate reduction becomes significantly more pronounced. The initial rise in velocity as mass flow rate is in decline can be explained by reconsidering how velocity is defined by equation 13. The density reduction due to a temperature rise (ideal gas law) combined with the area reduction both initially outweigh the decline in mass flow rate. This is true until $LC \approx 0.22$ when mass flow rate begins its more significant decline, and causes velocity to reach an apex and eventually decrease. Reynolds number reduces in response to a decreasing LC meaning the flow is becoming more laminar, which means convection heat transfer should be reduced excluding any other variables. Opposing initial trends of velocity and Reynolds number are explained by reexamining the Reynolds number definition (equation 11). The effect of temperature rise on density and viscosity combine with geometry reductions to outweigh increasing velocities, thus leading to a reduction in Reynolds number. Competing flow characteristics such as this play a critical role in determining the effect of each parameter on convection heat transfer.

4.1.3. Impact on Heat Transfer Efficiency

As indicated in the *MathCAD* calculations, the flow through the pot gap is simplified using an internal channel flow assumption characterized by a pressure drop due to associated head losses (24). Nusselt number values are obtained based on tabulated values dependent on the geometric properties of the channel (25). The previous definition for convection coefficient (equation 14) is dependent on Nusselt number, gas thermal conductivity and hydraulic diameter of the channel. The magnitude that the convection coefficient and convection heat transfer to the pot bottom change with respect to LC is shown in Figure 4.4.

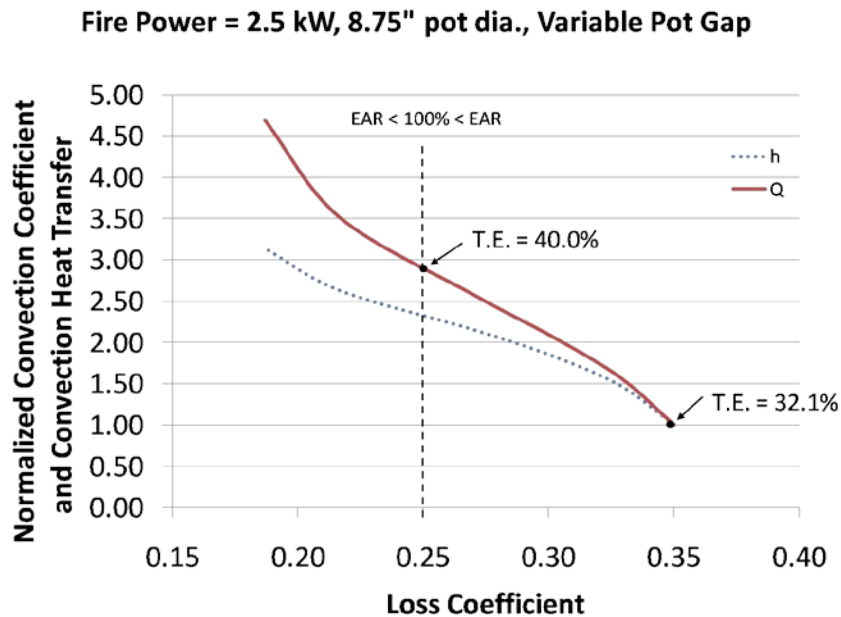


Figure 4.2. Normalized convection coefficient and convection heat transfer plotted against loss coefficient.

As LC decreases, both the convection coefficient (h) and convection heat transfer (Q) increase. These parameters are presented as normalized values, which means each calculated number “ h ” and “ Q ” for the respective LC value are divided by the nominal number at $LC = 0.35$. It is presented in this manner since the actual convection coefficient and consequent heat transfer for simplified channel flow is calculated differently than for impingement flow.

Therefore, normalized values provide a relative difference between values from reduced pot gaps to those from the nominal 18mm case.

The vertical dotted line in Figure 4.4 represents the location along the LC axis where $EAR = 100\%$ ($LC \approx 0.25$) and if $LC < 0.25$, then $EAR < 100\%$. When $EAR > 100\%$ the stove performs well, but when $EAR < 100\%$, stove performance begins to suffer noticeably. Theoretical calculations provided by Agenbroad suggest EAR reaches 100% when $LC \approx 0.25$ given a firepower of 2.5kW (17). This EAR constraint provides a lower limit to the LC which doesn't exactly coincide with the $LC \approx 0.22$ value mentioned previously. This could be because the previous LC limitation value ($LC \approx 0.22$) was dictated by the dramatic reduction in mass flow rate which may occur when $EAR < 100\%$.

Based on the limitations set by EAR , Figure 4.4 shows that the convection coefficient and convection heat transfer can potentially improve ~ 2.3 and ~ 2.8 times their nominal values if pot gap is reduced to approximately 9.2mm. This dimension translates to a pot gap coefficient ($PGC \approx 0.75$) which is less than the conventionally used boundary of $PGC = 1$. Returning back to the original energy balance calculations provided in Appendix C, if the convection heat transfer contribution to the bottom of the pot is multiplied by 2.8, it causes overall thermal efficiency to increase from 32.1% ($LC = 0.35$) to 40.0%.

As the $LC < 0.25$, EAR is less than the stove's practical operating limit, but an interesting phenomenon occurs as theoretical LC continues to decrease. Gas temperature in Figure 4.2 continues to increase while velocity in Figure 4.3 reaches a peak and then begins to decrease. Despite this decrease in velocity at this specific location, theoretical convection coefficient and convection heat transfer both continue to rise. This shows the dominance of temperature over velocity with respect to their influence on both convection coefficient and convection heat transfer. These results also present how much more influential temperature is on convection

than the Reynolds number. Reynolds number is decreasing but is still in the laminar regime ($Re < 1000$), so the temperature rise caused by a reduced pot gap causes both convection coefficient and convection heat transfer to also rise.

4.1.4. Experimental Validation

When burning biomass stoves, it is nearly impossible to reliably maintain a constant instantaneous firepower while changing other variables that strongly influence performance such as pot gap. Therefore an experimental validation of this study must be in the form of an indirect correlation between experimental and theoretical EAR, theoretical LC, and the relationship each of them have with temperature. Research conducted here at the EECL by Agenbrood experimentally measures how EAR and temperature are affected as the average firepower of the stove changes, while LC remains constant. Recall that by reducing pot gap, the effective firepower of the stove increases relative to the firepower of the stove at the nominal pot gap. Therefore the predicted rise in temperature based on a decreasing LC can be validated against the experimental relationship between temperature and EAR, as in Figure 4.5.

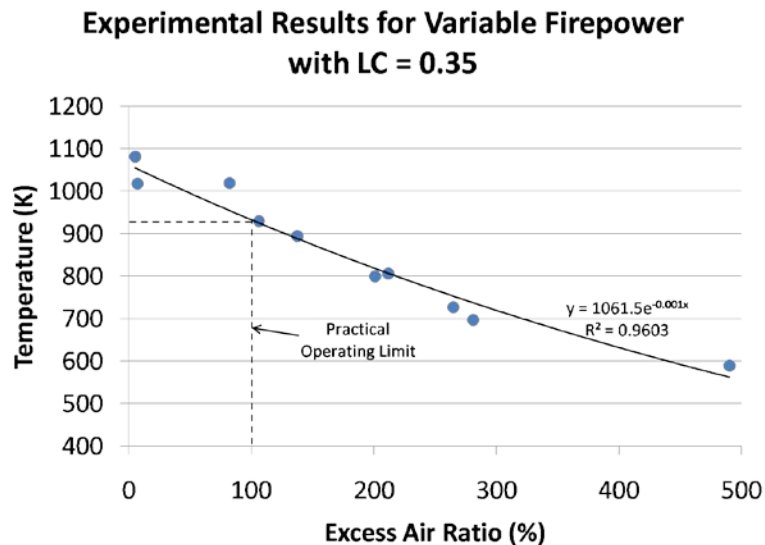


Figure 4.3. Excess Air Ratio (EAR) vs. Temperature [raw data used with permission from Agenbrood (17)].

Experimental temperature from Figure 4.5 at EAR = 100% is equal to $\sim 925\text{K}$. This measurement along with the observed trend of increasing temperature with decreasing EAR is compared against the theoretical trend of temperature in association with theoretical LC from Figure 4.2. Recalling that a theoretical EAR of 100% coincides with a LC = 0.25, theoretical temperature associated with this loss coefficient value in Figure 4.2 ($T \approx 910\text{K}$) is very close to the experimental value for temperature ($T \approx 925\text{K}$) indicated by Figure 4.5 for EAR = 100%. Analyzing EAR in this fashion provides a link between theoretical and experimental data which enables one to confidently predict the relationship between pot gap, temperature and heat transfer.

4.2. Case Study #2 – Hot Gas Path Geometry and Flow Characteristics

This case study considers the lessons learned from the previous case study, and applies them to practical stove design configurations such as a pot skirt and a double-pot accessory. The objective of both the pot skirt and double pot attachment is the same: increase surface area exposure of the pot(s) while at the same time modifying characteristic flow parameters such as velocity and temperature to enhance heat transfer efficiency. Figure 4.6 provides examples of each of these design configurations relative to their placement upon a standard cookstove.



Figure 4.4. Pot skirt (left) and double pot attachment (right) shown as integrated accessories to a standard biomass cookstove.

4.2.1. Pot Skirt

4.2.1.1. Theory and Practice

As hot combustion gases exit the pot gap area, natural buoyancy effects cause them to travel upwards along the sides of the pot. Despite this fact, the gases do not have much guidance and therefore tend to lose much of their thermal energy to the ambient environment. If a pot skirt is placed around this pot gap exit area, it forces the gases to follow closer to the side surface of the pot, exposing it to higher gas temperatures. This relocation of existing hot gases closer to the pot is accompanied by an actual rise in gas exit temperature due to a decreased loss coefficient from the added flow restriction of the pot skirt. This rise in gas temperature combined with the constricted flow area causes a rise in flow velocity, despite a decreasing mass flow rate. This rise in flow velocity seems like it should cause a rise in convection coefficient through its influence on the Nusselt number, but the effect of rising gas thermal conductivity (through temperature) has a far greater impact on convection coefficient.

Nonetheless, placing a pot skirt around the side of a pot leads to heat transfer efficiency gains due to increased temperatures, a higher convection coefficient and more exposed surface area of the pot. The effects that a pot skirt has on these flow characteristics do not hold true for all pot skirt configurations, as they are limited by the impact that the pot skirt has on EAR and the ensuing stove combustion efficiency. Striking the right balance between improving flow characteristics and maintaining an appropriate combustion environment is the focus of the next section.

4.2.1.2. Optimizations

An optimization of certain pot skirt parameters is possible by adopting the same theoretical calculation strategy as is implemented for the pot gap study. A firepower of 2.5kW is assumed with a LC = 0.35 along with the appropriate mass flow rate, temperature and ensuing

variables. Pot gap is fixed at 18mm and instead of reducing the pot gap to observe a rise in pressure loss as before, either the pot skirt gap (t) is reduced or the skirt height (h) is increased. As before with pot gap, flow through the pot skirt is represented as a simplified channel flow. Minor losses due to the 90 degree bend at the pot perimeter are ignored since this is a path already taken without the pot skirt, and it is assumed to be accounted for by $LC = 0.35$.

Calculations using *MathCAD* shown in Appendix G provide a way to determine the additional heat flux into the pot sides relative to the bottom due to the presence of a pot skirt of varying gaps and heights. A correction factor is determined to account for the discrepancy between experimental relative improvements (in terms of thermal efficiency) from using a pot skirt (26.3% improvement) versus the theoretical value derived in the preliminary energy balance calculations in Appendix C. This correction factor is used to better estimate the heat flux into the bottom of the pot alone, based on variable temperatures and flow rates for different loss coefficients created by the pot skirt restriction.

Theoretical calculations in *MathCAD* (Appendix G) are paired with *Excel* (Appendix H) to iterate through various pot skirt/height combinations while monitoring the effect each has on convection efficiency. Convection efficiency ($\eta_{convection}$) as defined by equation 17 is used as a metric to measure pot skirt effects in order to isolate radiative effects from the model. Two plots are created from the *Excel* data in Appendix H and are shown in Figures 4.7 and 4.8.

$$\frac{Q_{bottom} + Q_{pot\ skirt}}{Q_{firepower}} * 100 = \eta_{convection} \quad [17]$$

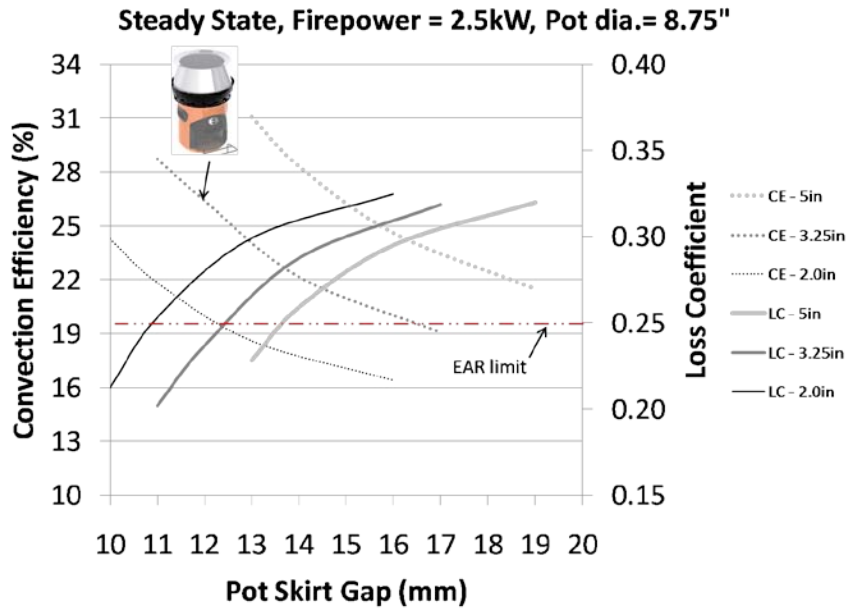


Figure 4.5. Convection efficiency and loss coefficient versus pot skirt gap for various skirt heights.

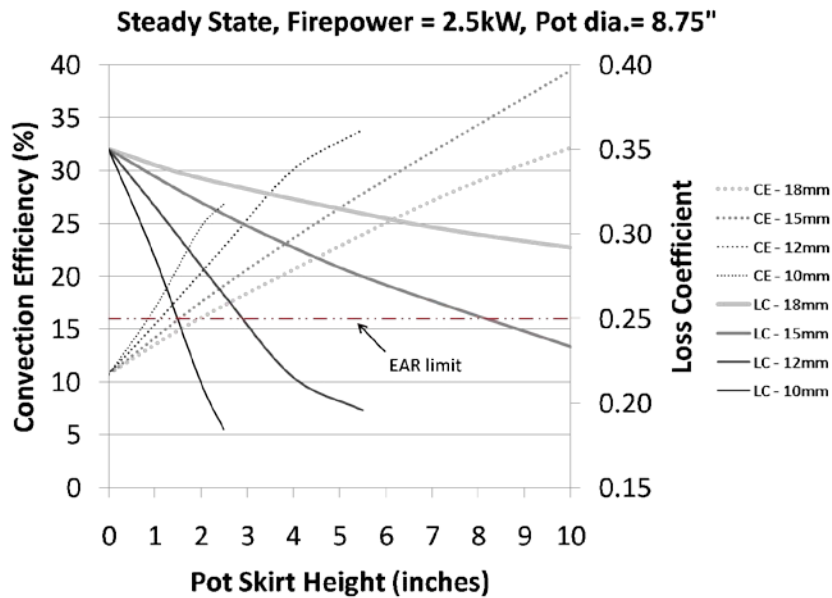


Figure 4.6. Convection efficiency and loss coefficient versus pot skirt height for various skirt gaps.

Each of the plots in the above figures assumes firepower = 2.5kW which has a minimum associated LC = 0.25 based on a minimum EAR = 100%. As indicated earlier, minimum LC is a function of firepower, so these exact plots are only applicable to this specific firepower. Figure 4.7 provides a curve based on skirt height from a commercially available pot skirt on the market

sold by *Envirofit* that I helped design. The optimal pot gap from Figure 4.7 for the *Envirofit* pot skirt may not be directly applicable to this data due to its adjustable nature and non-uniform pot gap along its height. Slight non-linearities present in the curves from Figure 4.8 are due to decreasing gas temperature with increasing skirt height as heat is transferred into the pot.

Optimal pot gap for any configuration is determined by following the horizontal “EAR limit” line across to where it intersects the “LC” curve and then following a straight line up to where it would intersect the respective “CE” curve. This intersection point not only provides the optimal pot skirt height or gap for a given gap or height, it also indicates an expected improvement in convection heat transfer efficiency. For example, from Figure 4.8 if a pot skirt gap is assumed to be 12mm, then this corresponds to an optimal pot skirt height equal to ~3 inches. Convection efficiency for this configuration jumps to a value of approximately 25% from a nominal value of 11%. This improvement is larger than experimental measurements that exhibit a convection efficiency improvement from 16.1% without a skirt to 20.0% with the adjustable skirt. These convection efficiency improvements correspond to thermal efficiencies of 29.3% and 37%, respectively. Disparities between theoretical and experimental data could be due to the inherent firepower variability of an experimental test which would influence the effectiveness of the pot skirt, the theoretical assumption to neglect any transient energy absorption of the pot skirt during operation, and the non-uniform pot skirt gap for the experimental test.

4.2.2. Double-pot attachment

When the overall stove geometry changes to accommodate a second pot and chimney, the flow dynamics and stove performance are altered to the point where a new energy balance on the system must be performed. The method used for the double-pot energy balance is similar to what is used for the single-pot version. The first step is to determine an appropriate

mass flow rate and temperature. For the single-pot stove configuration, these values were obtained using experimental and theoretical data from previous research done by Agenbrood here at the EECL. He did not follow similar procedures for a double pot configuration, so temperatures and flow rates must be obtained through theoretical means. This is accomplished by starting with flow parameters for $LC = 0.5$ and adjusting them based on a calculated theoretical LC value associated with double-pot flow path geometry. This procedure is identical to the one carried out to adjust for temperatures and mass flow rates in the pot gap study, except here the LC is influenced by pressure losses and gains from a double-pot attachment and chimney. The new LC value accounts for both 90 degree bends in the flow starting from the stove, connects them with fully developed laminar channel flow beneath the pots, and includes both pressure losses and gains from a six foot chimney at the exit. The newly calculated temperature and mass flow rate are used to represent more realistic values from which a more accurate energy balance can be derived. Detailed calculations including both the loss coefficient derivation and energy balance assessment are provided in Appendix J.

The energy balance assessment is simplified by assuming radiation contributions are of equal % to the total firepower input as the single-pot stove energy balance. Firepower changes from 3.5kW in the single-pot stove to 5kW in the double-pot, so the magnitude of radiation in the double pot increases proportionally to this ratio. Also, the amount of heat transferred through the bottom of the stove via conduction is assumed to be of equal magnitude as the single-pot stove. Convection contributions throughout the gas path account for a continually reducing gas temperature as heat is drawn away into the body of the stove and into the pots. Contribution percentages of radiation, conduction, and convection are presented in Figure 4.9 along with other pertinent contributions.

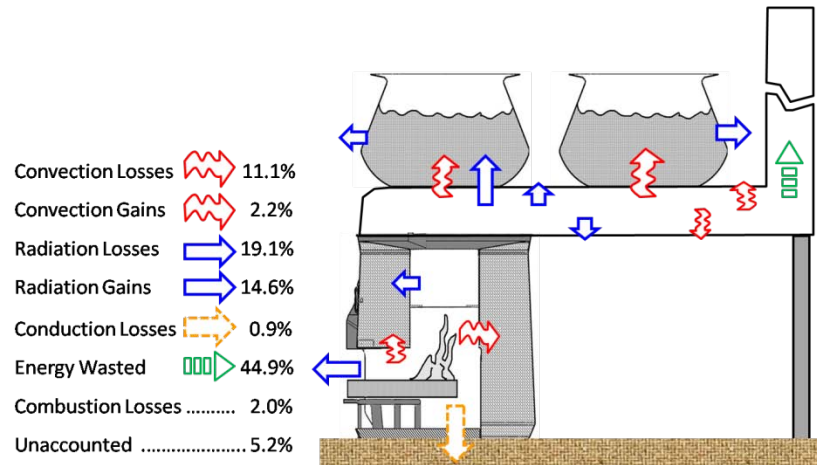


Figure 4.7. Summary of energy balance for double-pot stove attachment.

Comparing these values to ones from the single-pot energy balance reveals a lower thermal efficiency, increased proportion of wasted energy, an increase in convection losses to the body and a decrease in convection gains to the pot. The double-pot attachment used for this assessment is *Envirofit's* G3355 that offers two separate 5 ¼ inch diameter openings on the top of the channel for pot placement. If these openings are enlarged to match the diameter of each pot (8.75 inches), then the convection gain contribution jumps from 2.2% as indicated in the figure to 6.0%. This translates to overall thermal efficiency improving from 16.8% to 20.7%. This reiterates the importance of increasing surface area to improve heat transfer efficiency. Experimental thermal efficiency values for the G3355 with the 5 ¼ inch holes range from 18.9% to 21.7%, which are closely approximated by the theoretical numbers.

If the pots are sunken into the horizontal flow path, it further increases surface area then but causes the LC to decrease due to increased pressure loss. Increasing induced pressure by lengthening chimney height could overcome this pressure loss, but the exact height increase would depend on the degree to which each pot is sunken into the horizontal flow path. Heat transfer effects from these modifications are unknown since performing such a study would

involve an integrated effort between modeling firepower, loss coefficient, excess air, temperature, mass flow rate and heat transfer efficiency all together.

4.3. Case Study #3 – Extended Surface Heat Transfer Experimentation

The first case study illustrated the importance of flow characteristics in influencing heat transfer. The second one took it a step further to investigate how both improving flow characteristics and increasing surface area can be combined to improve heat transfer. The focus of this case study is to keep flow characteristics the same, but increase the surface area of the pot exposed to the hot gases through the utilization of extended surfaces, or fins. These fins are attached to the bottom of a pot so as to capture heat from the flow and direct it to the water. This is achieved using two different approaches, both of which combine principles of conduction and convection to improve heat transfer.

4.3.1. First Approach – Heat Exchanger Plate

4.3.1.1. Design Objective and Development Strategy

The objective of this approach is to offer a heat plate stove accessory to people in the developing world that reduces time to boil (TTB), improves thermal efficiency (TE), and is a low-cost alternative to a finned pot. Attaching fins to a pot improves the convection heat transfer by increasing surface area, but finned pots tend to be very costly which prohibits many people from purchasing one, especially if they already have a (unfinned) pot of their own. If a heat plate accessory is sold as a separate unit to be used with any pot that somebody already owns, then this is an effective way to improve heat transfer efficiency (HTE) and reduce TTB. After collaborating with some experienced professionals, including Dr. Steven Schaeffer, and performing some temperature tests, I learned that a sand casting of ductile iron would be the lowest cost method of manufacturing such a plate at high volumes. Dr. Schaeffer is a mechanical engineering professor at CSU, is the director of the university's Manufacturing

Instructional Laboratory, and offers extensive knowledge in the realm of general manufacturing practices. Some preliminary calculations showed that such a plate would actually worsen TTB and HTE but a die or investment casting may offer more favorable results. Therefore, despite higher costs associated with more complex manufacturing, the heat plate which is investigated here both in theory and in practice replicates one which could potentially be manufactured at high volume using either a die or investment casting method.

4.3.1.2. Fundamental Physics

Three physical principles govern the performance of the heat plate: contact resistance, thermal capacitance, and surface area. Contact resistance between the bottom surface of the pot and the top surface of the plate that it rests on reduces the magnitude of heat that is conducted between them. The thermal capacitance of the plate itself causes it to absorb heat from the fire during start-up phases of the stove instead of transferring it to the pot. Competing against these two principles is increasing surface area, which causes a rise in heat transfer. The magnitude that each of these principles influence heat transfer relative to each other is what decides whether a heat plate will result in an improvement or a detriment. This quandary is represented schematically in Figure 4.10.

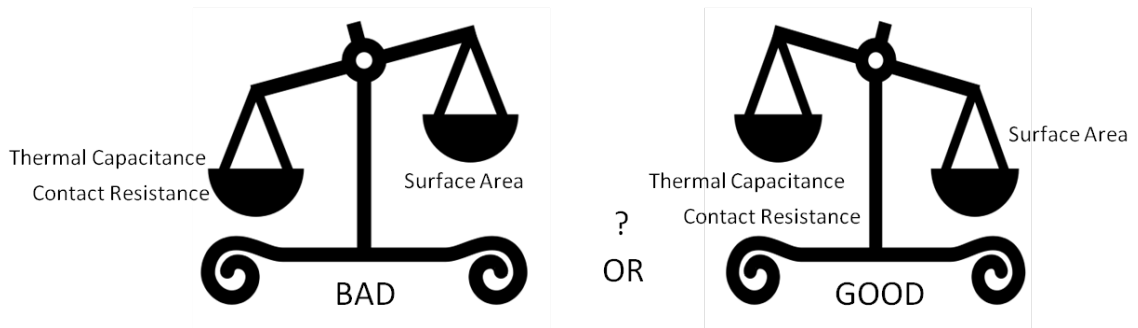


Figure 4.8. Competing relationships between thermal capacitance, contact resistance, and surface area in relation to heat transfer.

4.3.1.2.1. Contact Resistance

Thermal contact resistance exists between two surfaces because the apparent contact area is much larger than the actual contact area shared between them, as illustrated in Figure 4.11.

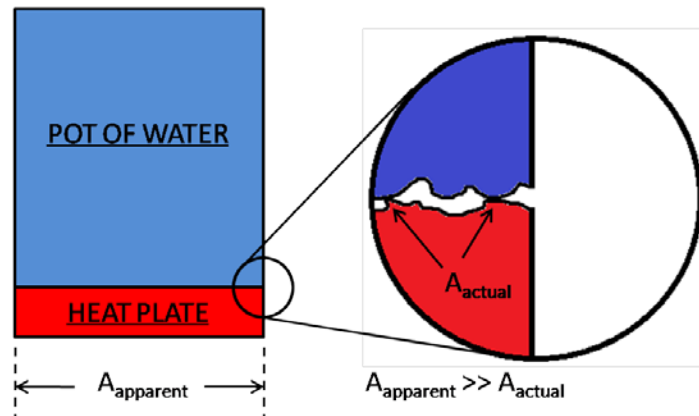


Figure 4.9. An Illustrative schematic representing contact resistance.

Voids that exist between the peaks of contact area act as microscopic layers of insulation as they are filled with air. Though these voids are small, they greatly affect the thermal conductivity between the two surfaces since the thermal conductivity of metal (i.e. steel) is more than 1000 times greater than air. Five factors determine the overall thermal contact resistance between two surfaces: thermal conductivity, surface roughness, contact pressure, microhardness and surface cleanliness. If either of the two surfaces is rough, then more voids will exist between them and contact resistance increases. If the microhardness of either of the materials is low, then the voids can be compressed so long as the contact pressure is high enough to do so, thus reducing contact resistance. These effects are more noticeable if the thermal conductivities of each material are high. Of course if a surface is dirty, then it forms an insulative layer between the contact areas, in addition to the insulative air occupying the voids. In the arena of biomass cookstoves, contact resistances have the potential to be very

high considering used pots are likely to have high surface roughness, low contact pressure (~1.2 kPa), and very dirty surfaces.

Little to no literature exists that provides empirical contact resistance values in the range applicable to the interface between a pot of water and heat plate. The most relevant data available to approximate contact resistance at such low contact pressures originates from a numerical model that suggests a range between 0.011 – 0.347 m²*K/W (26). This translates to a resistance contribution equivalent to 30-93% of the total thermal resistance of the plate/pot assembly. This large range of potential values compounded by the many assumptions built into a numerical model provides an incentive to experimentally measure the contact resistance specific to a 5L pot of water and heat plate. More details in regard to this experiment are provided in Section 4.3.1.4.

4.3.1.2.2. Thermal Capacitance

Thermal capacitance is directly proportional to the amount of internal energy absorbed by an object while it undergoes a temperature change. More literally, it is equal to the mass of a particular object multiplied by its specific heat. The magnitude of these two physical properties multiplied together represents the ability of a certain object to resist a change in temperature. Low thermal capacitance is a desirable trait for a heat plate since it will take less time absorbing thermal energy from the fire and spend more time conducting energy to the pot. This is most important for improving TTB for a cold start test when the plate must undergo a large temperature change. Since this particular heat plate design must be made from steel, the specific heat cannot be modified since it is an inherent material property. This leaves mass as the only plate characteristic that can be reduced to improve heat plate performance. Reducing mass to lower thermal capacitance must be balanced by the added mass of the fins to increase

surface area. Therefore the most optimally designed heat plate will provide fins with the maximum possible surface area-to-mass ratio.

4.3.1.2.3. Surface Area

In order to maximize the surface area-to-mass ratio, the side profile of the fin must be very thin, thereby allowing a larger quantity of fins to be placed on one surface such as the bottom surface of a pot or heat plate. Besides increasing the quantity of fins, surface area of the fin array can be improved by increasing either the length (L) or the width (w) of each individual fin, as presented in Figure 4.12.

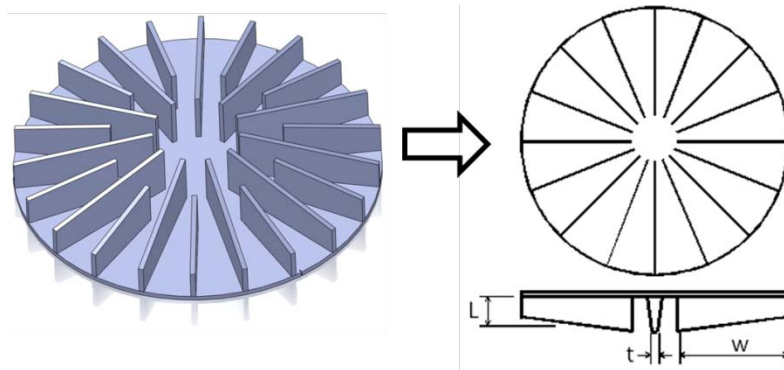


Figure 4.10. 3D image of potential heat plate design (left) with top and side views (right).

For steady state operation, the width dimension should theoretically be elongated as much as possible until the temperature of the gas equals the temperature of the fin. This point has not been reached with this design configuration; therefore the width dimension is constrained by the outer diameter of the plate (determined by pot diameter) and the circular gap in the center (based on manufacturing guidelines for a casting). The length dimension of the fin reaches an optimal value once the added benefit from increased surface area is dominated by the increased conductive resistance due to an elongated conduction path. Based on the definition of conductive resistance (equation 18), fins with smaller thickness (lower cross-sectional area, A) have a smaller optimal design length than thicker fins (larger A).

$$R_{conductive} = \frac{L}{kA} \quad [18]$$

Once again, the length dimension of the heat plate is constrained by the interface with the stove in order to preserve the same pot gap as when an ordinary pot is used. This upper limit for fin length could be reduced if a different manufacturing method is used to provide thinner fin wall thickness. More is discussed in relation to this trade-off in the next section.

4.3.1.3. Theoretical Model

Theoretical calculations are used to predict the influence of a heat plate on TTB based on inputs including plate and pot diameter, plate material, fin profile geometry and fin quantity. Details of these calculations are provided in Appendix K. This model is used as a tool to predict how changing each of these variables can either lengthen or shorten the time to boil. Convection coefficient is assumed not to change with the introduction of additional fins, and it is theoretically calculated the same way as in Sections 3.4 and 3.5 and as shown in Appendix A. This theoretical convection coefficient value is validated against a semi-empirical convection coefficient, with details provided in Appendix B and summarized as follows.

Total internal energy absorbed by the pot of water during an experimental water boil test is calculated and divided by the time required complete the test. This provides the total rate of heat transferred into the pot of water, accounting for both convection and radiation. In order to isolate convective heat transfer from this value, estimated radiation contributions from the energy balance (Appendix C) are subtracted from it, resulting in energy contributions from convection only. Convection coefficient is calculated from here assuming the pot/gas interface is represented using a thermal circuit with plane wall conduction. Values from both the theoretical and semi-empirical calculations are in close proximity to each other (8.5-9.6 W/m²*K) which inspires confidence in the accuracy of ensuing calculations.

Validation of this theoretical model is necessary before proceeding with fabrication of a heat plate prototype. According to data found in literature, an optimal fin length can be calculated simply by knowing the fin thickness, material, and convection coefficient (27). The theoretical value for optimal fin length for a steel fin of thickness = 0.055" based on literature is compared against my theoretical data through a TTB correlation, as presented in Figure 4.13.

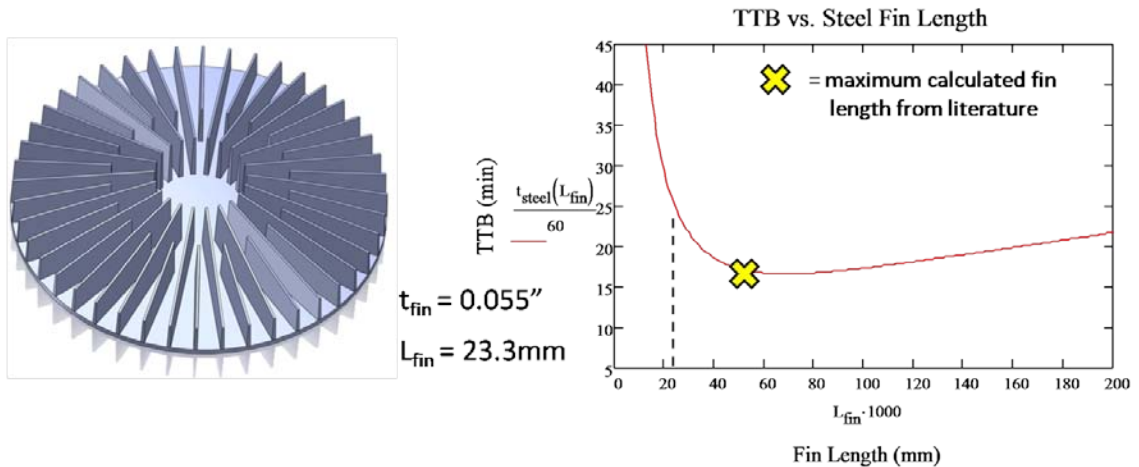


Figure 4.11. Comparison of optimal theoretical fin length value with literature findings.

The curve plotted in Figure 4.13 is based on data from theoretical TTB calculations using an experimentally derived contact resistance value, which is described in Section 4.3.1.4. The “X” marked on the line indicates the location along the x-axis (54mm) for an optimal length fin from literature. The lowest point on the curve indicates the theoretical optimal fin length since this is the location where TTB is at a minimum. Note how closely the literature-based value coincides with this low point on the plot. Based on this assessment, TTB for various heat plate design configurations can be confidently predicted before they are fabricated. This provides a very useful tool to evaluate how changing certain design parameters such as plate material, wall thickness, contact resistance etc. can influence performance, as shown in Figure 4.14. This plot shows the times to boil corresponding from the range of contact resistance values obtained from literature (26).

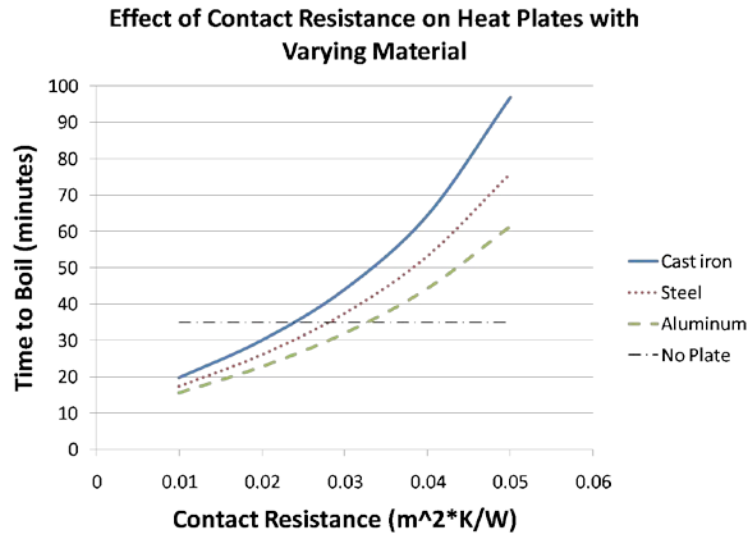


Figure 4.12. Effect of plate material and contact resistance on TTB using heat plate.

Knowing this information, the decision is made to develop a test to experimentally determine the expected contact resistance between a typical pot and a heat plate. Since contact resistance is the biggest unknown with the greatest potential to have an impact on TTB, a more reliable experimental value is critical in determining if it is prudent to move forward with fabricating a heat plate prototype.

4.3.1.4. Contact Resistance Experimentation

Equipment used for this experiment include an adjustable electric range as a constant and reliable heat source, a variac controller to adjust the amperage being supplied to the burner, a *Fluke* current meter/multi-meter to monitor the amperage, a custom-fabricated experimental test bucket outfitted with several thermocouples and designed to replicate a heat plate, and two different pots (2.5L India-style and 5.0L stainless) used to hold the water when placed inside of the bucket. A collection of images for each of the equipment listed above is shown in Figure 4.15.

Quantifying Contact Resistance – Experimental Setup:



Figure 4.13. Collection of images from contact resistance experiment.

The first segment of the test involves filling either of the two pots with water and placing it inside of the test bucket while the bucket sits on the electric range. The range is powered on while *Labview* software records instantaneous temperature measurements for each of the surface-mounted thermocouples on the bucket. A similar procedure is carried out for the second segment of the test, except the same amount of water is placed directly inside of the bucket to eliminate all contact resistance. Only the first test segment with the pot inside of the bucket is required to measure thermal contact resistance, but this realization was made after both tests were already completed for each pot configuration. Temperature profiles corresponding to each thermocouple location are shown in Figure 4.16 along with a schematic showing the location of each thermocouple on the bucket.

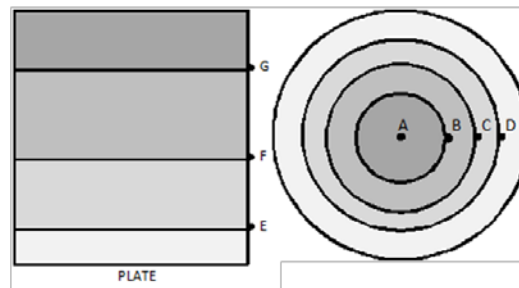
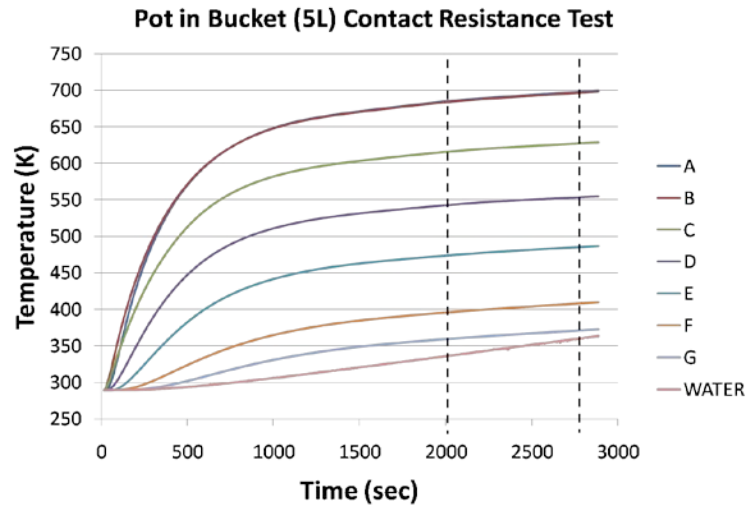


Figure 4.14. Temperature profiles of each thermocouple location with illustrative schematic showing the relevant locations on bucket.

These temperature profiles are examined at the time interval indicated by the dotted lines and used to calculate the internal energies absorbed by the system (i.e. water, bucket, pot). The internal energy absorbed by the system during this time interval can be used to solve for contact resistance by representing the pot/bucket interface with a thermal resistive circuit based on known material and geometrical properties of the assembly. Specific details related to the calculation of contact resistance are provided in Appendix L. Test results yielded contact resistance values from 0.0123 to 0.0185 $m^2 \cdot K/W$ for the 2.5L and 5L pots respectively. Plugging these contact resistance values back into theoretical TTB calculations indicates that if a heat plate were fabricated according to sand casting specifications, then it would only offer a TTB \approx 52 minutes; however, if it is fabricated to replicate a die casting (thinner walls) then the

presence of a larger quantity of thinner fins would reduce TTB \approx 26 minutes. This TTB is close to the nominal TTB for a pot placed on a stove without any heat plate, which means the plate could potentially be an improvement considering the slight inaccuracies built in to the theoretical model. This potential for improvement warrants the fabrication of a prototype heat plate to be tested against theoretical predictions.

4.3.1.5. Testing

After several weeks in the lab attempting a variety of different methods to fabricate a prototype heat plate that would accurately represent a die casting, a functional working model was finally created and is pictured below in Figure 4.17.

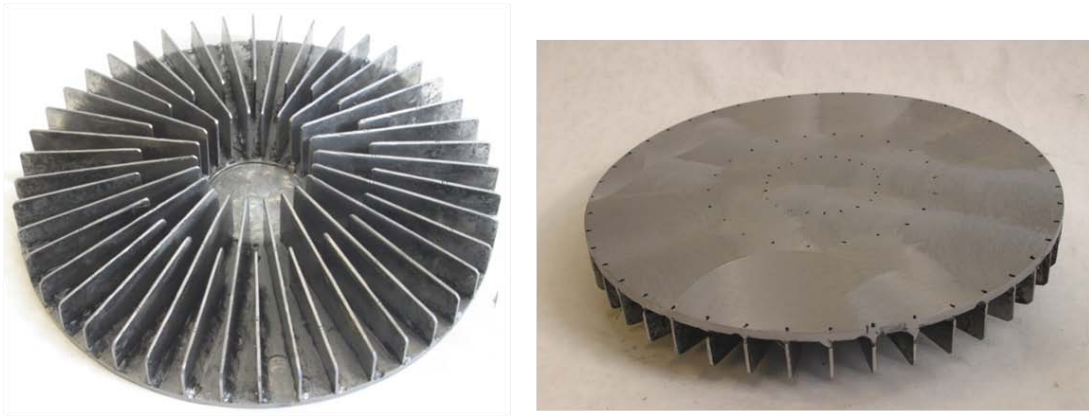


Figure 4.15. Heat plate die cast replicate prototype.

The performance of this heat plate is tested according to the same water boil test (WBT) procedure outlined and established from previous research here at the EECL (28). The plate is placed fin-side-down on top of the stove where the pot would normally sit, and then a pot is placed on top of the plate, as shown in the two photos in Figure 4.18. The stove is then burned as per normal protocol and performance metrics are quantified.



Figure 4.16. Images of the heat plate placed on top of the cookstove before and during testing.

This design configuration multiplies the exposed surface area to the combustion gases by 5x and interfaces nicely with both the pot and stove. Unfortunately for the cold start test, the increased surface area does not provide enough of a boost in convection heat transfer to significantly overcome the losses associated with the thermal capacitance and contact resistance. In fact these contributions nearly cancel each other out since average TTB hardly changes compared to the nominal case of the same stove being burned using an ordinary pot. A summary of these results is presented in Table 4.1.

Table 4.1. Summary of results for WBT with heat plate.

Test	Tester	Date	Thermal Efficiency	Simmer Fuel (g)	Shell Benchmark Data			
					Fuel (g)	CO (g)	TTB (min)	PM (mg)
1	Dan	4/13/2010	26.6	219.6	572.0	25.0	32.2	-
2	Sean	4/13/2010	27.8	205.6	554.7	25.7	26.9	-
3	Melanie	4/14/2010	28.7	269.2	655.2	27.7	24.0	-
Average	-	-	27.7	231.5	594.0	26.1	27.7	-
G3300 Cert.	Melanie	-	29.0	337.0	669.3	16.0	27.5	1221.5

Smoke being emitted from the stove is significantly more prominent using the heat plate, especially during the beginning of each phase. This is most likely attributed to the quenching of gases and/or flames as they impinge upon the relatively cool fin surface directly

above the combustion zone. The qualitative observation of increased smokiness is manifest in the higher CO production evident from Table 4.1. If thermal capacitance of the overall plate assembly is reduced, the duration of smoke and CO production would be lessened and performance improved. The benefit of using such a heat plate is highlighted during the simmer phase when fuel usage plummets to use 20-39% less fuel than the nominal case. This is a real advantage, but trade-offs in terms of cost, lack of TTB improvement, and higher pollutant formation make the heat plate a difficult purchase for consumers in developing countries.

Even still, the fact that both thermal capacitance and contact resistance were capable of being nearly overcome by surface area improvements is significant. This indicates how influential extended surface heat transfer is in terms of biomass cookstove performance. In light of these observations, it is logical to proceed further down this path by testing a purpose-built, extended surface pot that is commercially available and capable of being modified to accommodate our test protocol.

4.3.2. Second Approach – Commercially Available Finned Pot

A handful of improved cooking pots exist on the market today, all of which offer significant convective heat transfer improvements, but are prohibitively expensive (\$60) from the perspective of a consumer in the developing world. Additionally, the largest size typically available (~3L) is too small to accommodate the daily cooking requirements of families in the developing world. Indeed, if one of these “heat exchanger pots” were to be made large enough to accommodate the cooking requirements of the average consumer, costs would certainly be even higher.

All considerations aside, from an engineering perspective a heat exchanger pot offers enormous potential to improve stove performance since contact resistance is eliminated from the equation. Eliminating contact resistance directly improves heat transfer independent of any

other design changes; however an indirect benefit stems from the lower fin surface temperature exposed to the combustion gases. Lower surface temperatures mean materials with lower melting temperatures and higher thermal conductivities such as aluminum can be used. Such is the case for *Jetboil*, a company offering improved backpacking cookstoves to outdoor enthusiasts here in the United States and abroad. The 3L capacity heat exchanger pot tested and pictured in Figure 4.19 was generously donated by *Jetboil* and modified with higher sides to accommodate 5L of water.






Figure 4.17. Unmodified *Jetboil* heat exchanger pot.

4.3.2.1. Testing

The same standard WBT protocol is followed using the finned pot from *Jetboil* as is used in any other WBT, except only a cold start (CS) phase is performed. This strategy is used in an effort to focus on both the benefits and drawbacks associated with the use of a finned pot. Reductions in TTB are expected along with improvements in heat transfer efficiency and a simultaneous increase in pollutant formation in the form of CO due to the transient nature of a CS test with more exposed surface area. CS test results from using this pot are compared against CS tests using a flat-bottom pot on the same stove, as presented in Table 4.2.

Table 4.2. Cold Start test results comparing a finned pot against a conventional flat-bottomed pot

	Cold Start	Wood Usage (kg)	CO emission (g)	Time to Boil (min)	Emission Factor (gCO/kg wood)	Thermal Efficiency (%)	Combustion Efficiency (%)
Flat-bottom Pot	Test #1	0.3411	8.0	36.0	23.5	27.8	98.0
	Test #2	0.3299	8.0	36.0	24.2	29.8	98.0
	Test #3	0.3215	6.5	33.0	20.2	30.1	98.4
	Averages	0.3355	8.0	36.0	23.9	28.8	98.0
Finned Pot	Test #1 (Sean)	0.2243	7.4	18.5	33.0	42	N/A
	Test #2 (Sean)	0.2374	7.8	18.3	32.9	41.1	N/A
	Test #3 (Mel)	0.2196	4.2	20.0	19.1	46.3	N/A
	Averages	0.2271	6.5	18.9	28.3	43.1	N/A

Note how a different person performed tests #1 and #2 (Sean) for the finned pot than test #3 (Melanie). Sean and Melanie each have a different burning style – Sean burns the stove at a higher fuel feed rate than Melanie. Hence, Sean’s tests have a lower TTb but also show a higher emission factor and lower thermal efficiency. Melanie performed each of the three tests using the flat-bottom pot, resulting in significantly lower thermal efficiencies, significantly higher TTb, and approximately equivalent emission factor as compared against the finned pot. Presenting results from two different users certainly introduces an extra variable into the comparison matrix; however, the benefits associated with using a finned pot are obvious and are not accompanied by any consistent trends showing a compromise in pollutant formation and estimated combustion efficiency. More tests are necessary to secure more repeatable trends between thermal efficiency and combustion efficiency, but the results presented here illustrate the potential for massive thermal efficiency gains.

4.3.3. Summary – Extended Surface Heat Transfer

Increasing the surface area of the pot exposed to the hot combustion gases clearly improves thermal efficiency and reduces TTb. Simultaneous increases in pollutant formation, and therefore combustion efficiency losses, are more noticeable for the heat plate than for the finned pot. This is likely due to the greater thermal capacitance of the heat plate combined with

its larger exposed surface area which more readily quenches the combustion gases. The heat plate offers neutral performance gains in TTB and thermal efficiency in regard to a CS test, but the large thermal capacitance proves to benefit the simmer performance. Despite this improvement from using a heat plate, the cost associated with such a stove accessory would not be low enough to warrant the investment from the consumer.

The finned pot offers the most promising performance enhancements, especially if more testing proves that combustion efficiency can be held relatively constant while experiencing such drastic thermal efficiency gains. Again, the Achilles' heel in attempting to sell to a market in the developing world is the cost. Perhaps some testing could be conducted using a finned pot placed over a three stone fire? Can improved pots be sold close to the same price as an improved stove while accomplishing close to the same performance improvements? These are questions worth considering before completely eliminating finned pots as an option to consumers in developing countries.

4.4. Case Study #4 – Radiation Heat Transfer: Diffusion vs. Premixed Flames

As is evident from the single-pot and double-pot energy balance calculations, radiation can account for anywhere between 45.5% and 87% of the total thermal energy addition to the pot(s), respectively. Most of this radiation originates from highly radiant flames instead of the charcoal bed since the flames are located closer to the pot, resulting in a more favorable view factor for heat transfer. Highly luminous and colorful diffusion flames exist due to numerous tiny soot particles which glow and give off significant radiative energy. This translates to elevated emissivity values compared against cleaner burning, lower luminosity premixed flames. This relationship has significant implications related to the effective heat transfer coefficient (includes effect of radiation on convection coefficient) of a cookstove depending on the type of flame created by the fire. Research from literature suggests that the effective heat transfer

coefficient can be 2.3 – 3.4 times greater for a reacting radiant flow than for an isothermal non-reacting flow (22).

4.4.1. Experimental Set-up and Results

The goal is to try to create a scenario in which the heat transfer from a clean, premixed flame with low emissivity is compared against the heat transfer from a dirty, highly luminous and emissive diffusion flame. A controlled experiment is set up using a Bunsen burner, pot support, propane tank and the inner combustion chamber from a G3300 cookstove. A premixed flame is created by allowing for the appropriate amount of air to be entrained into the Bunsen burner at the fuel orifice. A simulated diffusion flame is created by closing off the air supply to the Bunsen burner, resulting in a highly luminous flame. Thermal efficiency related to each of these flame configurations are measured for two different pot heights and equivalent chamber heights, as shown in Figure 4.20. Results are presented in Table 4.3.



Figure 4.18. Pot configuration for tests #1 and #2.

Table 4.3. Flame radiation test results.



	Test #	Separation Distance (in)	Water Used (L)	Fuel Used (g)	TTB (min)	Thermal Efficiency (%)
Diffusion Flame	1	3.25	5	71	46	46.5
	2	11.5	3	90.5	33.1	22.6
Pre-mixed Flame	1	3.25	5	66.5	42.2	50.2
	2	11.5	3	91.5	33.2	22.2

Results do not turn out as expected. Expectations were to see higher thermal efficiencies from the diffusion flame due to its higher emissivity, but this does not turn out to be the case. In fact for test #1, the premixed flame has a higher thermal efficiency than the diffusion flame. Results from test #1 can possibly be explained due to interactions between the flame and pot as they are positioned relatively close together. The length of the premixed flame is short compared to the diffusion flame; however, this difference in flame length makes very little difference in terms of heat flux between the two flames. Flame temperature plays a much more influential role in determining thermal efficiencies for test #1 since the flame-to-pot distance is nearly the same for each flame type. The premixed flame temperature is higher than the diffusion flame due to more complete combustion, which means it will be providing a greater amount of heat flux to the pot. The larger temperature of the premixed flame outweighs the greater emissivity of the diffusion flame to yield a slightly higher thermal efficiency.

In an effort to eliminate these effects, the pot is raised in test #2 so the radiative benefits of the diffusion flame are mostly maintained but the gas temperature from the premixed flame is reduced due to more entrainment of cooler ambient air, and the loss of heat to the walls of the chamber. In this scenario the flame length influences heat flux more

significantly since the pot is positioned further away from the burner than in test #1. The premixed flame temperature is still higher than the diffusion flame temperature in test #2, but this effect is not as influential on thermal efficiency since the gas temperature is drastically reduced by the time it makes it to the pot. The resulting thermal efficiency values for test #2 are almost identical for each flame type. These results are closer to the original expectations, but do not produce conclusive evidence to suggest which flame type offers a higher thermal efficiency. It is clear that data from literature cannot be verified by using such a simple setup as this. Perhaps more testing will reveal more interesting trends from which additional lessons can be learned.

5. Conclusions and Future Work

Approaching heat transfer efficiency of biomass cookstoves from a perspective rooted in the fundamental physics of its operation has proven to be useful in understanding why certain design strategies are more successful than others. The heat transfer mode that offers the most potential for efficiency gains is convection. This is achievable by either increasing surface area of the pot exposed to hot combustion gases or by modifying the characteristic flow parameters of mass flow rate and temperature. Temperature has a significantly larger impact on heat transfer than mass flow rate, both through its direct effect on temperature difference and also through the indirect effect it has on convection coefficient.

When considering potential design improvement strategies for cookstoves, many of them are dependent upon the firepower which is inherently variable and continually fluctuating depending on user inputs. This makes it difficult to optimize a universal solution to improve heat transfer at an affordable price. This is especially true for methods of heat transfer improvement that modify the gas temperature and flow rate of the stove such as pot gap, pot skirt, and the double-pot attachment. The effect of different flame types (i.e. premixed vs. diffusion) on radiation heat transfer is not fully understood, although it is shown that the separation distance between the flame and the pot has more of an influence on thermal efficiency than flame type. More work in this area is needed to secure a more thorough understanding of the variety of trade-offs that exist. A Finned pot holds the most promise in offering heat transfer enhancements to biomass cookstoves since the benefits from increased

surface area are independent of firepower constraints. The major drawbacks of this option are the increased production costs of such a product.

Future work is possible that could further improve the understanding of biomass cookstove operation. One relationship that would be helpful in producing better predictive models for heat transfer is one that ties together minimum loss coefficient and firepower at a fixed excess air ratio (i.e. 100%). Such a curve is predicted to look something similar to one shown in Figure 5.1.

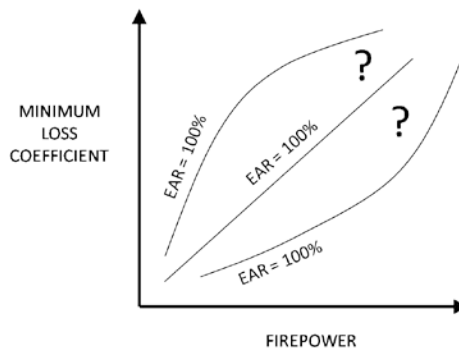


Figure 5.1. Predicted relationship between minimum loss coefficient and firepower for a fixed excess air ratio.

Another relationship that would be helpful in addressing heat transfer concerns is one relating the firepower/loss coefficient ratio to temperature and mass flow rate for a select few EAR values, as suggested by Figure 5.2.

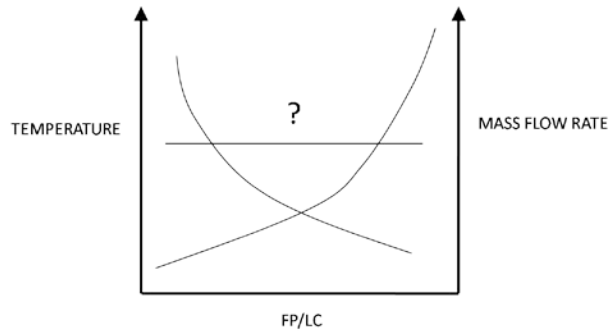


Figure 5.2. Unknown predicted relationship between firepower/loss coefficient, temperature and mass flow rate.

Works Cited

1. *Indoor Air Pollution in Developing Countries: a major environmental and public health challenge*. **Bruce, Nigel**. 2000, Bulletin of the World Health Organization, pp. 1078-1092.
2. World Health Organization. [Online] [Cited: May 4, 2010.] <http://www.who.int/indoorair/en/>.
3. *Indoor Air Pollution and Its Impact on Children Under 5 Years Old in Bangladesh*. **Khalequzzaman, M.** 2007, Indoor Air, pp. 468-474.
4. *Indoor Smoke Exposures from Traditional and Improved Cookstoves Caparissons Among Rural Nepali Women*. **Reid, H.** 1986, Mountain Research and Development, pp. 293-304.
5. *Health, Energy, and Greenhouse-Gas Impacts of Biomass Combustion in Household Stoves*. **Smith, K.** 1994, Energy for Sustainable Development, pp. 23-29.
6. World Resources Institute - Climate Analysis Indicators Tool. [Online] [Cited: May 4, 2010.] <http://cait.wri.org/figures/World-FlowChart.pdf>.
7. *Research Needs for Improving Biofuel Burning Cookstove Technologies*. **Ahuja, D.** 1990, Natural Resources Forum, pp. 125-134.
8. **Solomon, S., et al.** *IPCC, 2007: Summary for Policymakers. In: Climate Change 2007: The Physical Science Basis. Contribution of Working Group 1 to the Fourth Assessment Report of the Intergovernmental Panel on Climate Change*. Cambridge, United Kingdom and New York, NY, USA : Cambridge University Press, 2007.
9. **Parry, M.L., et al.** *IPCC, 2007: Summary for Policymakers. In: Climate Change 2007: Impacts, Adaptation and Vulnerability. Contribution of working Group 2 to the Fourth Assessment Report of the Intergovernmental Panel on Climate Change*. Cambridge, UK : Cambridge University Press, 2007. 7-22.
10. **V., Ramanathan.** *Role of Black Carbon on Global and Regional Climate Change*. Washington, DC : Testimonial to the House Committee on Oversight and Government Reform, 2007. Testimonial.
11. *Radiative Forcing From Household Fuel Burning in Asia*. **Aunan K., Berntsen T., Myhre G., Rypdal K., Streets D., Woo J., Smith K.** 2009, Atmospheric Environment, pp. 5674-5681.

12. **Bryden, Mark.** Aprovecho Research Center - Advanced Studies in Appropriate Technology. [Online] [Cited: May 6, 2010.] <http://bioenergylists.org/stovesdoc/PCia/Design Principles for Wood Burning Cookstoves.pdf>.
13. *Comparison of Five Rural, Wood-Burning Cooking Devices: Efficiencies and Emissions.* **Ballard-Tremeer, G.** 1996, Biomass and Bioenergy, pp. 419-430.
14. **MacCarty, Nordica.** Aprovecho Research Center - Advanced Studies in Appropriate Technology. [Online] January 2007. [Cited: May 6, 2010.] http://www.aprovecho.org/web-content/publications/assets/India CCT Paper_1.7.08.pdf.
15. *What Makes People Cook with Improved Biomass Stoves?* **Barnes, D.** s.l. : World Bank Technical Paper, 1994. WTP 242.
16. *Models to Predict Emissions of Health-damaging Pollutants and Global Warming Contributions of Residential Fuel/stove Combinations in China.* **Edwards, Rufus D., et al.** Berkeley, CA 94720-7360 : Pergamon, 2003, Chemosphere, Vol. 50, pp. 201-215.
17. **Agenbroad, Joshua Nicholas.** Thesis - A Simplified Model for Understanding Natural Convection Driven Biomass Cooking Stoves. Fort Collins, CO : Colorado State University, 2010.
18. *Calculation of the Emissivity of Luminous Flames.* **Felske, J. D. and Tien, C. L.** Berkeley, California : Gordon and Breach, Science Publishers Ltd., 1973, Combustion Science and Technology, Vol. 7, pp. 25-31.
19. *Modelling and Measurements of Heat Transfer in Charcoal from Pyrolysis of Large Wood Particles.* **Larfeldt, Jenny, Leckner, Bo and Melaen, Morten Chr.** Goteborg, Sweden : Pergamon, 2000, Biomass and Bioenergy, Vol. 18.
20. *Combustion of Wood Charcoal.* **Evans, D.D. and Emmons, H.W.** Cambridge, MA : Elsevier Sequoia S.A., Lausanne, 1977, Vol. 1.
21. *The Engineering Tool Box.* [Online] [Cited: May 10, 2010.] http://www.engineeringtoolbox.com/emissivity-coefficients-d_447.html.
22. *Heat Transfer to Impinging Isothermal Gas and Flame Jets.* **Viskanta, R.** s.l. : Elsevier Science Publishing Co., Inc., 1993, Experimental Thermal and Fluid Science, Vol. 6.
23. *A study of free jet impingement. Part 2. Free jet turbulent structure and impingement heat transfer.* **Donaldson, Coleman Dup.** Great Britain : s.n., 1971, Fluid Mechanics, Vol. 45, pp. 477-512.
24. **White, Frank M.** *Fluid Mechanics - Sixth Edition.* New York, NY : McGraw-Hill, 2008. 978-0-07-293844-9.

25. **Incropera, Frank P. and DeWitt, David P.** *Introduction to Heat Transfer*. s.l. : John Wiley & Sons, 2002. 0-471-38649-9.

26. *Thermal Contact Resistance at Low Contact Pressure: Effect of Elastic Deformation*. **Bahrami, Majid, Yovanovich, Michael M. and Culham, Richard J.** s.l. : Elsevier Ltd., 2005, Vol. 48, pp. 3284-3293.

27. *A Critical Review of Extended Surface Heat Transfer*. **Razelos, Panagiotis.** 6, New York : Taylor & Francis Inc., 2003, Vol. 24. 0145-7632.

28. **L'Orange, Christian Colin Per.** Thesis - Testing Methodologies for Biomass Cook Stoves and Their Effects on Emissions. Fort Collins, CO : Colorado State University, 2009.

APPENDIX

Appendix A – Theoretical Convection Coefficient using MathCAD

$$\dot{m}_{\text{dotStove}} := 2.87 \cdot 10^{-3} \frac{\text{kg}}{\text{s}}$$

overall mass flowrate through the stove (input from Josh's calculations, assuming 3.5 kW fire power, LC = 0.35), adapted to a slightly larger value for G3300 geometry instead of 4" elbow.

$$T_{\text{gas}} := 792\text{K}$$

estimated flue gas temperature (input from Josh's calculations, assuming 3.5 kW fire power, LC = 0.35)

$$T_{\text{pot}} := 326\text{K}$$

average pot surface temperature

$$R_{\text{universal}} := 8.3143 \frac{\text{J}}{\text{K} \cdot \text{mol}}$$

universal gas constant

$$m_{\text{air}} := 28.97 \frac{\text{gm}}{\text{mol}}$$

molecular mass of air

$$P_{\text{atm}} := 101325\text{Pa}$$

atmospheric pressure

$$d_{\text{stack}} := 100\text{mm}$$

diameter of combustion chamber stack

$$R_{\text{air}} := \frac{R_{\text{universal}}}{m_{\text{air}}}$$

$$R_{\text{air}} = 286.997 \frac{\text{J}}{\text{K} \cdot \text{kg}}$$

specific gas constant of combusting gases. (assuming combusting gases primarily consist of air).

$$\rho_{\text{gas}} := \frac{P_{\text{atm}}}{R_{\text{air}} \cdot T_{\text{gas}}}$$

$$\rho_{\text{gas}} = 0.446 \frac{\text{kg}}{\text{m}^3}$$

estimated density of flue gases

$$A_{\text{stack}} := \frac{\pi \cdot d_{\text{stack}}^2}{4}$$

$$A_{\text{stack}} = 7.854 \times 10^{-3} \text{m}^2$$

cross-sectional area of stack

$$v_{\text{gas_stack}} := \frac{\dot{m}_{\text{dotStove}}}{\rho_{\text{gas}} \cdot A_{\text{stack}}}$$

estimated flue gas velocity flowing through stack.

$$v_{\text{gas_stack}} = 0.82 \frac{\text{m}}{\text{s}}$$

$$\frac{P_1}{\rho} + \frac{1}{2} \cdot v_1^2 + gz_1 = \frac{P_2}{\rho} + \frac{1}{2} \cdot v_2^2 + gz_2$$

Bernoulli's equation - basic form

$$P_{\text{gauge}} = P_1 - P_2 = \rho \cdot \frac{1}{2} \cdot (v_2^2 - v_1^2)$$

where $v_1 = 0$

Bernoulli's equation - reduced to fit boundary conditions at stove inlet

$$P_{\text{gauge}} := \rho_{\text{gas}} \cdot \frac{1}{2} \cdot v_{\text{gas_stack}}^2 \quad \text{Gauge pressure at stove inlet}$$

$$P_{\text{gauge}} = 0.15 \text{ Pa} \quad \text{This calculation is only applicable to CFD simulations}$$

$$\mu_{\text{O}} := 1.71 \cdot 10^{-5} \frac{\text{kg}}{\text{m}\cdot\text{s}} \quad \text{Nominal absolute viscosity of air at 1 atm} \quad T_{\text{O}} := 273\text{K}$$

$$\mu_{\text{gas}} := \mu_{\text{O}} \cdot \left(\frac{T_{\text{gas}}}{T_{\text{O}}} \right)^{0.7} \quad \mu_{\text{gas}} = 3.604 \times 10^{-5} \frac{\text{kg}}{\text{m}\cdot\text{s}} \quad \text{Curve fit power law approximation from Fluid Mechanics Text, App. A, p.816 (White, Frank).}$$

$$\text{Re}_{\text{stack}} := \frac{\rho_{\text{gas}} \cdot v_{\text{gas_stack}} \cdot d_{\text{stack}}}{\mu_{\text{gas}}} \quad \text{Reynolds number approximation for fully developed internal flow through a circular pipe.}$$

$$\text{Re}_{\text{stack}} = 1.014 \times 10^3 \quad \begin{array}{l} 100 < \text{Re} < 10^3 \text{ laminar flow} \\ 10^3 < \text{Re} < 10^4 \text{ transition to turbulence} \\ 10^4 < \text{Re} \text{ turbulent flow} \end{array}$$

Assume the space created by pot gap behaves like two parallel plates:

$$d_{\text{pot}} := 228\text{mm} = 8.976\text{in} \quad \text{diameter of pot}$$

$$A_{\text{pot_bottom}} := \frac{d_{\text{pot}}^2 \cdot \pi}{4} = 0.041 \text{ m}^2$$

$$h_{\text{potgap}} := 17.8\text{mm} \quad \text{height of air gap between pot and drip pan (i.e. pot gap)}$$

$$A_{\text{potgap}} := \pi \cdot d_{\text{pot}} \cdot h_{\text{potgap}} \quad A_{\text{potgap}} = 0.013 \text{ m}^2 \quad \text{Total cross-sectional area of pot gap space.}$$

$$v_{\text{gas_potgap}} := \frac{\dot{m}_{\text{dotStove}}}{\rho_{\text{gas}} \cdot A_{\text{potgap}}} \quad \text{estimated gas velocity flowing through pot gap area}$$

$$v_{\text{gas_potgap}} = 0.505 \frac{\text{m}}{\text{s}}$$

$$D_{\text{h}} := 2 \cdot h_{\text{potgap}} \quad D_{\text{h}} = 0.036 \text{ m} \quad \text{Hydraulic diameter definition for flow between two parallel plates}$$

$$Re_{\text{potgap}} := \frac{\rho_{\text{gas}} \cdot v_{\text{gas_potgap}} \cdot D_h}{\mu_{\text{gas}}}$$

$$Re_{\text{potgap}} = 222.35$$

Therefore, the theoretical flow through the pot gap area is less turbulent than through the stack.

$$c_{p_gas} := 1.087 \cdot 10^3 \frac{\text{J}}{\text{kg} \cdot \text{K}}$$

Specific heat of air (based on average gas temperature = 750K)

$$k_{\text{gas}} := 5.7 \cdot 10^{-2} \frac{\text{W}}{\text{m} \cdot \text{K}}$$

Thermal conductivity of air (dependent on gas temperature = 879K)

$$Pr := \frac{\mu_{\text{gas}} \cdot c_{p_gas}}{k_{\text{gas}}}$$

Pr = 0.687 Prandtl Number (ratio of thermal dissipation:conduction)

$$Re_{\text{average}} := Re_{\text{stack}}$$

Assume the average Re Number is at least equal to the value through the stack

$$Nu := .565 \cdot Pr^{.5} \cdot Re_{\text{average}}^{.5} = 14.915$$

Stagnation Point Nusselt Number

Area-averaged Nusselt number correlation from Donaldson, C., assuming a fully developed free jet impinging on a flat surface. (Also referenced by Viskanta, R.)

$$h_{\text{conv}} := \frac{Nu \cdot k_{\text{gas}}}{d_{\text{stack}}} = 8.502 \cdot \frac{\text{W}}{\text{m}^2 \cdot \text{K}}$$

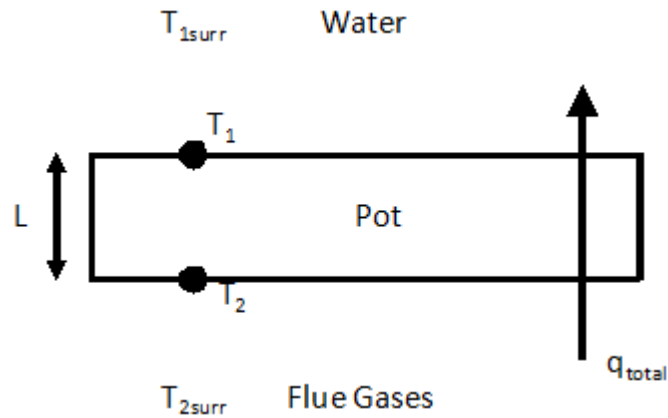
Theoretical convection coefficient for isothermal, non-combusting impinging flow upon pot bottom.

Accounting for combustion and therefore flame radiation can increase the magnitude of the convection heat transfer coefficient anywhere from 2.3x to 3.4x (Viskanta, R.). This is a more realistic representation of the "impinging flame jet" flow exhibited by the stove.

$$h_{\text{conv_lowflame}} := h_{\text{conv}} \cdot 2.3 = 19.553 \cdot \frac{\text{W}}{\text{m}^2 \cdot \text{K}}$$

$$h_{\text{conv_highflame}} := h_{\text{conv}} \cdot 3.4 = 28.905 \cdot \frac{\text{W}}{\text{m}^2 \cdot \text{K}}$$

Appendix B – Semi-empirical Convection Coefficient using MathCAD



$m_i := 5.002\text{kg}$ mass of water at beginning of test

$m_f := 4.968\text{kg}$ mass of water at end of test

$T_f := 363\text{K}$ Final water temp at end of test

$T_i := 288\text{K}$ Initial water temp at beginning of test

$h_{fg} := 2.283 \cdot 10^6 \frac{\text{J}}{\text{kg}}$ Enthalpy of evaporation of water at 363K

$C_p := 4180 \frac{\text{J}}{\text{kg} \cdot \text{K}}$ Specific heat of water at constant pressure

$t := 25\text{min}$ average time required to boil 5L of water

$$U := m_f \cdot C_p \cdot (T_f - T_i) + (m_i - m_f) \cdot h_{fg}$$

$U = 1.646 \times 10^6 \text{ J}$ Total Internal Energy required to bring 5L of water to a boil.

$Q_{\text{total}} := \frac{U}{t} = 1.097 \times 10^3 \text{ W}$ Total rate of Heat Transfer from stove to a 5L pot of water.

Radiation Heat Transfer Contribution

$\%_{\text{rad}} := 0.45$ fraction of total heat transfer to stove attributed to radiation gains from calculations entitled, "Appendix C - Single-pot Stove Energy Balance".

$$Q_{\text{rad_pot}} := Q_{\text{total}} \cdot \%_{\text{rad}} = 493.725 \text{ W}$$

Estimation of Convection Heat Transfer

$$Q_{\text{conv_pot}} := Q_{\text{total}} - Q_{\text{rad_pot}}$$

$Q_{\text{conv_pot}} = 603.441 \text{ W}$	Total rate of convection heat transfer to pot
--	---

Estimating Total Thermal Resistance of Pot of Water on Top of Stove

$d_{\text{pot}} := 8.75 \text{ in}$ Pot diameter

$h_{\text{side}} := 5 \text{ in}$ estimated vertical distance from pot bottom where hot gases flow

$A_{\text{side_pot}} := \pi \cdot d_{\text{pot}} \cdot h_{\text{side}}$ $A_{\text{side_pot}} = 0.089 \text{ m}^2$ Area along side of pot where hot gases flow

$A_{\text{bottom_pot}} := \frac{\pi \cdot d_{\text{pot}}^2}{4}$ $A_{\text{bottom_pot}} = 0.039 \text{ m}^2$ Area of pot bottom

$A_{\text{total_pot}} := A_{\text{side_pot}} + A_{\text{bottom_pot}}$ $A_{\text{total_pot}} = 0.127 \text{ m}^2$ Total exposed area of pot

$T_{2\text{surr}} := 819 \text{ K}$ Surrounding flue gas temperature inside stove

$T_{1\text{surr}} := \frac{T_f + T_i}{2} = 325.5 \text{ K}$ Surrounding water temperature inside pot

$q_{\text{conv_pot}} = \frac{T_{2\text{surr}} - T_{1\text{surr}}}{R_{\text{total}}}$ Definition of Heat Transfer in terms of overall temperature difference and convective and conductive thermal resistances.

$R_{\text{total}} := \frac{(T_{2\text{surr}} - T_{1\text{surr}}) \cdot A_{\text{bottom_pot}}}{Q_{\text{conv_pot}}}$ $R_{\text{total}} = 0.032 \text{ m}^2 \cdot \frac{\text{K}}{\text{W}}$

Using Total Thermal Resistance to find convection coefficient

$$R_{\text{conv}} = \frac{1}{h \cdot A_{\text{bottom_pot}}} \quad \text{Thermal resistance due to convection of hot gases}$$

$$R_{\text{cond}} = \frac{L}{k \cdot A_{\text{bottom_pot}}} \quad \text{Thermal resistance due to conduction through pot bottom}$$

$$R_{\text{total}} = R_{\text{conv}} + R_{\text{cond}} \quad \text{Total thermal resistance defined in terms of convective resistance and conductive resistance.}$$

$$k_{\text{pot}} := 16 \frac{\text{W}}{\text{m} \cdot \text{K}} \quad \text{Thermal conductivity of pot material, stainless steel}$$

$$L_{\text{pot}} := .011 \text{in} \quad \text{thickness of pot}$$

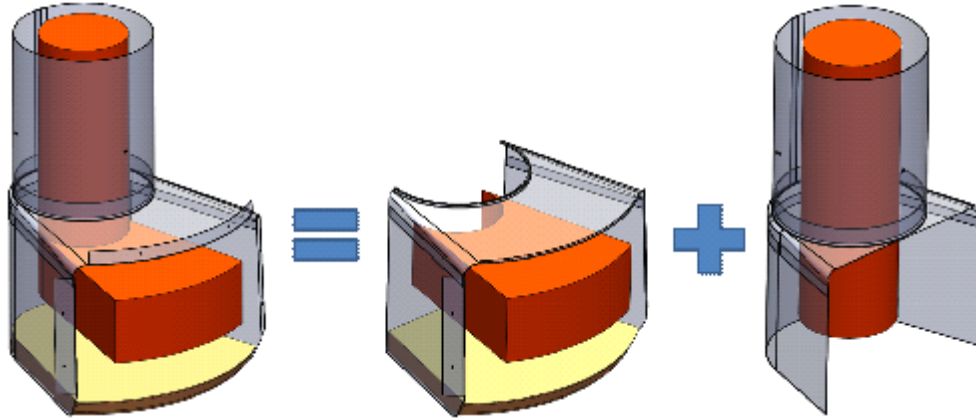
$$R_{\text{cond}} := \frac{L_{\text{pot}} \cdot A_{\text{bottom_pot}}}{k_{\text{pot}} \cdot A_{\text{bottom_pot}}} \quad R_{\text{cond}} = 1.746 \times 10^{-5} \text{m}^2 \cdot \frac{\text{K}}{\text{W}}$$

$$R_{\text{conv}} := R_{\text{total}} - R_{\text{cond}} \quad R_{\text{conv}} = 0.032 \text{m}^2 \cdot \frac{\text{K}}{\text{W}}$$

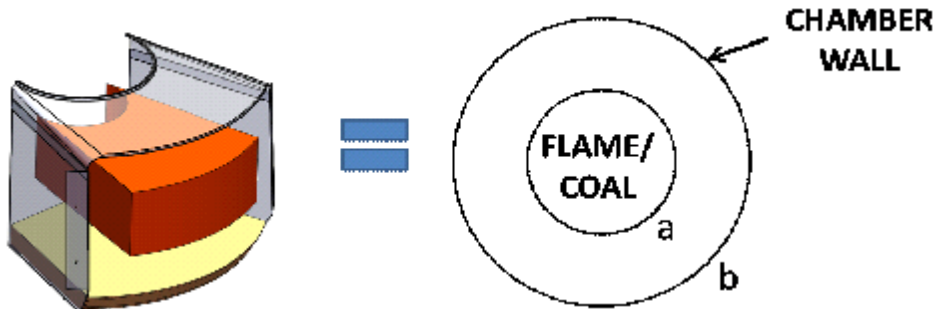
$$h := \frac{1 \cdot A_{\text{bottom_pot}}}{R_{\text{conv}} \cdot A_{\text{total_pot}}} = 9.598 \cdot \frac{\text{W}}{\text{m}^2 \cdot \text{K}} \quad \text{Semi-empirical convection heat transfer coefficient.}$$

Appendix C – Single-pot Stove Energy Balance using MathCAD

1. Radiation



1.1. Radiation From Flames/coal Bed to Lower Combustion Chamber



Lower chamber portion is represented by a simplified diffuse, gray, two surface enclosure consisting of two (infinitely) long concentric cylinders.

$L_{low} := 105\text{mm}$ Estimated length of cylindrical enclosure

$P_{low_a} := 276\text{mm}$ Estimated effective perimeter of inner cylinder

$r_{low_a} := \frac{P_{low_a}}{2 \cdot \pi} = 0.044\text{ m}$ effective radius of inner cylinder

$P_{low_b} := 484\text{mm}$ Effective perimeter of outer cylinder

$r_{low_b} := \frac{P_{low_b}}{2 \cdot \pi} = 0.077\text{ m}$ effective radius of outer cylinder

$$A_{\text{low}_a} := p_{\text{low}_a} \cdot L_{\text{low}} = 0.029 \text{ m}^2 \quad \text{Surface area of inner cylinder}$$

$$T_{\text{charcoal}} := 1127 \text{ K} \quad \text{Temperature of charcoal bed}$$

$$T_{\text{flame}} := 819 \text{ K} \quad \text{Temperature of flames in between bottom of pot and drip pan}$$

$$T_{\text{low}_a} := 0.6 \cdot T_{\text{charcoal}} + 0.4 \cdot T_{\text{flame}} = 1.004 \times 10^3 \text{ K} \quad \text{Average steady state surface temperature of flames and coal}$$

$$T_{\text{low}_b} := 870 \text{ K} \quad \text{Average steady state surface temperature of chamber walls}$$

$$\epsilon_{\text{charcoal}} := 0.83 \quad \text{Estimated emissivity value of burning charcoal surface from literature}$$

$$\epsilon_{\text{flame}} := 0.72 \quad \text{Estimated emissivity value of diffusion flame from literature}$$

$$\epsilon_{\text{low}_a} := 0.7 \epsilon_{\text{charcoal}} + 0.3 \epsilon_{\text{flame}} = 0.797 \quad \text{Mean emissivity value between flames and burning charcoal surface}$$

$$\epsilon_{\text{clay}} := 0.75 \quad \text{emissivity of fire clay brick base plate}$$

$$\epsilon_{\text{fecral}} := 0.26 \quad \text{emissivity of metal chamber}$$

$$A_{\text{clay}} := 16538 \text{ mm}^2 \quad \text{Area of base plate tile exposed to radiation}$$

$$A_{\text{fecral}} := 37830 \text{ mm}^2 \quad \text{Area of metal chamber exposed to radiation}$$

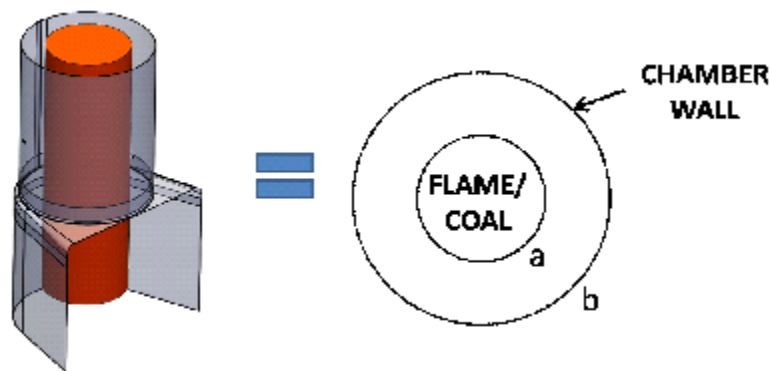
$$\epsilon_{\text{low}_b} := \frac{\epsilon_{\text{clay}} \cdot A_{\text{clay}} + \epsilon_{\text{fecral}} \cdot A_{\text{fecral}}}{A_{\text{clay}} + A_{\text{fecral}}} = 0.409 \quad \text{area weighted average emissivity of outer surfaces (i.e. metal and clay)}$$

$$\sigma_{\text{stefan}} := 5.67 \cdot 10^{-8} \frac{\text{W}}{\text{m}^2 \cdot \text{K}^4} \quad \text{Stefan-Boltzmann constant}$$

$$Q_{\text{rad_low_ab}} := \frac{\sigma_{\text{stefan}} \cdot A_{\text{low}_a} \cdot (T_{\text{low}_a}^4 - T_{\text{low}_b}^4)}{\frac{1}{\epsilon_{\text{low}_a}} + \frac{1 - \epsilon_{\text{low}_b}}{\epsilon_{\text{low}_b}} \cdot \left(\frac{r_{\text{low}_a}}{r_{\text{low}_b}} \right)} = 349.727 \text{ W}$$

Steady state radiative loss to walls of lower combustion chamber (Eq 13.25)*

1.2. Radiation From Flames to Upper Combustion Chamber



Upper chamber portion is represented by a simplified diffuse, gray, two surface enclosure consisting of two (infinitely) long concentric cylinders.

$L_{up} := 167\text{mm}$ Estimated length of cylindrical enclosure

$r_{up_a} := 32\text{mm}$ Estimated effective radius of inner cylinder

$P_{up_a} := 2 \cdot \pi \cdot r_{up_a}$ Perimeter of inner cylinder

$r_{up_b} := 50\text{mm}$ effective radius of outer cylinder

$A_{up_a} := P_{up_a} \cdot L_{up} = 0.034\text{m}^2$ Surface area of inner cylinder

$T_{up_a} := 0.6T_{\text{flame}} + 0.4T_{\text{charcoal}} = 942.2\text{K}$ Average steady state surface temperature of flames and coal

$T_{up_b} := 825\text{K}$ Average steady state surface temperature of chamber walls

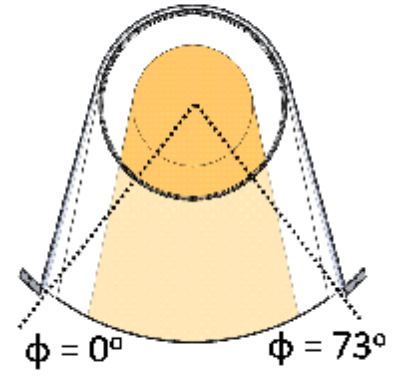
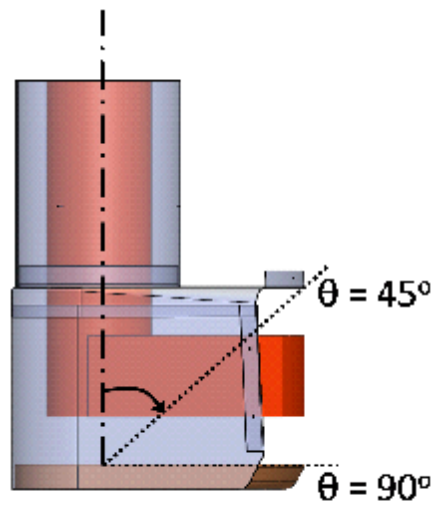
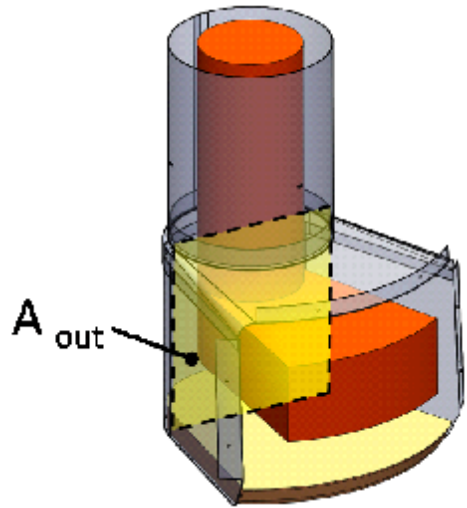
$\epsilon_{up_a} := \epsilon_{\text{flame}} \cdot 0.70 + \epsilon_{\text{charcoal}} \cdot 0.30 = 0.753$ estimated weighted average of emissivity for this region

$\epsilon_{up_b} := \epsilon_{\text{fecral}} = 0.26$ emissivity of metal chamber

$$Q_{\text{rad_up_ab}} := \frac{\sigma_{\text{stefan}} \cdot A_{up_a} \cdot (T_{up_a}^4 - T_{up_b}^4)}{\frac{1}{\epsilon_{up_a}} + \frac{1 - \epsilon_{up_b}}{\epsilon_{up_b}} \cdot \left(\frac{r_{up_a}}{r_{up_b}}\right)} = 196.354\text{ W}$$

Steady state radiative loss to walls of lower combustion chamber (Eq. 13.25)*

1.3. Radiation emission out mouth of stove



$$T_{\text{coalbed}} := 1125\text{K}$$

$$E_b := \sigma_{\text{stefan}} \cdot (T_{\text{coalbed}})^4 = 9.082 \times 10^4 \cdot \frac{\text{W}}{\text{m}^2}$$

Blackbody emissive power of coal bed and flames

$$E_{\text{actual}} := E_b \cdot \epsilon_{\text{low_a}} = 7.239 \times 10^4 \cdot \frac{\text{W}}{\text{m}^2}$$

Estimated Actual Emissive power of coal bed and flames

$$I_e := \frac{E_{\text{actual}}}{\pi} = 2.304 \times 10^4 \cdot \frac{\text{W}}{\text{m}^2}$$

Intensity of Emitted Radiation

$A_{out} := 11000\text{mm}^2$ Equivalent area of emitting surface

$\theta_{mouth2} := 90\text{deg}$ $\theta_{mouth1} := 45\text{deg}$ Zenith angles

$\phi_{mouth2} := 73\text{deg}$ $\phi_{mouth1} := 0\text{deg}$ Azimuth angles

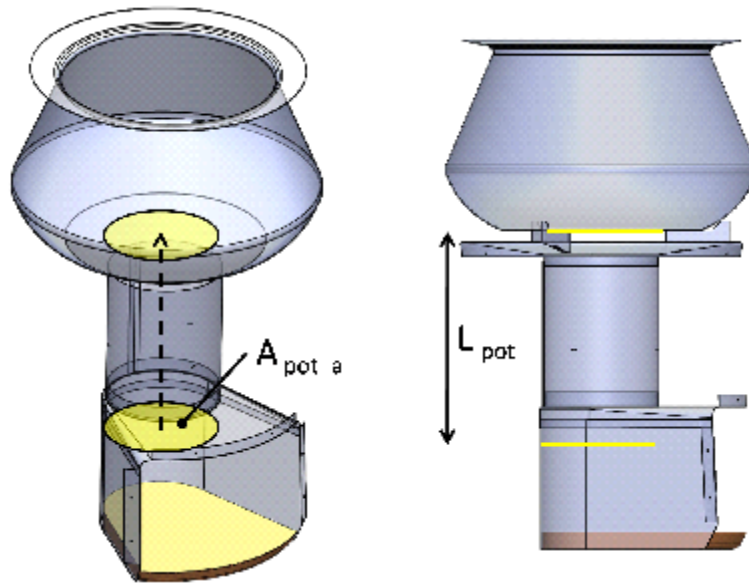
$$Q_{rad_out_mouth} := \int_{\phi_{mouth1}}^{\phi_{mouth2}} \int_{\theta_{mouth1}}^{\theta_{mouth2}} I_e \cdot A_{out} \cdot \cos(\theta) \sin(\theta) \, d\theta \, d\phi \quad (\text{Eq 12.7})^*$$

*Introduction to Heat Transfer, Incropera & DeWitt

$Q_{rad_out_mouth} = 80.73 \text{ W}$

Total rate of radiation heat transfer out the mouth of stove (assuming no irradiation from ambient)

1.4. Radiation Transfer to Pot From Coal Bed Only



$r_a := 50\text{mm}$ radius of effective emitting area

$r_b := 50\text{mm}$ radius of projected emitted area on pot

$L_{pot} := 200\text{mm}$ separation distance between two effective areas

$$A_{\text{pot}_a} := \pi \cdot r_a^2 = 7.854 \times 10^{-3} \text{ m}^2 \quad \text{effective emitting area}$$

$$A_{\text{pot}_b} := A_{\text{pot}_a} \quad \text{effective projected area on pot}$$

$$S_{\text{view}} := 1 + \frac{1 + \left(\frac{r_b}{L_{\text{pot}}}\right)^2}{\left(\frac{r_a}{L_{\text{pot}}}\right)^2} = 18 \quad \text{Variable simplification for view factor calculation}$$

$$F_{ab} := \frac{1}{2} \cdot \left[S_{\text{view}} - \left[S_{\text{view}}^2 - 4 \left(\frac{r_b}{r_a}\right)^2 \right]^{\frac{1}{2}} \right] = 0.056 \quad \text{View factor}$$

$$F_{ba} := F_{ab}$$

$$T_{\text{pot}_a} := T_{\text{charcoal}} = 1.127 \times 10^3 \text{ K} \quad \text{Average temperature of emitting area}$$

$$T_{\text{pot}_b} := 325 \text{ K} \quad \text{Average temperature of pot surface}$$

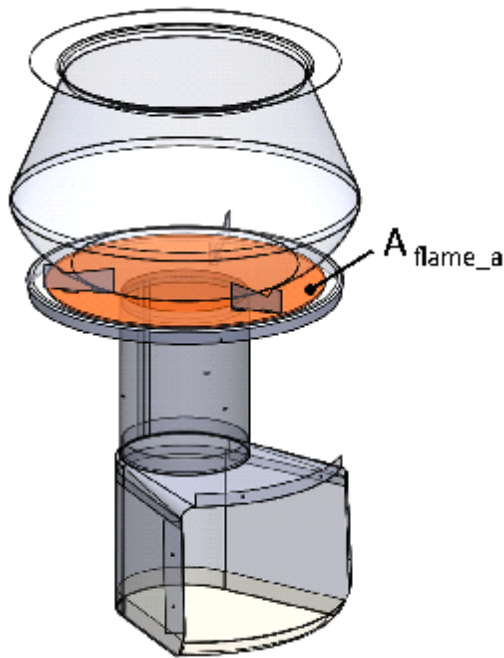
$$Q_{\text{rad}_\text{pot}_\text{ab}} := A_{\text{pot}_a} \cdot F_{ab} \cdot \sigma_{\text{stefan}} \cdot \left(\epsilon_{\text{charcoal}} \cdot T_{\text{pot}_a}^4 - T_{\text{pot}_b}^4 \right) = 32.952 \text{ W}$$

(Eq 13.13)*

*Introduction to Heat Transfer, Incropera & DeWitt

Total radiation heat transfer supplied to pot bottom from charcoal bed. Assuming no radiation from flames, pot is a black body (i.e. $\epsilon = \alpha = 1$, and radiation is diffuse, or directionally independent), and reflectivity of charcoal bed is negligible.

1.5. Radiation to pot from high flames



$$r_{\text{flame_a}} := 3.25\text{in} \quad \text{radius of effective emitting flame area}$$

$$r_{\text{flame_a}} = 82.55\text{mm}$$

$$r_{\text{flame_b}} := 4.25\text{in} \quad \text{radius of pot bottom}$$

$$r_{\text{flame_b}} = 107.95\text{mm}$$

$$L_{\text{flame}} := 10\text{mm} \quad \text{separation distance between two effective areas}$$

$$A_{\text{flame_a}} := \pi \cdot r_{\text{flame_a}}^2 = 0.021\text{m}^2$$

effective emitting flame area

$$A_{\text{flame_b}} := \pi \cdot r_{\text{flame_b}}^2 = 0.037\text{m}^2$$

effective area intercepted by pot bottom

$$S_{\text{flame_view}} := 1 + \frac{1 + \left(\frac{r_{\text{flame_b}}}{L_{\text{flame}}}\right)^2}{\left(\frac{r_{\text{flame_a}}}{L_{\text{flame}}}\right)^2} = 2.725$$

Variable simplification for view factor calculation

$$F_{\text{flame_ab}} := \frac{1}{2} \cdot \left[S_{\text{flame_view}} - \left[S_{\text{flame_view}}^2 - 4 \left(\frac{r_{\text{flame_b}}}{r_{\text{flame_a}}} \right)^2 \right]^{\frac{1}{2}} \right] = 0.98 \quad \text{View factor}$$

$$T_{\text{flame_a}} := T_{\text{flame}} = 819\text{K}$$

Average temperature of emitting area

$$T_{\text{flame_b}} := T_{\text{pot_b}} = 325\text{K}$$

Average temperature of pot surface

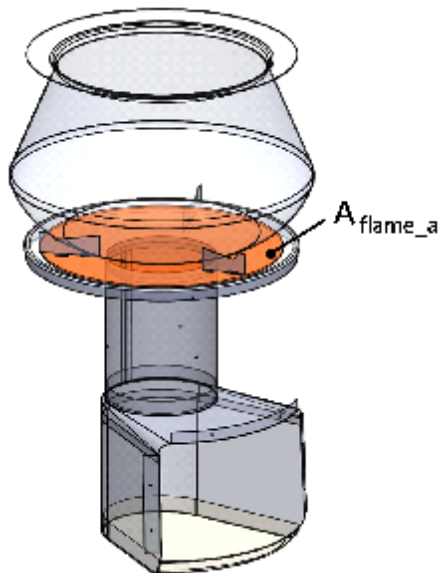
$$Q_{\text{rad_flame_ab}} := A_{\text{flame_a}} \cdot F_{\text{flame_ab}} \cdot \sigma_{\text{stefan}} \cdot \left(\varepsilon_{\text{flame}} \cdot T_{\text{flame_a}}^4 - T_{\text{flame_b}}^4 \right) = 372.193 \text{ W}$$

(Eq 13.13)*

*Introduction to Heat Transfer, Incropera & DeWitt

Total radiation heat transfer supplied to pot bottom from flame sheet. Assuming pot is a black body (i.e. $\varepsilon = \alpha = 1$, radiation is diffuse, or directionally independent), and reflectivity of flames is negligible.

1.6. Radiation to drip pan from high flames



$\varepsilon_{\text{pan}} := 0.26$ emissivity of drip pan assuming oxidized steel surface

$\rho_{\text{pan}} := 1 - \varepsilon_{\text{pan}} = 0.74$

reflectivity of drip pan, assuming pan is gray surface where $\alpha = \varepsilon$. (Eq. 12.59)*

$r_{\text{flame_a}} = 82.55 \cdot \text{mm}$ radius of effective emitting flame area

$r_{\text{flame_c_out}} := 4.75 \text{ in}$ outer radius of drip pan

$r_{\text{flame_c_out}} = 120.65 \cdot \text{mm}$

$L_{\text{flame}} = 10 \cdot \text{mm}$ separation distance between two effective areas

$A_{\text{flame_a}} = 0.021 \text{ m}^2$ effective emitting flame area

$A_{\text{flame_c_out}} := \pi \cdot r_{\text{flame_c_out}}^2 = 0.046 \text{ m}^2$ area of drip pan if it were a solid circle

$$S_{\text{flame_ac_out}} := 1 + \frac{1 + \left(\frac{r_{\text{flame_c_out}}}{L_{\text{flame}}} \right)^2}{\left(\frac{r_{\text{flame_a}}}{L_{\text{flame}}} \right)^2} = 3.151$$

Variable simplification for view factor calculation

$$F_{\text{flame_ac_out}} := \frac{1}{2} \cdot \left[S_{\text{flame_ac_out}} - \left[S_{\text{flame_ac_out}}^2 - 4 \left(\frac{r_{\text{flame_c_out}}}{r_{\text{flame_a}}} \right)^2 \right]^{\frac{1}{2}} \right] = 0.987$$

View factor from flame sheet to drip pan

$$T_{\text{flame_a}} = 819 \text{ K} \quad \text{Average temperature of emitting area}$$

$$T_{\text{flame_c}} := 668 \text{ K} \quad \text{Estimated average steady state drip pan surface temperature from experimental test results (10/20/2008)}$$

$$J_{\text{a_to_c}} := \varepsilon_{\text{flame}} \cdot \sigma_{\text{stefan}} \cdot T_{\text{flame_a}}^4 = 1.837 \times 10^4 \cdot \frac{\text{W}}{\text{m}^2}$$

Radiosity (emission + reflected irradiation) from flame to drip pan surface. Assume flames have negligible reflectivity.

$$Q_{\text{a_to_c_out}} := A_{\text{flame_a}} \cdot F_{\text{flame_ac_out}} \cdot J_{\text{a_to_c}} = 388.26 \text{ W} \quad \text{rate at which radiation leaves flames and is intercepted by drip pan}$$

(Eq 13.9)*

*Introduction to Heat Transer, Incropera & DeWitt

$$J_{\text{c_to_a}} := \varepsilon_{\text{pan}} \cdot \sigma_{\text{stefan}} \cdot T_{\text{flame_c}}^4 + \rho_{\text{pan}} \cdot J_{\text{a_to_c}} = 1.653 \times 10^4 \cdot \frac{\text{W}}{\text{m}^2}$$

Radiosity (emission + reflected irradiation) from drip pan to virtual flame sheet.

$$Q_{\text{c_to_a_out}} := A_{\text{flame_a}} \cdot F_{\text{flame_ac_out}} \cdot J_{\text{c_to_a}} = 349.361 \text{ W} \quad \text{rate at which radiation leaves drip pan and is intercepted by flames}$$

$$Q_{\text{flame_ac_out}} := Q_{\text{a_to_c_out}} - Q_{\text{c_to_a_out}} = 38.899 \text{ W} \quad \text{Total radiation heat transfer supplied to drip pan if it were a solid plate.}$$

$$r_{\text{flame_c_in}} := 50 \text{ mm} \quad \text{inner radius of drip pan (outer radius of combustion chamber)}$$

$$A_{\text{flame_c_in}} := \pi \cdot r_{\text{flame_c_in}}^2 = 7.854 \times 10^{-3} \text{ m}^2 \quad \text{area of combustion chamber}$$

$$S_{\text{flame_ac_in}} := 1 + \frac{1 + \left(\frac{r_{\text{flame_c_in}}}{L_{\text{flame}}}\right)^2}{\left(\frac{r_{\text{flame_a}}}{L_{\text{flame}}}\right)^2} = 1.382$$

Variable simplification for view factor calculation

$$F_{\text{flame_ac_in}} := \frac{1}{2} \cdot \left[S_{\text{flame_ac_in}} - \left[S_{\text{flame_ac_in}}^2 - 4 \left(\frac{r_{\text{flame_c_in}}}{r_{\text{flame_a}}} \right)^2 \right]^{\frac{1}{2}} \right] = 0.359$$

$$Q_{\text{a_to_c_in}} := A_{\text{flame_a}} \cdot F_{\text{flame_ac_in}} \cdot J_{\text{a_to_c}} = 141.031 \text{ W}$$

rate at which radiation leaves flames and is intercepted by drip pan

(Eq 13.9)* *Introduction to Heat Transfer, Incropera & DeWitt

$$Q_{\text{c_to_a_in}} := A_{\text{flame_a}} \cdot F_{\text{flame_ac_in}} \cdot J_{\text{c_to_a}} = 126.902 \text{ W}$$

rate at which radiation leaves drip pan and is intercepted by flames

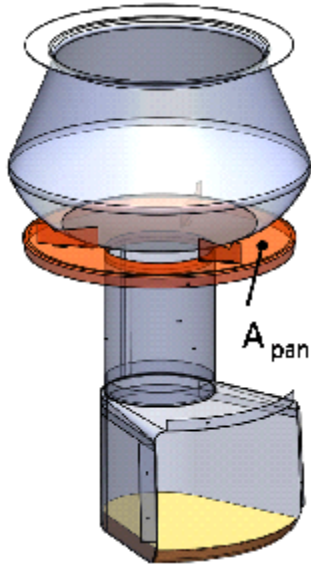
$$Q_{\text{flame_ac_in}} := Q_{\text{a_to_c_in}} - Q_{\text{c_to_a_in}} = 14.13 \text{ W}$$

Amount of radiation not absorbed by drip pan due to 100mm dia. hole in center.

$$Q_{\text{rad_flame_ac}} := Q_{\text{flame_ac_out}} - Q_{\text{flame_ac_in}} = 24.769 \text{ W}$$

Radiation absorbed by drip pan from high flames passing between pot gap.

1.7. Radiation reflected to pot from drip pan



$$r_{\text{pan_a_out}} := r_{\text{flame_c_out}} = 0.121 \text{ m} \quad \text{drip pan outer radius}$$

$$r_{\text{pan_a_in}} := r_{\text{flame_c_in}} = 0.05 \text{ m} \quad \text{drip pan inner radius}$$

$$r_{\text{pan_b}} := r_{\text{flame_b}} = 0.108 \text{ m} \quad \text{pot bottom radius}$$

$$A_{\text{pan_a_out}} := A_{\text{flame_c_out}} = 0.046 \text{ m}^2$$

$$A_{\text{pan_a_in}} := A_{\text{flame_c_in}} = 7.854 \times 10^{-3} \text{ m}^2$$

$$A_{\text{pan_a}} := A_{\text{pan_a_out}} - A_{\text{pan_a_in}} = 0.038 \text{ m}^2$$

$$L_{\text{panpot}} := 23.5 \text{ mm} \quad \text{average distance from drip pan to pot.}$$

$$\tau_{\text{flame}} := 1 - \varepsilon_{\text{flame}} = 0.28$$

transmissivity of flame assuming flame reflectivity is negligible. (Eq. 12.57)*

*Introduction to Heat Transfer, Incropera & DeWitt

$$S_{\text{pan_ab_out}} := 1 + \frac{1 + \left(\frac{r_{\text{pan_b}}}{L_{\text{panpot}}} \right)^2}{\left(\frac{r_{\text{pan_a_out}}}{L_{\text{panpot}}} \right)^2} = 1.838$$

$$F_{\text{pan_ab_out}} := \frac{1}{2} \left[S_{\text{pan_ab_out}} - \left[S_{\text{pan_ab_out}}^2 - 4 \left(\frac{r_{\text{pan_b}}}{r_{\text{pan_a_out}}} \right)^2 \right]^{\frac{1}{2}} \right] = 0.708$$

$$J_{\text{pan}} := \tau_{\text{flame}} \cdot J_{\text{c_to_a}} = 4.628 \times 10^3 \cdot \frac{\text{W}}{\text{m}^2} \quad \text{Radiosity (emission + reflected irradiation) transmitted from drip pan, through flames to pot}$$

$$Q_{a_to_b_out} := A_{pan_a_out} \cdot F_{pan_ab_out} \cdot J_{pan} = 149.913 \text{ W}$$

rate at which radiation leaves drip pan and is intercepted by pot

$$J_{pot} := \tau_{flame} \cdot \sigma_{stefan} \cdot T_{pot_b}^4 = 177.123 \cdot \frac{\text{W}}{\text{m}^2}$$

Radiosity from pot, through flame, to drip pan

$$Q_{b_to_a_out} := A_{pan_a_out} \cdot F_{pan_ab_out} \cdot J_{pot} = 5.738 \text{ W}$$

radiation from pot to pan

$$Q_{pan_ab_out} := Q_{a_to_b_out} - Q_{b_to_a_out} = 144.175 \text{ W}$$

Rate of radiation exchange between drip pan and pot if drip pan were a continuous circle without a hole for combustion chamber.

$$S_{pan_ab_in} := 1 + \frac{1 + \left(\frac{r_{pan_b}}{L_{panpot}} \right)^2}{\left(\frac{r_{pan_a_in}}{L_{panpot}} \right)^2} = 5.882$$

$$F_{pan_ab_in} := \frac{1}{2} \cdot \left[S_{pan_ab_in} - \left[S_{pan_ab_in}^2 - 4 \left(\frac{r_{pan_b}}{r_{pan_a_in}} \right)^2 \right]^{\frac{1}{2}} \right] = 0.944$$

$$Q_{a_to_b_in} := A_{pan_a_in} \cdot F_{pan_ab_in} \cdot J_{pan} = 34.307 \text{ W}$$

rate at which radiation leaves effective combustion chamber area and is intercepted by pot bottom.

$$Q_{b_to_a_in} := A_{pan_a_in} \cdot F_{pan_ab_in} \cdot J_{pot} = 1.313 \text{ W}$$

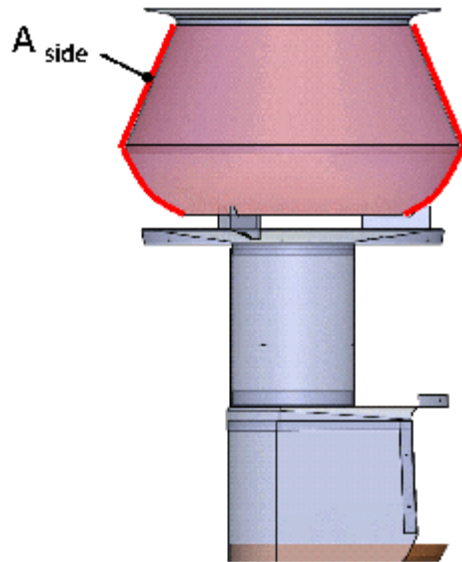
$$Q_{pan_ab_in} := Q_{a_to_b_in} - Q_{b_to_a_in} = 32.994 \text{ W}$$

radiation exchange from the virtual comb. chamber area.

$$Q_{rad_pan_ab} := Q_{pan_ab_out} - Q_{pan_ab_in} = 111.181 \text{ W}$$

Total radiation from drip pan to pot

1.8. Radiation lost by outer pot surface to ambient



$$T_{\text{side}} := 325\text{K}$$

Average side surface temperature of pot

$$E_{\text{b_side}} := \sigma_{\text{stefan}} \cdot (T_{\text{side}})^4 = 632.582 \cdot \frac{\text{W}}{\text{m}^2}$$

Blackbody emissive power of coal bed and flames

$$E_{\text{actual_side}} := E_{\text{b_side}} \cdot \varepsilon_{\text{fecral}} = 164.471 \cdot \frac{\text{W}}{\text{m}^2}$$

Estimated Actual Emissive power of pot surface

$$I_{\text{e_side}} := \frac{E_{\text{actual_side}}}{\pi} = 52.353 \cdot \frac{\text{W}}{\text{m}^2}$$

Intensity of Emitted Radiation

$$A_{\text{side}} := 132553\text{mm}^2$$

Equivalent area of emitting surface

$$\theta_{\text{side2}} := 90\text{deg}$$

$$\theta_{\text{side1}} := 0\text{deg}$$

Zenith angles

$$\phi_{\text{side2}} := 360\text{deg}$$

$$\phi_{\text{side1}} := 0\text{deg}$$

Azimuth angles

$$Q_{\text{rad_side}} := \int_{\phi_{\text{side1}}}^{\phi_{\text{side2}}} \int_{\theta_{\text{side1}}}^{\theta_{\text{side2}}} I_{\text{e_side}} \cdot A_{\text{side}} \cdot \cos(\theta) \sin(\theta) \, \theta \, \phi \quad (\text{Eq 12.7})^*$$

*Introduction to Heat Transfer, Incropera & DeWitt

$$Q_{\text{rad_side}} = 21.801 \text{ W}$$

Total rate of radiation heat transfer out from the sides of the pot.

Total Radiation Energy Balance:

$$Q_{\text{rad_total}} := Q_{\text{rad_side}} + Q_{\text{rad_flame_ab}} + Q_{\text{rad_flame_ac}} + Q_{\text{rad_pot_ab}} \dots \\ + Q_{\text{rad_out_mouth}} + Q_{\text{rad_up_ab}} + Q_{\text{rad_low_ab}} + Q_{\text{rad_pan_ab}}$$

$$Q_{\text{rad_total}} = 1.19 \times 10^3 \text{ W}$$

Relative Radiation Contributions:

$$\frac{Q_{\text{rad_low_ab}}}{Q_{\text{rad_total}}} \cdot 100 = 29.396 \quad (\text{LOSS}) \quad \frac{Q_{\text{rad_flame_ab}}}{Q_{\text{rad_total}}} \cdot 100 = 31.284 \quad (\text{GAIN})$$

$$\frac{Q_{\text{rad_up_ab}}}{Q_{\text{rad_total}}} \cdot 100 = 16.504 \quad (\text{LOSS}) \quad \frac{Q_{\text{rad_flame_ac}}}{Q_{\text{rad_total}}} \cdot 100 = 2.082 \quad (\text{LOSS})$$

$$\frac{Q_{\text{rad_out_mouth}}}{Q_{\text{rad_total}}} \cdot 100 = 6.786 \quad (\text{LOSS}) \quad \frac{Q_{\text{rad_side}}}{Q_{\text{rad_total}}} \cdot 100 = 1.832 \quad (\text{LOSS})$$

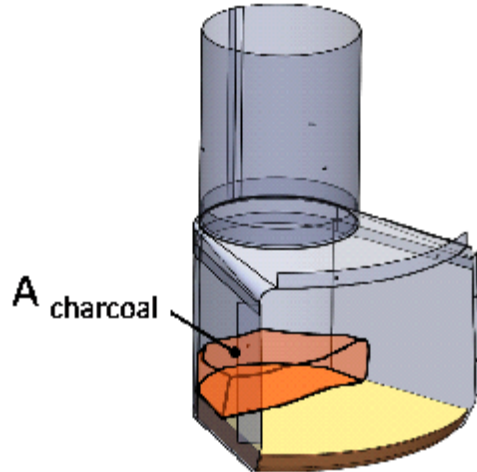
$$\frac{Q_{\text{rad_pot_ab}}}{Q_{\text{rad_total}}} \cdot 100 = 2.77 \quad (\text{GAIN}) \quad \frac{Q_{\text{rad_pan_ab}}}{Q_{\text{rad_total}}} \cdot 100 = 9.345 \quad (\text{GAIN})$$

$$Q_{\text{rad_gain}} := Q_{\text{rad_pot_ab}} + Q_{\text{rad_flame_ab}} + Q_{\text{rad_pan_ab}} = 516.326 \text{ W}$$

$$Q_{\text{rad_loss}} := Q_{\text{rad_total}} - Q_{\text{rad_gain}} = 673.382 \text{ W}$$

2. Conduction

2.1. Conduction of Coal Bed Through Stove Tile



$L_{\text{tile}} := 0.6\text{in}$ tile thickness

$A_{\text{charcoal}} := 6700\text{mm}^2$ Area where charcoal conducts through tile

$k_{\text{tile}} := 1.08 \frac{\text{W}}{\text{m}\cdot\text{K}}$ thermal conductivity of Mizzou Castable ceramic

$R_{\text{cond_tile}} := \frac{L_{\text{tile}}}{k_{\text{tile}}} = 0.014 \frac{\text{m}^2\text{K}}{\text{W}}$ Conductive resistance from tile

$R_{\text{contact_tile}} := 0.05 \frac{\text{m}^2\text{K}}{\text{W}}$ Estimated contact resistance being slightly higher than that of contact resistance of pot on steel plate. See Calculations entitled, "Contact Resistance Calculations for 5.0L (EECL standard) Pot in Bucket".

$R_{\text{total}} := R_{\text{cond_tile}} + R_{\text{contact_tile}}$ Total thermal resistance between inner surface of stove body and exposed surface of tile to charcoal

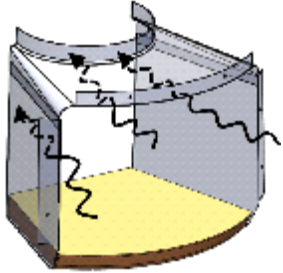
$T_{\text{tile}} := T_{\text{charcoal}} = 1.127 \times 10^3 \text{K}$ Temperature of exposed tile surface assuming same temp as charcoal.

$T_{\text{stove}} := 716\text{K}$ Steady state surface temperature of stove body beneath tile placed in indicated location.

$Q_{\text{cond}} := \frac{A_{\text{charcoal}} \cdot (T_{\text{tile}} - T_{\text{stove}})}{R_{\text{total}}} = 42.952 \text{W}$ Total steady state rate of conduction heat transfer through the tile

3. Convection

3.1. Convection from Gases to Lower Combustion Chamber Walls



$T_{\text{gas}} := 1050\text{K}$ Theoretical gas temperature for 3.5kW fire, loss coef. = 0.35 (Agenbrood).

$\dot{m}_{\text{dotstove}} := 3.0 \cdot 10^{-3} \frac{\text{kg}}{\text{s}}$ Theoretical mass flow rate for 3.5kW fire, loss coef. = 0.35 (Agenbrood).

$d_{\text{low}} := r_{\text{low_b}} \cdot 2 = 0.154\text{ m}$ Effective diameter of lower chamber if it were circular

$L_{\text{low}} = 0.105\text{ m}$ Effective chamber length

$A_{\text{low}} := \pi \cdot d_{\text{low}} \cdot L_{\text{low}} = 0.051\text{ m}^2$ Effective chamber surface area

$T_{\text{low}} := T_{\text{low_b}} = 870\text{ K}$ Average chamber wall surface temperature

$C_{\text{Re}} := 4000$ Correction factor for Reynolds number to account for turbulence effects from fuel obstruction, entrance region characteristics, elbow geometry and flame interaction.

$Re := 900 + C_{\text{Re}}$ Reynolds number calculation using correction factor and derived mass flow rate and temperature values from Agenbrood. See calculations entitled, "Theoretical Convection Heat Transfer Coefficient Calculations".

$100 < Re < 10^3$ laminar flow

$10^3 < Re < 10^4$ transition to turbulence

$10^4 < Re$ turbulent flow

$f := (.79 \cdot \ln(Re) - 1.64)^{-2} = 0.039$ Empirically derived friction factor between gases and walls of chamber. Assuming fully developed internal flow contained by smooth walls. (Eq. 8.21)

$c_{p_gas} := 1.141 \cdot 10^3 \frac{\text{J}}{\text{kg} \cdot \text{K}}$ Specific heat of air (dependent on Temperature)

$k_{\text{gas}} := 6.67 \cdot 10^{-2} \frac{\text{W}}{\text{m} \cdot \text{K}}$ Thermal conductivity of air (dependent on Temperature)

$$\mu_o := 1.71 \cdot 10^{-5} \frac{\text{kg}}{\text{m}\cdot\text{s}} \quad T_o := 273\text{K}$$

Nominal absolute viscosity and temperature of air at 1 atm

$$\mu_{\text{gas}} := \mu_o \cdot \left(\frac{T_{\text{gas}}}{T_o} \right)^{0.7} = 4.391 \times 10^{-5} \frac{\text{kg}}{\text{m}\cdot\text{s}}$$

Curve fit power law approximation from Fluid Mechanics Text, App. A, p.816 (White, Frank).

$$\text{Pr} := \frac{\mu_{\text{gas}} \cdot c_{p_gas}}{k_{\text{gas}}} = 0.751$$

Prandtl Number (ratio of thermal dissipation:conduction)

$$\text{Nu} := \frac{\left(\frac{f}{8} \right) \cdot (\text{Re} - 1000) \cdot \text{Pr}}{1 + 12.7 \left(\frac{f}{8} \right)^{\frac{1}{2}} \cdot \left(\frac{\text{Pr}^2}{3} - 1 \right)} = 16.815$$

Nusselt Number approximation for turbulent flow in circular tubes. Nusselt Number represents a dimensionless temperature gradient at the surface. (Eq. 8.63)

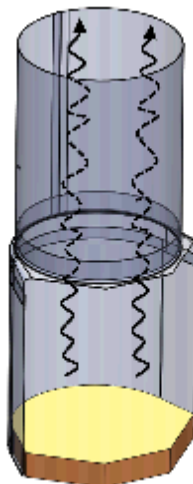
$$h_{\text{low}} := \frac{\text{Nu} \cdot k_{\text{gas}}}{d_{\text{low}}} = 7.28 \cdot \frac{\text{W}}{\text{m}^2\text{K}}$$

convection coefficient through lower chamber

$$Q_{\text{conv_low}} := h_{\text{low}} \cdot A_{\text{low}} \cdot (T_{\text{gas}} - T_{\text{low}}) = 66.595 \text{ W}$$

Convection heat transfer to lower combustion chamber

3.2. Convection from Gases to Upper Chamber Walls



$$d_{\text{up}} := r_{\text{up_b}} \cdot 2 = 0.1 \text{ m}$$

Effective diameter of lower chamber if it were circular

$$L_{\text{up}} = 0.167 \text{ m}$$

Effective chamber length

$$A_{\text{up}} := \pi \cdot d_{\text{up}} \cdot L_{\text{up}} = 0.052 \text{ m}^2$$

Effective chamber surface area

$$T_{\text{up}} := T_{\text{up_b}} = 825 \text{ K}$$

Average upper chamber wall surface temperature

$$\text{Re}_{\text{up}} := 900 + C_{\text{Re}}$$

Reynolds number calculation using correction factor and derived mass flow rate and temperature values from Agenbrood. See calculations entitled, "Theoretical Convection Heat Transfer Coefficient Calculations".

$$f_{up} := (.79 \cdot \ln(Re_{up}) - 1.64)^{-2} = 0.039$$

Empirically derived friction factor between gases and walls of chamber. Assuming fully developed internal flow contained by smooth walls. (Eq. 8.21)

$$Nu_{up} := \frac{\left(\frac{f_{up}}{8}\right) \cdot (Re_{up} - 1000) \cdot Pr}{1 + 12.7 \left(\frac{f_{up}}{8}\right)^{\frac{1}{2}} \cdot \left(\frac{2}{Pr^3} - 1\right)} = 16.815$$

Nusselt Number approximation for turbulent flow in circular tubes. Nusselt Number represents a dimensionless temperature gradient at the surface. (Eq. 8.63)

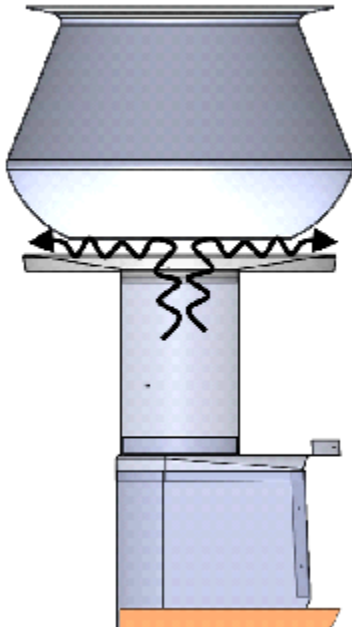
$$h_{up} := \frac{Nu_{up} \cdot k_{gas}}{d_{up}} = 11.216 \cdot \frac{W}{m^2 \cdot K}$$

convection coefficient through lower chamber

$$Q_{conv_up} := h_{up} \cdot A_{up} \cdot (T_{gas} - T_{up}) = 132.398 \text{ W}$$

Convection heat transfer to upper combustion chamber

3.3. Convection from gases to pot bottom



$$h_{conv_pot} := 9.5 \frac{W}{m^2 \cdot K}$$

Calculated convection coefficient for isothermal, impinging jet flow upon pot bottom. See calculations entitled, "Theoretical Convection Heat Transfer Coefficient Calculations"

$$d_{pot} := 8.5 \text{ in} \quad \text{average pot diameter}$$

$$A_{pot} := \frac{\pi \cdot d_{pot}^2}{4} = 0.037 \text{ m}^2 \quad \text{pot surface area}$$

$$T_{pot} := T_{pot_b} = 325 \text{ K} \quad \text{average pot surface temperature}$$

$$Q_{stove_losses} = \dot{m}_{stove} \cdot c_{p_gas} \cdot (T_{gas} - T_{gas2})$$

Solve the above equation (from for T_{gas2} to determine the gas temperature exposed to pot bottom

$$Q_{stove_losses} := Q_{conv_up} + Q_{rad_up_ab} = 328.752 \text{ W}$$

$Q_{\text{stove_losses}}$ represents the rate of thermal energy (heat) lost from the fire to the upper part of the stove, before the combustion gases make it to the pot.

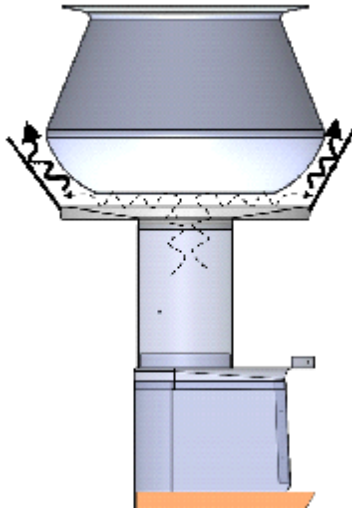
$$T_{\text{gas2}} := T_{\text{gas}} - \frac{Q_{\text{stove_losses}}}{\dot{m}_{\text{stove}} \cdot c_{p_gas}} = 953.958 \text{ K} \quad \text{Gas temperature exposed to pot bottom}$$

$$Q_{\text{conv_pot}} := h_{\text{conv_pot}} \cdot A_{\text{pot}} \cdot (T_{\text{gas2}} - T_{\text{pot}}) = 218.746 \text{ W} \quad \text{Convection heat transfer to pot bottom}$$

$$T_{\text{gasNL}} := 1530 \text{ K} \quad \text{Gas temperature exposed to pot bottom, not accounting for losses to chamber}$$

$$Q_{\text{conv_potNL}} := h_{\text{conv_pot}} \cdot A_{\text{pot}} \cdot (T_{\text{gasNL}} - T_{\text{pot}}) = 419.089 \text{ W}$$

3.4. Convection from gases to sides of the pot by using a pot skirt



$$Q_{\text{pot_losses}} = \dot{m}_{\text{stove}} \cdot c_{p_gas} \cdot (T_{\text{gas2}} - T_{\text{gas3}})$$

Solve this equation for T_{gas3} to determine temperature of gases exposed to sides of pot

$$Q_{\text{pot_losses}} := Q_{\text{rad_pot_ab}} + Q_{\text{rad_flame_ab}} + Q_{\text{rad_flame_ac}} \dots = 759.842 \text{ W} \\ + Q_{\text{rad_pan_ab}} + Q_{\text{conv_pot}}$$

$$T_{\text{gas3}} := T_{\text{gas2}} - \frac{Q_{\text{pot_losses}}}{\dot{m}_{\text{stove}} \cdot c_{p_gas}} = 731.977 \text{ K} \quad \text{Gas temperature as it exits the pot gap and travels up the sides of the pot.}$$

$$t_{\text{skirt}} := .375 \text{ in} \quad \text{thickness of the air gap between the pot skirt and pot}$$

$$h_{\text{skirt}} := 3.25 \text{ in} = 0.083 \text{ m} \quad \text{height of pot skirt from bottom of pot}$$

$$d_i := d_{\text{pot}} = 0.216 \text{ m} \quad d_o := d_i + 2 \cdot t_{\text{skirt}} = 0.235 \text{ m}$$

$$d_h := d_o - d_i = 0.019 \text{ m} \quad \text{hydraulic diameter of circular tube annulus formed by pot skirt and pot}$$

$$\frac{d_i}{d_o} = 0.919 \quad \text{Based on this value, Nusselt number can be interpolated from Table 8.2 in Heat Transfer text, p. 469.}$$

$$\text{Nu}_i := 5 \quad \text{Nusselt number for inner surface (pot) of annulus. Assuming fully developed laminar flow, with outer wall of pot skirt perfectly insulated and side pot surface held at uniform temperature.}$$

$$h_{\text{conv_sides}} := \frac{\text{Nu}_i \cdot k_{\text{gas}}}{d_h} = 17.507 \cdot \frac{\text{W}}{\text{m}^2 \text{K}}$$

$$A_{\text{sides}} := \pi \cdot d_{\text{pot}} \cdot h_{\text{skirt}} = 0.056 \text{ m}^2$$

$$Q_{\text{conv_sides}} := h_{\text{conv_sides}} \cdot A_{\text{sides}} \cdot (T_{\text{gas3}} - T_{\text{pot}}) = 398.924 \text{ W}$$

Relative Convection Contributions

$$Q_{\text{conv_total}} := Q_{\text{conv_low}} + Q_{\text{conv_up}} + Q_{\text{conv_pot}} + Q_{\text{conv_sides}} = 816.663 \text{ W}$$

$$\frac{Q_{\text{conv_low}}}{Q_{\text{conv_total}}} \cdot 100 = 8.155 \quad (\text{LOSS}) \quad \frac{Q_{\text{conv_pot}}}{Q_{\text{conv_total}}} \cdot 100 = 26.785 \quad (\text{GAIN})$$

$$\frac{Q_{\text{conv_up}}}{Q_{\text{conv_total}}} \cdot 100 = 16.212 \quad (\text{LOSS}) \quad \frac{Q_{\text{conv_sides}}}{Q_{\text{conv_total}}} \cdot 100 = 48.848 \quad (\text{GAIN})$$

$$Q_{\text{conv_loss}} := Q_{\text{conv_low}} + Q_{\text{conv_up}} = 198.993 \text{ W}$$

$$Q_{\text{conv_gain}} := Q_{\text{conv_pot}} + Q_{\text{conv_sides}} = 617.67 \text{ W}$$

4. Wasted heat out the top of the stove

$$T_{\text{gas_exit}} := T_{\text{gas3}} - \frac{Q_{\text{conv_sides}}}{\dot{m}_{\text{dotstove}} \cdot c_{p_gas}} = 615.435 \text{ K}$$

$$T_{\text{ambient}} := 290 \text{ K}$$

$$c_{p_gas_exit} := 1.051 \cdot 10^3 \frac{\text{J}}{\text{kg} \cdot \text{K}} \quad \text{Specific heat of gas at exit (temperature dependent)}$$

$$Q_{\text{waste}} := m_{\text{dotstove}} \cdot c_{p_gas_exit} \cdot (T_{\text{gas_exit}} - T_{\text{ambient}}) = 1.026 \times 10^3 \text{ W}$$

5. Total Energy Balance

5.1. Total Contributions

$$Q_{\text{total}} := Q_{\text{rad_total}} + Q_{\text{cond}} + Q_{\text{conv_total}} + Q_{\text{waste}} = 3.075 \times 10^3 \text{ W}$$

$$\text{LHV} := 1.828 \cdot 10^7 \frac{\text{J}}{\text{kg}} \quad \text{lower heating value of wood (dry basis)}$$

$$m_{\text{wood}} := 290 \text{ gm} \quad \text{Average equivalent dry mass of wood consumed by Envirofit's G3300 cookstove for a "hot start" stove test.}$$

$$t_{\text{boil}} := 25 \text{ min} \quad \text{Average hot start TTB for G3300 certification test}$$

$$\text{Energy}_{\text{fuel}} := \frac{\text{LHV} \cdot (m_{\text{wood}})}{t_{\text{boil}}} = 3.534 \times 10^3 \cdot \text{W} \quad \text{chemical energy contained in the fuel}$$

$$\eta_{\text{combustion}} := 0.98 \quad \text{typical combustion efficiency for existing stove}$$

$$\text{Energy}_{\text{combustion}} := \text{Energy}_{\text{fuel}} \cdot (1 - \eta_{\text{combustion}}) = 70.683 \text{ W} \quad \text{Energy from fuel lost due to incomplete combustion}$$

$$\text{Energy}_{\text{balance}} := \text{Energy}_{\text{fuel}} - \text{Energy}_{\text{combustion}} - Q_{\text{total}} = 388.032 \text{ W}$$

$$\frac{\text{Energy}_{\text{balance}}}{\text{Energy}_{\text{fuel}}} \cdot 100 = 10.98 \quad \text{Total percentage of heat released from the fuel which is unaccounted for (LOSS/GAIN)}$$

$$\frac{\text{Energy}_{\text{combustion}}}{\text{Energy}_{\text{fuel}}} \cdot 100 = 2 \quad \text{Total percentage of heat lost due to incomplete combustion (LOSS)}$$

$$\frac{Q_{\text{rad_low_ab}}}{\text{Energy}_{\text{fuel}}} \cdot 100 = 9.896 \quad \text{Total percentage of radiation heat lost to lower chamber walls (LOSS)}$$

$\frac{Q_{\text{rad_up_ab}}}{\text{Energy}_{\text{fuel}}} \cdot 100 = 5.556$	Total percentage of radiation heat lost to upper chamber walls (LOSS)
$\frac{Q_{\text{rad_out_mouth}}}{\text{Energy}_{\text{fuel}}} \cdot 100 = 2.284$	Total percentage of radiation heat lost from mouth to ambient (LOSS)
$\frac{Q_{\text{rad_pot_ab}}}{\text{Energy}_{\text{fuel}}} \cdot 100 = 0.932$	Total percentage of radiation heat gained from charcoal bed to pot (GAIN)
$\frac{Q_{\text{rad_flame_ab}}}{\text{Energy}_{\text{fuel}}} \cdot 100 = 10.531$	Total percentage of radiation heat gained from high flames to pot (GAIN)
$\frac{Q_{\text{rad_flame_ac}}}{\text{Energy}_{\text{fuel}}} \cdot 100 = 0.701$	Total percentage of radiation heat lost from flames to drip pan (LOSS)
$\frac{Q_{\text{rad_pan_ab}}}{\text{Energy}_{\text{fuel}}} \cdot 100 = 3.146$	Total percentage of radiation heat gained drip pan to pot (GAIN)
$\frac{Q_{\text{rad_side}}}{\text{Energy}_{\text{fuel}}} \cdot 100 = 0.617$	Total percentage of radiation heat lost from pot sides to ambient (LOSS)
$\frac{Q_{\text{cond}}}{\text{Energy}_{\text{fuel}}} \cdot 100 = 1.215$	Total percentage of conduction heat lost through bottom of stove (LOSS)
$\frac{Q_{\text{conv_low}}}{\text{Energy}_{\text{fuel}}} \cdot 100 = 1.884$	Total percentage of convection heat lost to lower chamber walls (LOSS)
$\frac{Q_{\text{conv_up}}}{\text{Energy}_{\text{fuel}}} \cdot 100 = 3.746$	Total percentage of convection heat lost to upper chamber walls (LOSS)
$\frac{Q_{\text{conv_pot}}}{\text{Energy}_{\text{fuel}}} \cdot 100 = 6.19$	Total percentage of convection heat gained from jet impingement on pot bottom (GAIN)
$\frac{Q_{\text{conv_sides}}}{\text{Energy}_{\text{fuel}}} \cdot 100 = 11.288$	Total percentage of convection heat gained from hot gases along sides of pot due to pot skirt. (GAIN)
$\frac{Q_{\text{waste}}}{\text{Energy}_{\text{fuel}}} \cdot 100 = 29.034$	Total percentage of wasted heat lost to ambient (LOSS)

5.2. Heat Transfer to Pot

$$Q_{\text{pot}} := Q_{\text{rad_pot_ab}} + Q_{\text{rad_flame_ab}} + Q_{\text{rad_pan_ab}} + Q_{\text{conv_pot}} = 735.073 \text{ W}$$

Heat into the pot without a skirt

$$TE_{\text{bottom}} := \frac{Q_{\text{pot}}}{\text{Energy}_{\text{fuel}}} \cdot 100 = 20.799 \quad \text{Nominal thermal efficiency}$$

$$Q_{\text{pot_w_skirt}} := Q_{\text{pot}} + Q_{\text{conv_sides}} = 1.134 \times 10^3 \text{ W} \quad \text{Heat into the pot with a pot skirt}$$

$$TE_{\text{skirt}} := \frac{Q_{\text{pot_w_skirt}}}{\text{Energy}_{\text{fuel}}} \cdot 100 = 32.087 \quad \text{Thermal efficiency of pot with skirt}$$

$$\frac{TE_{\text{skirt}} - TE_{\text{bottom}}}{TE_{\text{bottom}}} \cdot 100 = 54.27 \quad \text{percentage improvement in thermal efficiency from using a pot skirt (compare to 26% improvement based on experimental results)}$$

$$\frac{Q_{\text{conv_sides}}}{Q_{\text{pot}}} \cdot 100 = 54.27$$

$$\frac{Q_{\text{conv_pot}} + Q_{\text{rad_flame_ab}}}{Q_{\text{conv_pot}}} = 2.701$$

Correction factor accounting for isothermal flow vs. flow with flame radiation (compare to literature values between 2.3 and 3.4).

5.3. Heat Transfer Contribution Summary

$$\frac{Q_{\text{conv_gain}}}{\text{Energy}_{\text{fuel}}} \cdot 100 = 17.477 \quad \text{Total percentage of energy to pot from convection}$$

$$\frac{Q_{\text{conv_loss}}}{\text{Energy}_{\text{fuel}}} \cdot 100 = 5.631 \quad \text{Total percentage of energy to stove from convection}$$

$$\frac{Q_{\text{rad_gain}}}{\text{Energy}_{\text{fuel}}} \cdot 100 = 14.61 \quad \text{Total percentage of energy to pot from radiation}$$

$$\frac{Q_{\text{rad_loss}}}{\text{Energy}_{\text{fuel}}} \cdot 100 = 19.054 \quad \text{Total percentage of energy lost to stove and ambient from radiation}$$

$$\frac{Q_{\text{cond}}}{\text{Energy}_{\text{fuel}}} \cdot 100 = 1.215$$

Total percentage of energy lost due to conduction

$$\frac{Q_{\text{waste}}}{\text{Energy}_{\text{fuel}}} \cdot 100 = 29.034$$

Total percentage of energy wasted at exit

$$\frac{\text{Energy}_{\text{combustion}}}{\text{Energy}_{\text{fuel}}} \cdot 100 = 2$$

Total percentage of energy lost due to combustion inefficiency

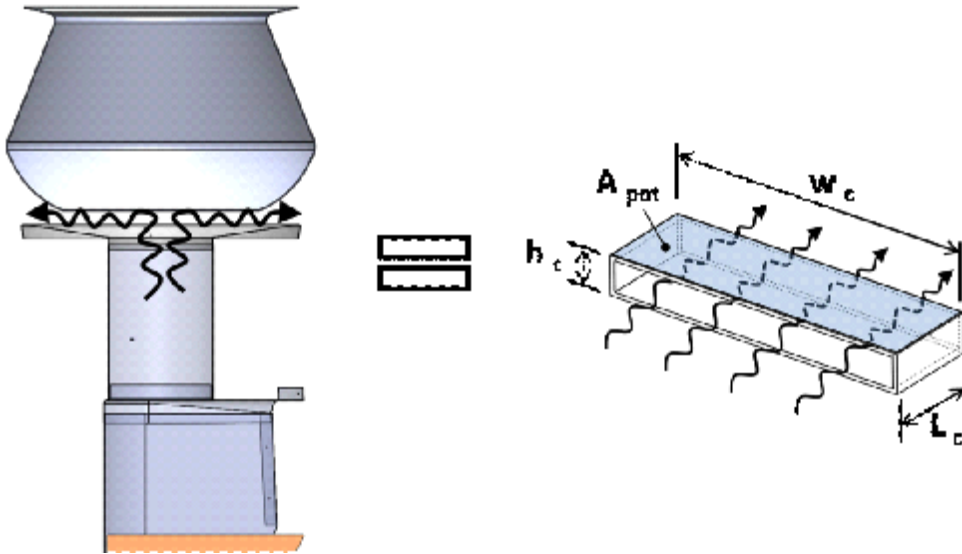
$$\frac{\text{Energy}_{\text{balance}}}{\text{Energy}_{\text{fuel}}} \cdot 100 = 10.98$$

Total percentage of heat released from the fuel which is unaccounted for

Appendix D – Mass Flow Rate, Temperature, Firepower, and Heat Transfer using Microsoft Excel

Section 3.4. Mass Flow Rate, Temperature, and Their Effects on Heat Transfer, LC = 0.5														
<i>input parameters are in italics</i>														
Q in (W)	Inlet gas temp (K)	Cp (J/kg*K)	<i>m dot stove (kg/s)</i>	Gas temp. exposed to pot bottom (K)	gas density (kg/m ³)	gas velocity (m/s)	Re	k (W/m*K)	Nu	h (W/m ² *K)	Q pot bottom (W)	Convection Efficiency (%), Q pot/Qin	Absolute Viscosity (kg/m*s)	Prandtl Number
4.00E+03	288	1.09E+03	<i>3.00E-03</i>	1515	0.233	1.64	673	0.100	11.5	11.5	1381		5.67E-05	6.17E-01
4.00E+03	288	1.09E+03	<i>3.20E-03</i>	1438	0.246	1.66	744	0.095	12.2	11.6	1303		5.47E-05	6.26E-01
4.00E+03	288	1.09E+03	<i>3.40E-03</i>	1370	0.258	1.68	818	0.089	13.0	11.5	1213		5.29E-05	6.46E-01
4.00E+03	288	1.09E+03	<i>3.60E-03</i>	1310	0.269	1.70	894	0.083	13.8	11.5	1143		5.13E-05	6.71E-01
4.00E+03	288	1.09E+03	<i>3.80E-03</i>	1256	0.281	1.72	972	0.079	14.6	11.5	1081		4.98E-05	6.85E-01
4.00E+03	288	1.09E+03	<i>4.00E-03</i>	1208	0.292	1.74	1052	0.077	15.2	11.7	1042		4.84E-05	6.84E-01
4.00E+03	288	1.09E+03	<i>4.20E-03</i>	1164	0.303	1.76	1133	0.074	15.8	11.7	990		4.72E-05	6.93E-01
4.00E+03	288	1.09E+03	<i>4.40E-03</i>	1124	0.314	1.78	1217	0.072	16.4	11.8	951		4.61E-05	6.95E-01
4.00E+03	288	1.09E+03	<i>4.60E-03</i>	1088	0.325	1.80	1301	0.071	17.0	12	924		4.50E-05	6.94E-01
Section 3.5. The influence of Firepower on Convection Efficiency - 4" Elbow with pot (LC = 0.35)														
Q in (W)	Inlet gas temp (K)	Cp (J/kg*K)	<i>m dot stove (kg/s)</i>	Gas temp. exposed to pot bottom (K)	gas density (kg/m ³)	gas velocity (m/s)	Re	k (W/m*K)	Nu	h (W/m ² *K)	Q pot bottom (W)	Convection Efficiency (%), Q pot/Qin	Absolute Viscosity (kg/m*s)	Prandtl Number
1.50E+03	288	1.09E+03	<i>3.08E-03</i>	619	0.570	0.72	1352	0.048	17.2	8.3	245	16.4	3.03E-05	6.87E-01
2.00E+03	288	1.09E+03	<i>3.00E-03</i>	705	0.501	0.78	1176	0.052	16.2	8.4	322	16.1	3.32E-05	6.95E-01
2.50E+03	288	1.09E+03	<i>2.87E-03</i>	792	0.446	0.83	1027	0.057	15.0	8.6	405	16.2	3.60E-05	6.87E-01
3.00E+03	288	1.09E+03	<i>2.67E-03</i>	879	0.402	0.88	911	0.061	14.2	8.6	480	16.0	3.88E-05	6.91E-01
3.50E+03	288	1.09E+03	<i>2.45E-03</i>	965	0.366	0.85	752	0.065	12.9	8.4	542	15.5	4.14E-05	6.92E-01
4.00E+03	288	1.09E+03	<i>1.51E-03</i>	1052	0.336	0.57	438	0.069	9.8	6.8	499	12.5	4.40E-05	6.93E-01

Appendix E – Pot Gap Calculations using MathCAD



$$m_{\text{dotStove5}} := 3.91 \cdot 10^{-3} \frac{\text{kg}}{\text{s}}$$

overall mass flowrate through the stove without pot where LC = 0.5 (input from Josh's calculations, assuming 4 kW fire power)

$$T_{\text{gas5}} := 1248\text{K}$$

estimated flue gas temperature without pot where LC = 0.5 (input from Josh's calculations, assuming 4 kW fire power)

$$m_{\text{dotStove35}} := 2.87 \cdot 10^{-3} \frac{\text{kg}}{\text{s}}$$

overall mass flowrate through the stove with pot where LC = 0.35 (input from Josh's calculations, assuming 2.5 kW fire power)

$$T_{\text{gas35}} := 792\text{K}$$

estimated flue gas temperature with pot where LC = 0.35 (input from Josh's calculations, assuming 2.5 kW fire power)

$C_5 := .5$ experimental loss coefficient (LC) without pot from Agenbroad, 2010

$C_{35} := .35$ experimental LC with pot and 18mm pot gap from Agenbroad, 2010

$T_o := 288\text{K}$ ambient temperature

$h := 230\text{mm}$ chimney height

$d_{\text{stack}} := 100\text{mm}$ diameter of combustion chamber stack

$$A_{\text{stack}} := \frac{\pi d_{\text{stack}}^2}{4} = 7.854 \times 10^{-3} \text{m}^2$$

cross sectional area of the stack

$$R_{\text{universal}} := 8.3143 \frac{\text{J}}{\text{K} \cdot \text{mol}} \quad \text{universal gas constant}$$

$$m_{\text{air}} := 28.97 \frac{\text{gm}}{\text{mol}} \quad \text{molecular mass of air}$$

$$P_{\text{atm}} := 101325 \text{Pa} \quad \text{atmospheric pressure}$$

$$R_{\text{air}} := \frac{R_{\text{universal}}}{m_{\text{air}}} \quad R_{\text{air}} = 286.997 \frac{\text{J}}{\text{K} \cdot \text{kg}} \quad \text{specific gas constant of combusting gases. (assuming combusting gases primarily consist of air).}$$

$$\rho_{\text{gas5}} := \frac{P_{\text{atm}}}{R_{\text{air}} \cdot T_{\text{gas5}}} = 0.283 \frac{\text{kg}}{\text{m}^3} \quad \text{estimated density of flue gases for LC=0.5}$$

$$\rho_{\text{gas35}} := \frac{P_{\text{atm}}}{R_{\text{air}} \cdot T_{\text{gas35}}} = 0.446 \frac{\text{kg}}{\text{m}^3} \quad \text{estimated density of flue gases for LC=0.35}$$

$$\rho_{\text{O}} := \frac{P_{\text{atm}}}{R_{\text{air}} \cdot T_{\text{O}}} = 1.226 \frac{\text{kg}}{\text{m}^3} \quad \text{density of ambient air}$$

$$\Delta P_{\text{chimney_lc5}} := g \cdot h \cdot \rho_{\text{O}} \cdot \left(1 - \frac{T_{\text{O}}}{T_{\text{gas5}}} \right) \cdot C_5 = 1.063 \text{Pa} \quad \text{Pressure difference due to chimney effect in stove that causes flow (LC = 0.5).}$$

$$\Delta P_{\text{chimney_lc35}} := g \cdot h \cdot \rho_{\text{O}} \cdot \left(1 - \frac{T_{\text{O}}}{T_{\text{gas35}}} \right) \cdot C_{35} = 0.616 \text{Pa} \quad \text{Pressure difference due to chimney effect in stove that causes flow (LC = 0.35).}$$

$$d_{\text{pot}} := 8.75 \text{in} \quad A_{\text{pot}} := \frac{\pi d_{\text{pot}}^2}{4} = 0.039 \text{m}^2 \quad \text{pot diameter and bottom area, respectively}$$

$$t_{\text{gap_nom}} := \frac{A_{\text{stack}}}{\pi d_{\text{pot}}} = 11.249 \cdot \text{mm} \quad \text{nominal pot gap to achieve equivalent cross sectional area as combustion chamber.}$$

$$t_{\text{gap_exp}} := 18 \text{mm} \quad \text{experimental pot gap distance}$$

$$A_{\text{gap_nom}} := \pi d_{\text{pot}} \cdot t_{\text{gap_nom}} = 7.854 \times 10^{-3} \text{m}^2 \quad \text{Nominal pot gap x-sec. area}$$

$$A_{\text{gap_exp}} := \pi d_{\text{pot}} \cdot t_{\text{gap_exp}} = 0.013 \text{m}^2 \quad \text{Experimental pot gap cross sectional area}$$

$$C_{\text{potgap}} := \frac{A_{\text{gap_exp}}}{A_{\text{gap_nom}}} = 1.6 \quad \text{pot gap coefficient}$$

$$L_c := \frac{d_{\text{pot}}}{2} = 0.111 \text{ m} \quad \text{channel length}$$

$$w_c := \frac{A_{\text{pot}}}{L_c} = 0.349 \text{ m} \quad \text{channel width}$$

$$h_{c_equivalent} := \frac{A_{\text{gap_exp}}}{w_c} = 0.036 \text{ m} \quad \text{equivalent channel height if it were to have the same x-sec area as experimental pot gap.}$$

$$h_c := 36 \text{ mm} \quad \text{channel height}$$

$$\frac{w_c}{h_c} = 9.697 \quad \text{Refer to Table 8.1 (Incropera & DeWitt) for an equivalent Nusselt Number and friction factor for non-circular ducts (ie } Nu_{Dh}, f_{ReDh} \text{)}$$

$$Nu_{Dh} := 5.8$$

$$f_{ReDh} := 82$$

$$k_{\text{gas}} := 5.70 \cdot 10^{-2} \frac{\text{W}}{\text{m}\cdot\text{K}} \quad \text{Thermal conductivity of gas at } T=792\text{K}$$

$$A_c := h_c \cdot w_c = 0.013 \text{ m}^2 \quad \text{x-sec area of channel}$$

$$D_h := 4 \cdot \frac{w_c \cdot h_c}{2w_c + 2h_c} = 0.065 \text{ m} \quad \text{hydraulic diameter of channel}$$

$$v_{\text{gas5}} := \frac{\dot{m}_{\text{Stove5}}}{\rho_{\text{gas5}} \cdot A_c} = 1.1 \frac{\text{m}}{\text{s}} \quad \text{estimated flue gas velocity flowing through stack (LC=0.5).}$$

$$v_{\text{gas35}} := \frac{\dot{m}_{\text{Stove35}}}{\rho_{\text{gas35}} \cdot A_c} = 0.512 \frac{\text{m}}{\text{s}} \quad \text{estimated flue gas velocity flowing through stack (LC = 0.35).}$$

$$\mu_o := 1.71 \cdot 10^{-5} \frac{\text{kg}}{\text{m}\cdot\text{s}} \quad \text{Nominal absolute viscosity of air at } 1 \text{ atm } T_{\text{oref}} := 273\text{K}$$

$$\mu_{\text{gas5}} := \mu_o \cdot \left(\frac{T_{\text{gas5}}}{T_{\text{oref}}} \right)^{0.7} = 4.955 \times 10^{-5} \frac{\text{kg}}{\text{m}\cdot\text{s}}$$

Curve fit power law approximation (LC = 0.5) from Fluid Mechanics Text, App. A, p.816 (White, Frank).

$$\mu_{\text{gas35}} := \mu_o \cdot \left(\frac{T_{\text{gas35}}}{T_{\text{oref}}} \right)^{0.7} = 3.604 \times 10^{-5} \frac{\text{kg}}{\text{m}\cdot\text{s}}$$

Curve fit power law approximation (LC = 0.5) from Fluid Mechanics Text, App. A, p.816 (White, Frank).

$$h_f = f \cdot \frac{L_c}{D_h} \cdot \frac{v_{\text{gas}}^2}{2g}$$

Head loss for non-circular duct representing pot gap area (Eqn. 6.58, White, Frank)

$$f = \frac{64}{\text{Re}_{D_h}}$$

friction factor for flow through circular duct, assuming laminar flow which neglects surface roughness of walls (Eqn 6.13, White, Frank), Table 8.1 (Incropera & Dewitt) offers values with differing cross-section.

$$\left(\frac{P_1}{\rho g} + \alpha_1 \cdot \frac{v_{\text{gas1}}^2}{2g} + z_1 \right) = \left(\frac{P_2}{\rho g} + \alpha_2 \cdot \frac{v_{\text{gas2}}^2}{2g} + z_2 \right) + h_f$$

The complete incompressible steady flow energy equation for channel flow (Eqn 6.7, White, Frank)

where

$$\alpha_1 = \alpha_2 \quad \text{kinetic energy correction factor (Eqn 3.71, White, Frank)}$$

$$v_{\text{gas1}} = v_{\text{gas2}} \quad \text{velocity is the same through channel (mass conservation)}$$

$$z_1 = z_2 \quad \text{potential energy change is negligible through channel}$$

rewriting steady flow energy equation accounting for above corrections:

$$\frac{\Delta P}{\rho g} = h_f \quad \text{or} \quad \Delta P = h_f \cdot \rho g$$

and substituting for h_f above where

$$\text{Re}_{D_h} = \frac{\rho_{\text{gas}} \cdot v_{\text{gas}} \cdot D_h}{\mu_{\text{gas}}} \quad \text{yields}$$

$$\Delta P_{c5} := \frac{64 \cdot \mu_{\text{gas5}} \cdot L_c \cdot v_{\text{gas5}}}{2D_h^2} = 0.045 \text{ Pa}$$

Pressure drop due to head losses through channel representing pot gap flow area for LC = 0.5

$$\Delta P_{c35} := \frac{f_{\text{ReDh}} \cdot \mu_{\text{gas35}} \cdot L_c \cdot v_{\text{gas35}}}{2D_h^2} = 0.020 \text{ Pa}$$

Pressure drop due to head losses through channel representing pot gap flow area for LC = 0.35

$$\text{Re}_{\text{Dh35}} := \frac{\rho_{\text{gas35}} \cdot v_{\text{gas35}} \cdot D_h}{\mu_{\text{gas35}}} = 413.559$$

$$h_{\text{conv}} := \frac{\text{Nu}_{\text{Dh}} \cdot k_{\text{gas}}}{D_h} = 5.065 \cdot \frac{\text{W}}{\text{m}^2 \text{K}}$$

convection coefficient for duct flow

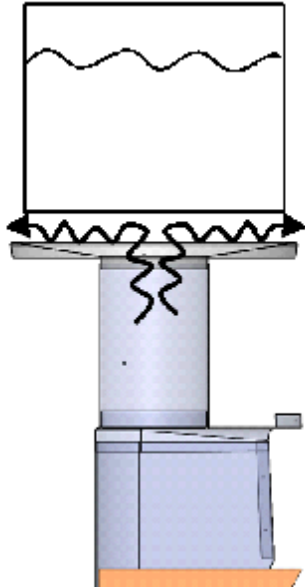
Appendix F – Pot Gap Calculations using Microsoft Excel

Pot Gap Calculations - Microsoft Excel																
Assumptions: Nominal Loss Coefficient = 0.35, fire power = 2.5kW, nominal pot gap = 18mm, pot dia.=8.75", semi-empirical mdot and temperature values																
This color fill represents data that is input from Mathcad or other data																
This color fill is calculated within Excel Spreadsheet																
Nominal values are in boldface font																
Section A - Constant mdot, temperature and induced pressure																
mdot (kg/s)	Temp (K)	Induced pressure from Chimney effect (Pa)	pot gap (mm)	pot gap coeff.	velocity (m/s)	Re	head loss pressure drop (Pa)	Loss Coefficient (prelim.)	Loss Coefficient (adjusted)	friction factor*Re	Nu	Hydraulic Diameter (mm)	channel h (W/m ² K)	normalized channel h	channel Q (W)	normalized channel Q
2.87E-03	792	0.616	8	0.71	1.153	436	0.227	0.23		92	7.2	31	13.4	0.38		
2.87E-03	792	0.616	10	0.89	0.922	431	0.116	0.29		90	6.6	38	9.9	0.52		
2.87E-03	792	0.616	12	1.07	0.768	427	0.066	0.32		87	6.3	45	8	0.64		
2.87E-03	792	0.616	14	1.25	0.659	422	0.042	0.34		85	6.1	52	6.7	0.76		
2.87E-03	792	0.616	16	1.42	0.576	418	0.028	0.35		83	5.9	59	5.7	0.89		
2.87E-03	792	0.616	18	1.6	0.512	414	0.020	0.35		82	5.8	65	5.1	1.00		
2.87E-03	792	0.616	20	1.78	0.461	409	0.015	0.35		82	5.7	72	4.5	1.13		
2.87E-03	792	0.616	22	1.96	0.419	405	0.011	0.36		81	5.5	78	4	1.28		
2.87E-03	792	0.616	24	2.13	0.384	401	0.009	0.36		80	5.4	84	3.6	1.42		
Section B - Variable mdot, temperature, and induced pressure																
2.87E-03	792	0.616	18	1.6	0.512	414	0.02	0.35	0.35	82	5.8	65	5.1	1.00	88.1	1.0
2.79E-03	823	0.593	13	1.2	0.717	402	0.054	0.33	0.33	86	6.2	48	7.5	1.47	138.2	1.6
2.73E-03	851	0.567	11	0.98	0.857	388	0.093	0.31	0.30	88.5	6.45	41	9.3	1.82	181.0	2.1
2.67E-03	885	0.541	9.8	0.871	0.98	372	0.138	0.29	0.27	90	6.7	37	11	2.16	227.9	2.6
2.49E-03	950	0.501	8.8	0.782	1.09	332	0.201	0.26	0.22	91	7	34	13.4	2.63	309.9	3.5
1.81E-03	1024	0.457	8	0.71	0.94	230	0.221	0.23	0.19	92	7.2	31	16	3.14	413.8	4.7

Experimental Test Measurements from Agenbrood FP = variable, LC = 0.35	
Temp (K)	Excess Air Ratio (EAR)
1081	5.2
1017	6.9
1018.4	82.4
929.1	106.3
894.6	137.5
798.9	200.9
806.4	211.8
726.9	264.8
696.5	281.2
589.4	490.3

Appendix G – Pot Skirt Calculations using MathCAD

1. Theoretical convection from gases to pot bottom only



inputs are colored in red

outputs are colored in yellow

relevant results have a border

$$d_{\text{pot}} := 8.75 \text{ in} \quad \text{average pot diameter}$$

$$A_{\text{pot}} := \frac{\pi \cdot d_{\text{pot}}^2}{4} = 0.039 \text{ m}^2 \quad \text{pot surface area}$$

$$T_{\text{pot}} := 326 \text{ K} \quad \text{average pot surface temperature}$$

$$d_{\text{chimney}} := 100 \text{ mm}$$

$$\dot{m}_{\text{dotStove35}} := 2.87 \cdot 10^{-3} \frac{\text{kg}}{\text{s}}$$

overall mass flowrate through the stove with pot where LC = 0.35 (input from Josh's calculations, assuming 2.5 kW fire power)

$$T_{\text{gas35}} := 792 \text{ K}$$

estimated flue gas temperature with pot where LC = 0.35 (input from Josh's calculations, assuming 2.5 kW fire power)

$$k_{\text{gas}} := \left(\frac{.0047}{\text{K}} \cdot T_{\text{gas35}} + 1.9403 \right) \cdot 10^{-2} \frac{\text{W}}{\text{m} \cdot \text{K}} = 0.057 \cdot \frac{\text{W}}{\text{m} \cdot \text{K}} \quad \text{Thermal conductivity of gas (increases with temperature)}$$

$$c_{p_gas} := 1.11 \cdot 10^3 \frac{\text{J}}{\text{kg} \cdot \text{K}}$$

Specific heat of air (assumed constant value at T=850K)

$$h_{\text{conv_pot}} := 8.5 \frac{\text{W}}{\text{m}^2 \cdot \text{K}}$$

Calculated convection coefficient for isothermal, impinging jet flow upon pot bottom using above values for \dot{m} and temp. See calculations entitled, "Theoretical Convection Heat Transfer Coefficient Calculations"

$$Q_{\text{bottom_theory}} := h_{\text{conv_pot}} \cdot A_{\text{pot}} \cdot (T_{\text{gas35}} - T_{\text{pot}}) = 153.666 \text{ W}$$

Theoretical convection heat transfer to pot bottom only

2. Experimental Correlation to Energy Balance for Realistic Convection Heat Transfer to Pot without Pot Skirt.

Use calculated values from "Single-pot Stove Energy Balance" worksheet to determine convection heat transfer to pot bottom and pot sides, without the presence of a pot skirt.

Initial Guesses:

$$Q_{\text{sides_balance}} := 1 \quad \text{Convection heat transfer to sides of pot from energy balance calculations. Theoretical value is } Q_{\text{sides_balance}} = 399\text{W}$$

$$Q_{\text{bottom_balance}} := 1 \quad \text{Convection heat transfer only to bottom of pot from energy balance calculations. Theoretical value is } Q_{\text{bottom_balance}} = 219\text{W}$$

Given

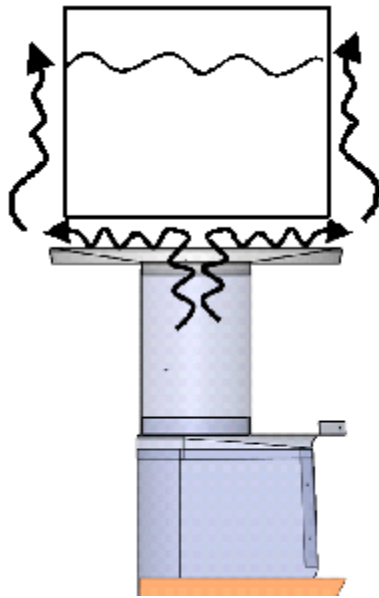
$$Q_{\text{sides_balance}} + Q_{\text{bottom_balance}} = 618 \quad \text{Summation of theoretical convection heat transfer values from the energy balance.}$$

$$\frac{Q_{\text{sides_balance}}}{Q_{\text{bottom_balance}} + 516} = .263 \quad \text{Experimentally derived improvement percentage from using a pot skirt over not using one is 26.3%. This equation is used to represent this relationship. Radiation heat transfer is = 516W. See Section 5.2 of "Single-pot Stove Energy Balance" for a more detailed history.}$$

$$\text{Find}(Q_{\text{sides_balance}}, Q_{\text{bottom_balance}}) = \begin{pmatrix} 236.138 \\ 381.862 \end{pmatrix}$$

$$Q_{\text{bottom_exper}} := 381.9\text{W} \quad \text{Experimentally corrected convection heat transfer to bottom of pot and to sides of pot, without a pot skirt.}$$

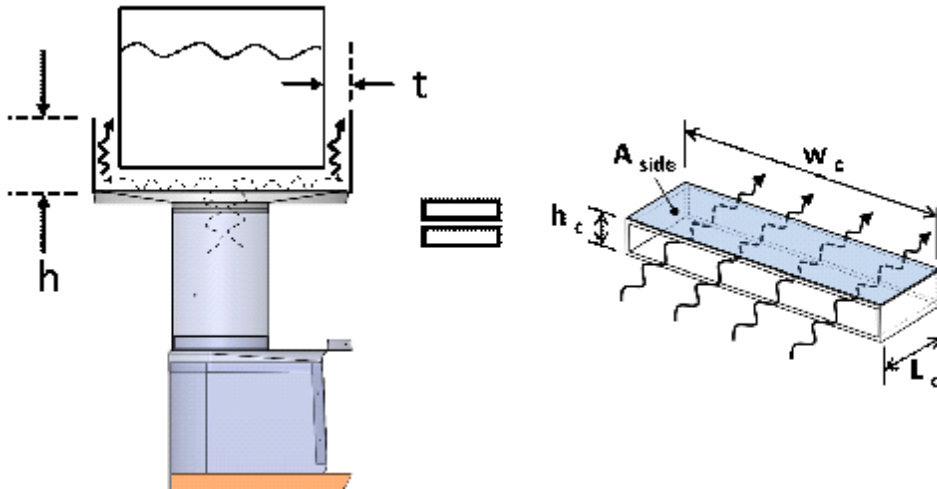
$$\text{CF} := \frac{Q_{\text{bottom_exper}}}{219\text{W}} = 1.744 \quad \text{Correction factor for theoretical convection heat transfer to pot to include convection to sides of pot.}$$



$$Q_{\text{pot}} := Q_{\text{bottom_theory}} \cdot \text{CF} = 267.969 \text{ W}$$

Realistic estimation for rate of convection heat transfer to pot without pot skirt, as pictured here.

3. Investigation of Pot Skirt on Convection Heat Transfer



The flow passing through the pot skirt is treated as flow through a rectangular channel. Minor losses due to the 90 degree bend are ignored since buoyancy already forces the flow to move in the upward direction.

$$C_{35} := .35 \quad \text{experimental LC with pot and pot gap} = 18\text{mm (Agenbroad, 2010)}$$

$$p := d_{\text{pot}} \cdot \pi = 0.698 \text{ m} \quad \text{perimeter of pot}$$

$$t := 18\text{mm} = 0.709\text{-in} \quad \text{pot skirt gap thickness}$$

$$h_{\text{skirt}} := 1\text{in} \quad \text{1st pot skirt section height}$$

$$A_{s1} := p \cdot h_{\text{skirt}} = 0.018 \text{ m}^2 \quad \text{surface area of pot exposed to gases from first skirt section}$$

$$h_2 := 1 \text{ in} \quad \text{additional height added by second section}$$

$$A_{s2} := p \cdot h_2 = 0.018 \text{ m}^2 \quad \text{additional area added by second skirt section}$$

$$h_3 := 0 \text{ in} \quad \text{additional height added by third section}$$

$$A_{s3} := p \cdot h_3 = 0 \quad \text{additional area added by third skirt section}$$

$$h_4 := 0 \text{ in} \quad \text{additional height added by fourth section}$$

$$A_{s4} := p \cdot h_4 = 0 \quad \text{additional area added by fourth skirt section}$$

$$h_c := t = 0.709 \text{ in} \quad \text{channel height} \quad w_c := p = 27.489 \text{ in} \quad \text{channel width}$$

$$L_c := h_{\text{skirt}} + h_2 + h_3 + h_4 \quad \text{channel length}$$

$$\frac{h_c}{w_c} = 0.0258 \quad \frac{w_c}{h_c} = 38.79$$

$$f_{\text{ReDh}} := -91.866 \cdot \left(\frac{h_c}{w_c} \right) + 94.707 = 92.339$$

Modified friction factor (f_{ReDh} = Darcy friction factor * Reynolds#) is calculated based on geometrical correlations for internal duct flow of various cross-sections, assuming fully developed laminar flow (Table 6.4, White)

$$\text{Nu}_{\text{Dh}} := 4.86 \quad \text{Nusselt number is calculated based on geometrical correlations for internal duct flow of various cross-sections, assuming fully developed laminar flow (Table 8.1, Incropera & DeWitt).}$$

$$A_c := h_c \cdot w_c = 0.013 \text{ m}^2 \quad \text{x-sec area of channel}$$

$$D_h := 4 \cdot \frac{w_c \cdot h_c}{2w_c + 2h_c} = 35 \cdot \text{mm} \quad \text{hydraulic diameter of channel}$$

$$T_o := 288 \text{ K} \quad \text{ambient temperature}$$

$$R_{\text{universal}} := 8.3143 \frac{\text{J}}{\text{K} \cdot \text{mol}} \quad \text{universal gas constant}$$

$$m_{\text{air}} := 28.97 \frac{\text{gm}}{\text{mol}} \quad \text{molecular mass of air}$$

$$P_{\text{atm}} := 101325 \text{ Pa} \quad \text{atmospheric pressure}$$

$$R_{\text{air}} := \frac{R_{\text{universal}}}{m_{\text{air}}} \quad R_{\text{air}} = 286.997 \frac{\text{J}}{\text{K} \cdot \text{kg}} \quad \text{specific gas constant of combusting gases. (assuming combusting gases primarily consist of air).}$$

$$\rho_{\text{gas35}} := \frac{P_{\text{atm}}}{R_{\text{air}} \cdot T_{\text{gas35}}} = 0.446 \frac{\text{kg}}{\text{m}^3} \quad \text{estimated density of flue gases for LC=0.35}$$

$$\rho_0 := \frac{P_{\text{atm}}}{R_{\text{air}} \cdot T_0} = 1.226 \frac{\text{kg}}{\text{m}^3} \quad \text{density of ambient air}$$

$$h_{\text{chimney}} := 230 \text{ mm} + h_{\text{skirt}} + h_2 + h_3 + h_4 = 0.281 \text{ m}$$

$$\Delta P_{\text{chimney_lc35}} := g \cdot h_{\text{chimney}} \cdot \rho_0 \cdot \left(1 - \frac{T_0}{T_{\text{gas35}}} \right) \cdot C_{35} = 0.752 \text{ Pa}$$

Pressure difference due to chimney effect in stove that causes flow.

$$v_{\text{gas35}} := \frac{\dot{m}_{\text{dotStove35}}}{\rho_{\text{gas35}} \cdot A_c} = 0.512 \frac{\text{m}}{\text{s}}$$

estimated flue gas velocity flowing through stack (LC = 0.35).

$$\mu_0 := 1.71 \cdot 10^{-5} \frac{\text{kg}}{\text{m} \cdot \text{s}} \quad \text{Nominal absolute viscosity of air at 1 atm } T_{\text{oref}} := 273 \text{ K}$$

$$\mu_{\text{gas35}} := \mu_0 \cdot \left(\frac{T_{\text{gas35}}}{T_{\text{oref}}} \right)^{0.7} = 3.604 \times 10^{-5} \frac{\text{kg}}{\text{m} \cdot \text{s}} \quad \text{Curve fit power law approximation (LC = 0.5) from Fluid Mechanics Text, App. A, p.816 (White, Frank).}$$

$$h_f = f_{\text{ReDh}} \cdot \frac{L_c}{D_h} \cdot \frac{v_{\text{gas}}^2}{2g} \quad \text{Head loss for non-circular duct representing pot gap area (Eqn. 6.58, White, Frank)}$$

$$\left(\frac{P_1}{\rho g} + \alpha_1 \cdot \frac{v_{\text{gas1}}^2}{2g} + z_1 \right) = \left(\frac{P_2}{\rho g} + \alpha_2 \cdot \frac{v_{\text{gas2}}^2}{2g} + z_2 \right) + h_f \quad \text{The complete incompressible steady flow energy equation for channel flow (Eqn 6.7, White, Frank)}$$

where

$$\alpha_1 = \alpha_2 \quad \text{kinetic energy correction factor (Eqn 3.71, White, Frank)}$$

$v_{\text{gas}1} = v_{\text{gas}2}$ velocity is the same through channel (mass conservation)

$z_1 = z_2$ potential energy change is negligible through channel

rewriting steady flow energy equation accounting for above corrections:

$$\frac{\Delta P}{\rho g} = h_f \quad \text{or} \quad \Delta P = h_f \cdot \rho g$$

and substituting for h_f above where $Re_{Dh} = \frac{\rho_{\text{gas}} \cdot v_{\text{gas}} \cdot D_h}{\mu_{\text{gas}}}$ yields

$$\Delta P_{\text{loss}35} := \frac{f_{ReDh} \cdot \mu_{\text{gas}35} \cdot L_c \cdot v_{\text{gas}35}}{2D_h^2} = 0.035 \text{ Pa}$$

Pressure loss due to head losses through channel representing specified pot gap flow area

$$Re_{Dh35} := \frac{\rho_{\text{gas}35} \cdot v_{\text{gas}35} \cdot D_h}{\mu_{\text{gas}35}} = 222.37$$

Reynolds number for internal channel flow

$$h_{\text{conv}} := \frac{Nu_{Dh} \cdot k_{\text{gas}}}{D_h} = 7.842 \cdot \frac{W}{m^2 K}$$

Convection coefficient for internal channel flow

$$A_{\text{chimney}} := \pi \cdot \frac{d_{\text{chimney}}^2}{4} = 7.854 \times 10^{-3} \text{ m}^2$$

$$C_{\text{potskirt}} := \frac{A_c}{A_{\text{chimney}}} = 1.6$$

pot skirt coefficient

$$Q_{\text{pot}} = \dot{m}_{\text{dotstove}} \cdot c_{p_gas} \cdot (T_{\text{gas}} - T_{\text{gas}2})$$

Solve the above equation for $T_{\text{gas}2}$ to determine the gas temperature exposed to pot skirt

$$Q_{\text{pot}} = 267.969 \text{ W}$$

Q_{pot} represents the rate of thermal energy (heat) lost from the fire to the pot bottom, before the combustion gases pass through the skirt.

$$T_{\text{gas}1} := T_{\text{gas}35} - \frac{Q_{\text{pot}}}{\dot{m}_{\text{dotStove}35} \cdot c_{p_gas}} = 707.884 \text{ K}$$

Gas temperature exposed to first pot skirt section

$T_{\text{skirt}} := (T_{\text{gas1}} + T_o) \cdot .5 = 497.942 \text{ K}$	estimated surface temperature of skirt based off of experimental drip pan measurements
$Q_{\text{loss1}} := h_{\text{conv}} \cdot A_{s1} \cdot (T_{\text{gas1}} - T_{\text{skirt}}) = 29.197 \text{ W}$	Convection heat transfer lost to pot skirt surface
$Q_{\text{skirt1}} := h_{\text{conv}} \cdot A_{s1} \cdot (T_{\text{gas1}} - T_{\text{pot}}) = 53.109 \text{ W}$	Convection heat transfer to pot from first skirt section
$T_{\text{gas2}} := T_{\text{gas1}} - \frac{Q_{\text{skirt1}} + Q_{\text{loss1}}}{m_{\text{dotStove35}} \cdot c_{p_gas}} = 682.048 \text{ K}$	Gas temperature exposed to second pot skirt section
$Q_{\text{loss2}} := h_{\text{conv}} \cdot A_{s2} \cdot (T_{\text{gas2}} - T_{\text{skirt}}) = 25.604 \text{ W}$	Convection heat transfer lost to pot skirt surface
$Q_{\text{skirt2}} := h_{\text{conv}} \cdot A_{s2} \cdot (T_{\text{gas2}} - T_{\text{pot}}) = 49.516 \text{ W}$	Convection heat transfer to pot from second skirt section
$T_{\text{gas3}} := T_{\text{gas2}} - \frac{Q_{\text{skirt2}} + Q_{\text{loss2}}}{m_{\text{dotStove35}} \cdot c_{p_gas}} = 658.468 \text{ K}$	Gas temperature exposed to third pot skirt section
$Q_{\text{loss3}} := h_{\text{conv}} \cdot A_{s3} \cdot (T_{\text{gas3}} - T_{\text{skirt}}) = 0$	Convection heat transfer lost to pot skirt surface
$Q_{\text{skirt3}} := h_{\text{conv}} \cdot A_{s3} \cdot (T_{\text{gas3}} - T_{\text{pot}}) = 0$	Convection heat transfer to pot from third skirt section
$T_{\text{gas4}} := T_{\text{gas3}} - \frac{Q_{\text{skirt3}} + Q_{\text{loss3}}}{m_{\text{dotStove35}} \cdot c_{p_gas}} = 658.468 \text{ K}$	Gas temperature exposed to fourth pot skirt section
$Q_{\text{skirt4}} := h_{\text{conv}} \cdot A_{s4} \cdot (T_{\text{gas4}} - T_{\text{pot}}) = 0$	Convection heat transfer to pot from fourth skirt section

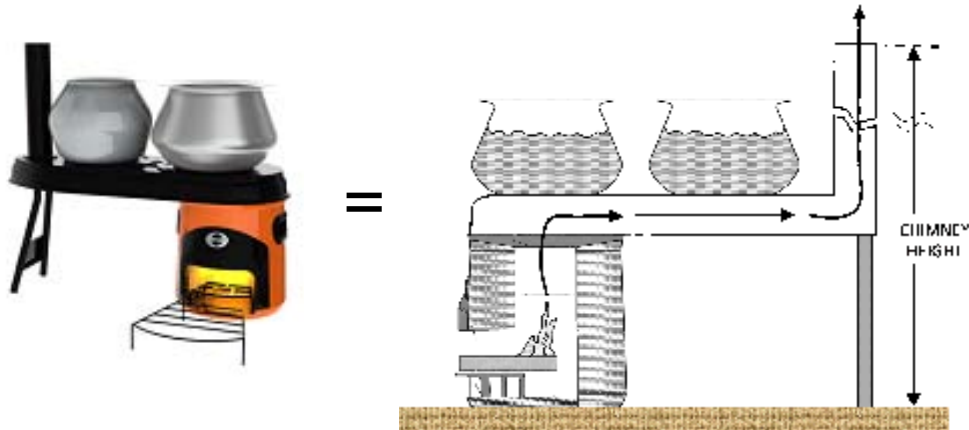
$$Q_{\text{skirttotal}} := Q_{\text{skirt1}} + Q_{\text{skirt2}} + Q_{\text{skirt3}} + Q_{\text{skirt4}} = 102.625 \text{ W}$$

Appendix H – Pot Skirt Calculations using Microsoft Excel

Pot Skirt Calculations with Variable Skirt Height - Microsoft Excel																
Assumptions: Nominal Loss Coefficient = 0.35, fire power = 2.5kW, nominal pot gap = 18mm, pot dia.=8.75", semi-empirical mdot and temperature values																
This color fill represents data that is input from Mathcad or other data																
This color fill is calculated within Excel Spreadsheet																
Nominal values are in boldface font																
Section A - Constant mdot, temperature and induced pressure only influenced by skirt height, skirt gap = 18mm																
mdot (kg/s)	Temp (K)	Induced pressure from Chimney effect (Pa)	skirt height (in)	velocity (m/s)	head loss pressure drop (Pa)	Loss Coefficient (prelim.)	Loss Coefficient (adjusted)	friction factor*Re	pot h Nu (W/m ² K)	skirt h (W/m ² K)	Q pot (W)	Q skirt (W)	convection efficiency (%)	Δ Conv. Heat Transfer (W/mm)		
2.87E-03	792	0.616	0	0.512	222	0.000	0.350	92.3	4.86	8.5	7.8					
2.87E-03	792	0.684	1	0.512	222	0.018	0.341	92.3	4.86	8.5	7.8					
2.87E-03	792	0.752	2	0.512	222	0.035	0.334	92.3	4.86	8.5	7.8					
2.87E-03	792	0.88	4	0.512	222	0.070	0.322	92.3	4.86	8.5	7.8					
2.87E-03	792	1.024	6	0.512	222	0.105	0.314	92.3	4.86	8.5	7.8					
2.87E-03	792	1.16	8	0.512	222	0.141	0.307	92.3	4.86	8.5	7.8					
2.87E-03	792	1.296	10	0.512	222	0.176	0.302	92.3	4.86	8.5	7.8					
Section B - Variable mdot, temperature, and induced pressure, 18mm																
2.87E-03	792	0.616	0	0.512	222	0	0.350	0.350	92.3	4.86	8.5	7.8	268	0	11	0.00
2.79E-03	823	0.733	2	0.517	210	0.036	0.334	0.333	92.3	4.86	8.5	8	286	115	16	57.50
2.73E-03	842	0.95	6	0.518	203	0.111	0.314	0.309	92.3	4.86	8.5	8.2	297	328	25	53.25
2.72E-03	858	1.062	8	0.526	199	0.153	0.307	0.300	92.3	4.86	8.5	8.3	306	418	29	45.00
2.71E-03	865	1.164	10	0.528	197	0.193	0.300	0.292	92.3	4.86	8.5	8.3	310	493	32	37.50
Section A - Constant mdot, temperature and induced pressure only influenced by skirt height, skirt gap = 12mm																
mdot (kg/s)	Temp (K)	Induced pressure from Chimney effect (Pa)	skirt height (in)	velocity (m/s)	head loss pressure drop (Pa)	Loss Coefficient (prelim.)	Loss Coefficient (adjusted)	friction factor*Re	pot h Nu (W/m ² K)	skirt h (W/m ² K)	Q pot (W)	Q skirt (W)	convection efficiency (%)	Δ Conv. Heat Transfer (W/mm)		
2.87E-03	792	0.616	0	0.768	224	0.000	0.350	93.1	4.86	8.5	11.7					
2.87E-03	792	0.684	1	0.768	224	0.059	0.320	93.1	4.86	8.5	11.7					
2.87E-03	792	0.786	2.5	0.768	224	0.147	0.285	93.1	4.86	8.5	11.7					
2.87E-03	792	0.88	4	0.768	224	0.235	0.257	93.1	4.86	8.5	11.7					
2.87E-03	792	0.99	5.5	0.768	224	0.324	0.235	93.1	4.86	8.5	11.7					
Section B - Variable mdot, temperature, and induced pressure, 12mm																
2.87E-03	792	0.616	0	0.768	224	0	0.350	0.350	93.1	4.86	8.5	11.7	268	0	11	0.00
2.76E-03	839	0.645	1	0.783	207	0.062	0.320	0.316	93.1	4.86	8.5	12.1	295	90	15	90.00
2.65E-03	898	0.683	2.5	0.804	190	0.168	0.285	0.264	93.1	4.86	8.5	12.7	329	240	23	100.00
2.43E-03	960	0.717	4	0.789	166	0.276	0.257	0.215	93.1	4.86	8.3	13.3	356	396	30	104.00
1.93E-03	1010	0.747	5.5	0.659	127	0.329	0.235	0.196	93.1	4.86	7.55	13.8	349	497	34	67.33
Section A - Constant mdot, temperature and induced pressure only influenced by skirt height, skirt gap = 15mm																
mdot (kg/s)	Temp (K)	Induced pressure from Chimney effect (Pa)	skirt height (in)	velocity (m/s)	head loss pressure drop (Pa)	Loss Coefficient (prelim.)	Loss Coefficient (adjusted)	friction factor*Re	pot h Nu (W/m ² K)	skirt h (W/m ² K)	Q pot (W)	Q skirt (W)	convection efficiency (%)	Δ Conv. Heat Transfer (W/mm)		
2.87E-03	792	0.616	0	0.615	223	0.000	0.350	92.7	4.86	8.5	9.4					
2.87E-03	792	0.752	2	0.615	223	0.061	0.322	92.7	4.86	8.5	9.4					
2.87E-03	792	0.88	4	0.615	223	0.121	0.302	92.7	4.86	8.5	9.4					
2.87E-03	792	1.024	6	0.615	223	0.182	0.288	92.7	4.86	8.5	9.4					
2.87E-03	792	1.296	10	0.615	223	0.303	0.268	92.7	4.86	8.5	9.4					
Section B - Variable mdot, temperature, and induced pressure, 15mm																
2.87E-03	792	0.616	0	0.615	223	0	0.350	0.350	92.7	4.86	8.5	9.4	268	0	11	0.00
2.76E-03	839	0.714	2	0.626	206	0.064	0.322	0.319	92.7	4.86	8.5	9.7	295	144	18	72.00
2.71E-03	865	0.803	4	0.634	198	0.133	0.302	0.292	92.7	4.86	8.5	9.9	310	280	24	68.00
2.66E-03	890	0.896	6	0.64	191	0.205	0.288	0.270	92.7	4.86	8.5	10.1	324	405	29	62.50
2.57E-03	934	1.079	10	0.649	178	0.359	0.268	0.234	92.7	4.86	8.5	10.5	350	637	39	58.00
Section A - Constant mdot, temperature and induced pressure only influenced by skirt height, skirt gap = 10mm																
mdot (kg/s)	Temp (K)	Induced pressure from Chimney effect (Pa)	skirt height (in)	velocity (m/s)	head loss pressure drop (Pa)	Loss Coefficient (prelim.)	Loss Coefficient (adjusted)	friction factor*Re	pot h Nu (W/m ² K)	skirt h (W/m ² K)	Q pot (W)	Q skirt (W)	convection efficiency (%)	Δ Conv. Heat Transfer (W/mm)		
2.87E-03	792	0.616	0	0.922	225	0.000	0.350	93.4	4.86	8.5	14					
2.87E-03	792	0.684	1	0.922	225	0.101	0.298	93.4	4.86	8.5	14					
2.87E-03	792	0.752	2	0.922	225	0.203	0.256	93.4	4.86	8.5	14					
2.87E-03	792	0.786	2.5	0.922	225	0.253	0.237	93.4	4.86	8.5	14					
Section B - Variable mdot, temperature, and induced pressure, 10mm																
2.87E-03	792	0.616	0	0.922	225	0	0.350	0.350	93.4	4.86	8.5	14	268	0	11	0.00
2.71E-03	865	0.61	1	0.951	200	0.111	0.298	0.286	93.4	4.86	8.5	14.8	310	114	17	114.00
2.43E-03	960	0.605	2	0.946	166	0.238	0.256	0.212	93.4	4.86	8.3	15.9	356	260	25	146.00
1.98E-03	1005	0.554	2.5	0.807	131	0.262	0.220	0.184	93.4	4.86	7.6	16.4	349	321	27	122.00

Pot Skirt Calculations with Variable Skirt Gap - Microsoft Excel																	
Assumptions: Nominal Loss Coefficient = 0.35, fire power = 2.5KW, nominal pot gap = 18mm, pot dia.=8.75", semi-empirical mdot and temperature values																	
This color fill represents data that is input from Mathcad or other data																	
This color fill is calculated within Excel Spreadsheet																	
Section A - Constant mdot, temperature and pressure drop only influenced by skirt gap, skirt height = 2.0 inches																	
mdot (kg/s)	Temp (K)	Induced pressure from Chimney effect (Pa)	skirt gap (mm)	pot skirt coeff.	velocity (m/s)	Re	head loss pressure drop (Pa)	Loss Coefficient (prelim.)	Loss Coefficient (adjusted)	friction factor*Re	Hydraulic Diameter (mm)	pot h (W/m^2K)	skirt h (W/m^2K)	Q pot (W)	Q skirt (W)	convection efficiency (%)	
2.87E-03	792	0.752	10	0.889	0.922	225	0.203	0.256		93.4	4.86	20	8.5	14			
2.87E-03	792	0.752	11	0.978	0.838	225	0.153	0.279		93.3	4.86	22	8.5	12.7			
2.87E-03	792	0.752	13	1.16	0.709	224	0.093	0.307		93	4.86	26	8.5	10.8			
2.87E-03	792	0.752	16	1.42	0.576	223	0.050	0.327		92.6	4.86	31	8.5	8.8			
Section B - Variable mdot, temperature, and induced pressure, skirt height = 2.0 inches																	
2.43E-03	960	0.605	10	0.889	0.946	166	0.238	0.256	0.212	93.4	4.86	20	8.3	15.9	356	251	24
2.65E-03	909	0.643	11	0.978	0.888	188	0.178	0.279	0.253	93.3	4.86	22	8.5	13.9	335	211	22
2.72E-03	857	0.688	13	1.16	0.727	201	0.100	0.307	0.299	93	4.86	26	8.5	11.4	305	160	19
2.78E-03	825	0.719	16	1.42	0.581	210	0.052	0.327	0.325	92.6	4.86	31	8.5	9	287	123	16
Section A - Constant mdot, temperature and pressure drop only influenced by skirt gap, skirt height = 3.25 inches																	
mdot (kg/s)	Temp (K)	Induced pressure from Chimney effect (Pa)	skirt gap (mm)	pot skirt coeff.	velocity (m/s)	Re	head loss pressure drop (Pa)	Loss Coefficient (prelim.)	Loss Coefficient (adjusted)	friction factor*Re	Hydraulic Diameter (mm)	pot h (W/m^2K)	skirt h (W/m^2K)	Q pot (W)	Q skirt (W)	convection efficiency (%)	
2.87E-03	792	0.837	11	0.978	0.838	225	0.248	0.246		93.3	4.86	22	8.5	12.7			
2.87E-03	792	0.837	12	1.1	0.768	224	0.191	0.270		93	4.86	24	8.5	11.7			
2.87E-03	792	0.837	14	1.2	0.656	224	0.121	0.299		92.9	4.86	27	8.5	10			
2.87E-03	792	0.837	17	1.5	0.54	223	0.068	0.322		92.5	4.86	33	8.5	8.3			
Section B - Variable mdot, temperature, and induced pressure, skirt height = 3.25 inches																	
2.22E-03	982	0.653	11	0.978	0.804	149	0.276	0.246	0.202	93.3	4.86	22	8	14.7	355	363	29
2.59E-03	927	0.699	12	1.1	0.812	181	0.226	0.270	0.237	93	4.86	24	8.5	13	346	314	26
2.71E-03	869	0.751	14	1.2	0.682	198	0.134	0.299	0.288	92.9	4.86	27	8.5	10.7	312	242	22
2.76E-03	832	0.791	17	1.5	0.548	207	0.071	0.322	0.319	92.5	4.86	33	8.5	8.6	291	186	19
Section A - Constant mdot, temperature and pressure drop only influenced by skirt gap, skirt height = 5.0 inches																	
mdot (kg/s)	Temp (K)	Induced pressure from Chimney effect (Pa)	skirt gap (mm)	pot skirt coeff.	velocity (m/s)	Re	head loss pressure drop (Pa)	Loss Coefficient (prelim.)	Loss Coefficient (adjusted)	friction factor*Re	Hydraulic Diameter (mm)	pot h (W/m^2K)	skirt h (W/m^2K)	Q pot (W)	Q skirt (W)	convection efficiency (%)	
2.87E-03	792	0.956	13	1.16	0.709	224	0.232	0.265		93	4.86	26	8.5	10.8			
2.87E-03	792	0.956	14	1.2	0.659	224	0.186	0.282		92.9	4.86	27	8.5	10			
2.87E-03	792	0.956	16	1.4	0.576	223	0.125	0.304		92.6	4.86	31	8.5	8.8			
2.87E-03	792	0.956	19	1.7	0.485	222	0.075	0.323		92.2	4.86	37	8.5	7.4			
Section B - Variable mdot, temperature, and induced pressure, skirt height = 5.0 inches																	
2.55E-03	938	0.788	13	1.16	0.746	177	0.274	0.265	0.228	93	4.86	26	8.5	12.1	352	425	31
2.65E-03	903	0.824	14	1.2	0.693	188	0.214	0.282	0.259	92.9	4.86	27	8.5	11	332	376	28
2.72E-03	861	0.868	16	1.4	0.594	199	0.136	0.304	0.295	92.6	4.86	31	8.5	9.3	308	307	25
2.76E-03	831	0.906	19	1.7	0.49	206	0.078	0.323	0.320	92.2	4.86	37	8.5	7.7	290	247	21

Appendix J – Double-pot calculations using MathCAD



Assume all previous radiation calculations from "Single-pot Stove Energy Balance" are upheld. Initial loss coefficient = 0.5 with associated temperatures at appropriate firepower.

Firepower Determination, Two 5L Pots and 6' Chimney:

$$\text{LHV} := 1.828 \cdot 10^7 \frac{\text{J}}{\text{kg}} \quad \text{lower heating value of wood (dry basis)}$$

$$m_{\text{wood}} := 580\text{gm} \quad \text{Average equivalent dry mass of wood consumed by Envirofit's G3355 double-pot accessory for a "hot start" stove test.}$$

$$t_{\text{boil}} := 36\text{min} \quad \text{Average hot start TTB for G3300 certification test}$$

$$\text{Energy}_{\text{fuel}} := \frac{\text{LHV} \cdot (m_{\text{wood}})}{t_{\text{boil}}} = 4.909 \times 10^3 \cdot \text{W} \quad \text{chemical energy contained in the fuel}$$

Flow Properties and Characteristics:

$$m_{\text{dot}} := 3.65 \cdot 10^{-3} \frac{\text{kg}}{\text{s}} \quad \text{mass flow rate and temperatures assuming LC = 0.5, with firepower = 5kW.}$$

$$T_{\text{gas}} := 1000\text{K}$$

$$k_{\text{gas}} := \left(\frac{.0047}{\text{K}} \cdot T_{\text{gas}} + 1.9403 \right) \cdot 10^{-2} \frac{\text{W}}{\text{m} \cdot \text{K}} = 0.066 \frac{\text{W}}{\text{m} \cdot \text{K}} \quad \text{Thermal conductivity of gas (increases with temperature)}$$

$C_{50} := 0.5$ Preliminary Loss Coefficient

$\mu_o := 1.71 \cdot 10^{-5} \frac{\text{kg}}{\text{m}\cdot\text{s}}$ Nominal absolute viscosity of air at 1 atm $T_{\text{oref}} := 273\text{K}$

$\mu_{\text{gas}} := \mu_o \cdot \left(\frac{T_{\text{gas}}}{T_{\text{oref}}} \right)^{0.7} = 4.243 \times 10^{-5} \frac{\text{kg}}{\text{m}\cdot\text{s}}$ Curve fit power law approximation (LC = 0.5) from Fluid Mechanics Text, App. A, p.816 (White, Frank).

$T_o := 288\text{K}$ ambient temperature

$R_{\text{universal}} := 8.3143 \frac{\text{J}}{\text{K}\cdot\text{mol}}$ universal gas constant

$m_{\text{air}} := 28.97 \frac{\text{gm}}{\text{mol}}$ molecular mass of air

$P_{\text{atm}} := 101325\text{Pa}$ atmospheric pressure

$R_{\text{air}} := \frac{R_{\text{universal}}}{m_{\text{air}}}$ $R_{\text{air}} = 286.997 \frac{\text{J}}{\text{K}\cdot\text{kg}}$ specific gas constant of combusting gases. (assuming combusting gases primarily consist of air).

$\rho_{\text{gas}} := \frac{P_{\text{atm}}}{R_{\text{air}} \cdot T_{\text{gas}}} = 0.353 \frac{\text{kg}}{\text{m}^3}$ estimated density of flue gases for LC=0.35

Channel Dimensions:

$h_c := 1.8\text{in}$ channel height $w_c := 7\text{in}$ channel width

$L_c := 25\text{in}$ channel length

$\frac{h_c}{w_c} = 0.2571$ $\frac{w_c}{h_c} = 3.889$

$$f_{\text{ReDh}} := 101.38 \cdot \left(\frac{h_c}{w_c} \right)^2 - 117 \cdot \left(\frac{h_c}{w_c} \right) + 95.625 = 72.243$$

Modified friction factor (f_{ReDh} = Darcy friction factor * Reynolds#) for channel flow is calculated based on geometrical correlations for internal duct flow of various cross-sections, assuming fully developed laminar flow (Table 6.4, White). This equation represents a curve fit from the data presented in the table.

$$\text{Nu}_{\text{Dh}} := 4.3$$

Nusselt number is calculated based on geometrical correlations for internal duct flow of various cross-sections, assuming fully developed laminar flow (Table 8.1, Incropera & DeWitt).

$$A_c := h_c \cdot w_c = 8.129 \times 10^{-3} \text{ m}^2$$

x-sec area of channel

$$D_h := 4 \cdot \frac{w_c \cdot h_c}{2w_c + 2h_c} = 73 \cdot \text{mm}$$

hydraulic diameter of channel

$$v_{\text{gas}} := \frac{\dot{m}}{\rho_{\text{gas}} \cdot A_c} = 1.272 \frac{\text{m}}{\text{s}}$$

estimated flue gas velocity flowing through channel

$$\text{Re}_{\text{Dh35}} := \frac{\rho_{\text{gas}} \cdot v_{\text{gas}} \cdot D_h}{\mu_{\text{gas}}} = 769.705$$

Reynolds number for internal channel flow

Chimney Geometry Characteristics:

$$d_{\text{chim}} := 3 \text{ in} \quad A_{\text{chim}} := \frac{\pi d_{\text{chim}}^2}{4}$$

diameter and cross sectional area of chimney

$$T_{\text{gas_chim}} := T_{\text{gas}} \cdot 0.7 = 700 \text{ K}$$

$$\rho_{\text{gas_chim}} := \frac{P_{\text{atm}}}{R_{\text{air}} \cdot T_{\text{gas_chim}}} = 0.504 \frac{\text{kg}}{\text{m}^3}$$

estimated density of flue gases for LC=0.35

$$v_{\text{gas_chim}} := \frac{\dot{m}}{\rho_{\text{gas_chim}} \cdot A_{\text{chim}}} = 1.587 \frac{\text{m}}{\text{s}}$$

velocity of gases traveling through chimney. Assuming initial gas density

$$L_{\text{chim}} := 6 \text{ ft} \quad \text{length of chimney}$$

$$\mu_{\text{gas_chim}} := \mu_o \cdot \left(\frac{T_{\text{gas_chim}}}{T_{\text{oref}}} \right)^{0.7} = 3.306 \times 10^{-5} \frac{\text{kg}}{\text{m} \cdot \text{s}}$$

Curve fit power law approximation (LC = 0.5) from Fluid Mechanics Text, App. A, p.816 (White, Frank).

$$\text{Re}_{\text{chim}} := \frac{\rho_{\text{gas_chim}} \cdot v_{\text{gas_chim}} \cdot d_{\text{chim}}}{\mu_{\text{gas_chim}}} = 1.845 \times 10^3$$

$$f_{\text{chim}} := \frac{64}{\text{Re}_{\text{chim}}} = 0.035 \quad \text{Poiseuille flow factor, assuming laminar, fully developed flow (Eqn. 6.13 White).}$$

$$\text{Nu}_{\text{chim}} := 3.66 \quad \text{Nusselt number assuming fully developed laminar flow through a circular pipe (Table 8.1, Incropera & DeWitt)}$$

Pressure Drop Characteristics:

$$\rho_o := \frac{P_{\text{atm}}}{R_{\text{air}} \cdot T_o} = 1.226 \frac{\text{kg}}{\text{m}^3} \quad \text{density of ambient air}$$

$$h_{\text{chimney}} := 230\text{mm} + L_{\text{chim}} = 2.059 \text{ m}$$

$$\Delta P_{\text{chimney}} := g \cdot h_{\text{chimney}} \cdot \rho_o \cdot \left(1 - \frac{T_o}{T_{\text{gas}}}\right) \cdot C_{50} = 8.811 \text{ Pa} \quad \text{Pressure difference due to chimney effect in stove that causes flow.}$$

$$h_f = f_{\text{ReDh}} \cdot \frac{L_c}{D_h} \cdot \frac{v_{\text{gas}}^2}{2g} \quad \text{Head loss for non-circular duct channel flow beneath pots (Eqn. 6.58, White, Frank)}$$

$$\left(\frac{P_1}{\rho g} + \alpha_1 \cdot \frac{v_{\text{gas}1}^2}{2g} + z_1\right) = \left(\frac{P_2}{\rho g} + \alpha_2 \cdot \frac{v_{\text{gas}2}^2}{2g} + z_2\right) + h_f \quad \text{The complete incompressible steady flow energy equation for channel flow (Eqn 6.7, White, Frank)}$$

where

$$\alpha_1 = \alpha_2 \quad \text{kinetic energy correction factor (Eqn 3.71, White, Frank)}$$

$$v_{\text{gas}1} = v_{\text{gas}2} \quad \text{velocity is the same through channel (mass conservation)}$$

$$z_1 = z_2 \quad \text{potential energy change is negligible through channel}$$

rewriting steady flow energy equation accounting for above corrections:

$$\frac{\Delta P}{\rho g} = h_f \quad \text{or} \quad \Delta P = h_f \cdot \rho g$$

$$\text{and substituting for } h_f \text{ above where} \quad \text{Re}_{\text{Dh}} = \frac{\rho_{\text{gas}} \cdot v_{\text{gas}} \cdot D_h}{\mu_{\text{gas}}} \quad \text{yields}$$

$$\Delta P_{\text{loss_channel}} := \frac{f_{\text{ReDh}} \cdot \mu_{\text{gas}} \cdot L_c \cdot v_{\text{gas}}}{2D_h^2} = 0.234 \text{ Pa} \quad \text{Pressure loss due to head losses through channel}$$

$$h_{f_chim} := f_{chim} \cdot \frac{L_{chim}}{d_{chim}} \cdot \frac{v_{gas_chim}^2}{2 \cdot g} = 0.107 \text{ m} \quad \text{head loss for circular chimney}$$

The same equation is deduced using the same assumptions as above for channel flow

$$\Delta P_{loss_chim} := h_{f_chim} \cdot \rho_{gas_chim} \cdot g = 0.529 \text{ Pa} \quad \text{Pressure loss due to head losses through chimney}$$

$K_{90bend} := 0.3$ Resistance coefficient for a 90 degree bend in a 4 in. nominal diameter pipe.

$$\Delta P_{loss_bend} := K_{90bend} \cdot \rho_{gas} \cdot v_{gas}^2 = 0.171 \text{ Pa} \quad \text{Pressure loss due to 90 degree bend at top of combustion chamber stack and at bottom of chimney stack.}$$

$$\Delta P_{loss} := \Delta P_{loss_channel} + \Delta P_{loss_chim} + \Delta P_{loss_bend} \cdot 2 = 1.105 \text{ Pa} \quad \text{Total pressure drop through stove}$$

$$C_{new} := \frac{\Delta P_{chimney} - \Delta P_{loss}}{\Delta P_{chimney}} \cdot C_{50} = 0.437 \quad \text{new loss coefficient for double pot attachment}$$

$$h_{conv} := \frac{Nu_{Dh} \cdot k_{gas}}{D_h} = 3.926 \cdot \frac{W}{m^2 K} \quad \text{Convection coefficient for internal channel flow}$$

$T_{35} := 1225 \text{ K}$ Theoretical temperature for 5kW fire at LC = 0.35

$\dot{m}_{dot35} := 2.3 \cdot 10^{-3} \frac{\text{kg}}{\text{s}}$ Theoretical mass flow rate for 5kW fire at LC = 0.35

$T_{new} := (T_{35} + T_{gas}) \cdot .5 = 1.113 \times 10^3 \text{ K}$ Revised Temperature and mass flow rate estimations based on new loss coefficient. Arrived by taking a mean between values associated with LC = 0.35 and LC = 0.50 at 5kw firepower.

$\dot{m}_{dotnew} := (\dot{m}_{dot35} + \dot{m}_{dot}) \cdot .5 = 2.975 \times 10^{-3} \frac{\text{kg}}{\text{s}}$

Energy Balance - Radiation and Conduction Contributions:

Assume Radiation and Conduction Contributions are the same as for single-pot stove energy balance, but scaled up proportionally with firepower.

$$CF_{\text{single_pot}} := 1.39$$

$$Q_{\text{rad_loss}} := 673\text{W} \cdot CF_{\text{single_pot}} = 935.47\text{ W}$$

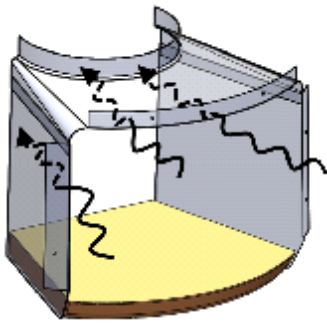
$$Q_{\text{rad_gain}} := 516\text{W} \cdot CF_{\text{single_pot}} = 717.24\text{ W}$$

$$Q_{\text{cond_loss}} := 43\text{W}$$

$$Q_{\text{rad_total}} := Q_{\text{rad_loss}} + Q_{\text{rad_gain}} = 1.653 \times 10^3\text{ W}$$

Energy Balance - Convection Contributions:

Convection from Gases to Lower Combustion Chamber Walls



$$P_{\text{low_b}} := 484\text{mm}$$

Effective perimeter of outer chamber

$$r_{\text{low}} := \frac{P_{\text{low_b}}}{2 \cdot \pi} = 0.077\text{ m}$$

effective radius of outer chamber

$$d_{\text{low}} := r_{\text{low}} \cdot 2 = 0.154\text{m}$$

Effective diameter of lower chamber if it were circular

$$L_{\text{low}} := .105\text{m}$$

Effective chamber length

$$A_{\text{low}} := \pi \cdot d_{\text{low}} \cdot L_{\text{low}} = 0.051\text{ m}^2$$

Effective chamber surface area

$$T_{\text{low}} := 870\text{K}$$

Average chamber wall surface temperature

$$C_{\text{Re}} := 4000$$

Correction factor for Reynolds number to account for turbulence effects from fuel obstruction, entrance region characteristics, elbow geometry and flame interaction.

$Re_{low} := 900 + C_{Re}$

Reynolds number calculation using correction factor and derived mass flow rate and temperature values from Agenbrood. See calculations entitled, "Theoretical Convection Heat Transfer Coefficient Calculations".

$100 < Re < 10^3$ laminar flow
 $10^3 < Re < 10^4$ transition to turbulence
 $10^4 < Re$ turbulent flow

$$f := (.79 \cdot \ln(Re_{low}) - 1.64)^{-2} = 0.039$$

Empirically derived friction factor between gases and walls of chamber. Assuming fully developed internal flow contained by smooth walls. (Eq. 8.21)

$$c_{p_gas} := 1.141 \cdot 10^3 \frac{J}{kg \cdot K}$$

Specific heat of air (assume constant for $T = 1000K$)

$$Pr := \frac{\mu_{gas} \cdot c_{p_gas}}{k_{gas}} = 0.729$$

Prandtl Number (ratio of thermal dissipation:conduction)

$$Nu := \frac{\left(\frac{f}{8}\right) \cdot (Re_{low} - 1000) \cdot Pr}{1 + 12.7 \left(\frac{f}{8}\right)^{\frac{1}{2}} \cdot \left(\frac{Pr}{3} - 1\right)} = 16.605$$

Nusselt Number approximation for turbulent flow in circular tubes. Nusselt Number represents a dimensionless temperature gradient at the surface. (Eq. 8.63)

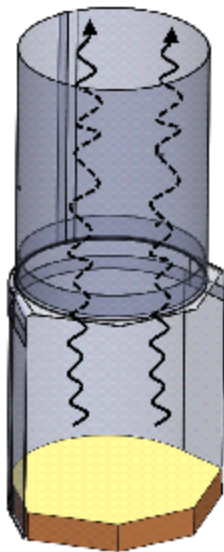
$$h_{low} := \frac{Nu \cdot k_{gas}}{d_{low}} = 7.157 \cdot \frac{W}{m^2 K}$$

convection coefficient through lower chamber

$$Q_{conv_low} := h_{low} \cdot A_{low} \cdot (T_{new} - T_{low}) = 88.2 W$$

Convection heat transfer to lower combustion chamber

3.2. Convection from Gases to Upper Chamber Walls



$d_{up} := 100\text{mm}$ Effective diameter of lower chamber if it were circular

$L_{up} := 167\text{mm}$ Effective chamber length

$A_{up} := \pi \cdot d_{up} \cdot L_{up} = 0.052\text{m}^2$ Effective chamber surface area

$T_{up} := 825\text{K}$ Average upper chamber wall surface temperature

$Re_{up} := 900 + C_{Re}$ Reynolds number calculation using correction factor and derived mass flow rate and temperature values from Agenbrood. See calculations entitled, "Theoretical Convection Heat Transfer Coefficient Calculations".

$f_{up} := (.79 \cdot \ln(Re_{up}) - 1.64)^{-2} = 0.039$ Empirically derived friction factor between gases and walls of chamber. Assuming fully developed internal flow contained by smooth walls. (Eq. 8.21)

$Nu_{up} := \frac{\left(\frac{f_{up}}{8}\right) \cdot (Re_{up} - 1000) \cdot Pr}{1 + 12.7 \left(\frac{f_{up}}{8}\right)^{\frac{1}{2}} \cdot \left(\frac{Pr}{3} - 1\right)} = 16.605$ Nusselt Number approximation for turbulent flow in circular tubes. Nusselt Number represents a dimensionless temperature gradient at the surface. (Eq. 8.63)

$h_{up} := \frac{Nu_{up} \cdot k_{gas}}{d_{up}} = 11.026 \cdot \frac{W}{m^2 K}$ convection coefficient through lower chamber

$Q_{conv_up} := h_{up} \cdot A_{up} \cdot (T_{new} - T_{up}) = 166.312\text{W}$ Convection heat transfer to upper combustion chamber

Convection to initial surface of attachment body:

$L_{initial} := 3.5\text{in}$ $A_{initial} := L_{initial} \cdot w_c \cdot 2 + L_{initial} \cdot h_c \cdot 2 = 0.04\text{m}^2$

$$T_{\text{initial}} := 592\text{K}$$

$$Q_{\text{initial}} := h_{\text{conv}} \cdot A_{\text{initial}} \cdot (T_{\text{new}} - T_{\text{initial}}) = 81.203 \text{ W}$$

Convection to First Pot Bottom:

$$d_{\text{pot}} := 8.75\text{in} \quad A_{\text{pot}} := \frac{\pi \cdot d_{\text{pot}}^2}{4} = 0.039\text{m}^2 \quad \text{diameter and area of exposed pot to hot gases in the channel}$$

$$T_{\text{pot1}} := 326\text{K} \quad \text{Average temperature of first pot}$$

$$h_{\text{conv_pot1}} := h_{\text{conv}} \cdot 1.6 = 6.281 \cdot \frac{\text{W}}{\text{m}^2 \text{K}} \quad \text{convection coefficient for first pot, multiplied by correction factor to account for partial impingement flow}$$

$$Q_{\text{pot1}} := h_{\text{conv_pot1}} \cdot A_{\text{pot}} \cdot (T_{\text{new}} - T_{\text{pot1}}) = 191.645 \text{ W}$$

Convection to Middle Body Surface:

$$T_{\text{gas2}} := T_{\text{new}} - \frac{Q_{\text{pot1}} + Q_{\text{initial}}}{\dot{m} \cdot c_{p_gas}} = 1.032 \times 10^3 \text{ K} \quad \text{Gas temperature exposed to middle body surface}$$

$$L_{\text{mid}} := 8.5\text{in} \quad \text{Effective middle section length, accounting for body surface directly beneath pot.}$$

$$A_{\text{mid}} := w_c \cdot L_{\text{mid}} \cdot 2 + h_c \cdot L_{\text{mid}} \cdot 2 = 0.097\text{m}^2 \quad \text{Surface area of section}$$

$$T_{\text{mid}} := 676\text{K} \quad \text{Average surface temperature of middle section (from experimentation)}$$

$$Q_{\text{mid}} := h_{\text{conv}} \cdot A_{\text{mid}} \cdot (T_{\text{gas2}} - T_{\text{mid}}) = 134.927 \text{ W}$$

Convection to Second Pot Bottom:

$$T_{\text{gas3}} := T_{\text{gas2}} - \frac{Q_{\text{mid}}}{\dot{m} \cdot c_{p_gas}} = 992.371 \text{ K} \quad \text{Gas temperature exposed 2nd pot bottom}$$

$$T_{\text{pot2}} := (288\text{K} + 321\text{K}) \cdot 0.5 = 304.5 \text{ K} \quad \text{Second pot average temperature = 321K when first pot reaches 363K.}$$

$$Q_{\text{pot2}} := h_{\text{conv}} \cdot A_{\text{pot}} \cdot (T_{\text{gas3}} - T_{\text{pot2}}) = 104.757 \text{ W}$$

Convection to End Body Surface:

$$T_{\text{gas4}} := T_{\text{gas3}} - \frac{Q_{\text{pot2}}}{\dot{m} \cdot c_{p_gas}} = 961.51 \text{ K} \quad \text{Gas temperature exposed to end body surface}$$

$$L_{\text{end}} := 2.75 \text{ in} \quad A_{\text{end}} := w_c \cdot L_{\text{end}} \cdot 2 + h_c \cdot L_{\text{end}} \cdot 2 = 0.031 \text{ m}^2$$

$$T_{\text{end}} := 517 \text{ K}$$

$$Q_{\text{end}} := h_{\text{conv}} \cdot A_{\text{end}} \cdot (T_{\text{gas4}} - T_{\text{end}}) = 54.488 \text{ W}$$

$$T_{\text{gas_exit}} := T_{\text{gas4}} - \frac{Q_{\text{end}}}{\dot{m} \cdot c_{p_gas}} = 945.458 \text{ K}$$

Convection Summary:

$$Q_{\text{conv_gain}} := Q_{\text{pot2}} + Q_{\text{pot1}} = 296.402 \text{ W}$$

$$Q_{\text{conv_loss}} := Q_{\text{end}} + Q_{\text{mid}} + Q_{\text{initial}} + Q_{\text{conv_up}} + Q_{\text{conv_low}} = 525.13 \text{ W}$$

$$Q_{\text{conv_total}} := Q_{\text{conv_gain}} + Q_{\text{conv_loss}}$$

Wasted heat out the chimney:

$$T_{\text{ambient}} := 290 \text{ K}$$

$$c_{p_gas_exit} := 1.051 \cdot 10^3 \frac{\text{J}}{\text{kg} \cdot \text{K}}$$

$$Q_{\text{waste}} := \dot{m} \cdot c_{p_gas_exit} \cdot (T_{\text{gas_exit}} - T_{\text{ambient}}) = 2.049 \times 10^3 \text{ W}$$

$$Q_{\text{total}} := Q_{\text{waste}} + Q_{\text{conv_total}} + Q_{\text{rad_total}} + Q_{\text{cond_loss}} = 4.567 \times 10^3 \text{ W}$$

Total Energy Balance:

$$\text{Energy}_{\text{fuel}} = 4.909 \times 10^3 \text{ W}$$

$$\eta_{\text{combustion}} := 0.98 \quad \text{typical combustion efficiency for existing stove}$$

$$\text{Energy}_{\text{combustion}} := \text{Energy}_{\text{fuel}} \cdot (1 - \eta_{\text{combustion}}) = 98.17 \text{ W} \quad \text{Energy from fuel lost due to incomplete combustion}$$

$$\text{Energy}_{\text{balance}} := \text{Energy}_{\text{fuel}} - \text{Energy}_{\text{combustion}} - Q_{\text{total}} = 243.669 \text{ W}$$

$$\frac{Q_{\text{conv_gain}}}{\text{Energy}_{\text{fuel}}} \cdot 100 = 6.039 \quad \text{Total percentage of energy to pot from convection}$$

$$\frac{Q_{\text{conv_loss}}}{\text{Energy}_{\text{fuel}}} \cdot 100 = 10.698 \quad \text{Total percentage of energy to stove from convection}$$

$$\frac{Q_{\text{rad_gain}}}{\text{Energy}_{\text{fuel}}} \cdot 100 = 14.612 \quad \text{Total percentage of energy to pot from radiation}$$

$$\frac{Q_{\text{rad_loss}}}{\text{Energy}_{\text{fuel}}} \cdot 100 = 19.058 \quad \text{Total percentage of energy lost to stove and ambient from radiation}$$

$$\frac{Q_{\text{cond_loss}}}{\text{Energy}_{\text{fuel}}} \cdot 100 = 0.876 \quad \text{Total percentage of energy lost due to conduction}$$

$$\frac{Q_{\text{waste}}}{\text{Energy}_{\text{fuel}}} \cdot 100 = 41.753 \quad \text{Total percentage of energy wasted at exit}$$

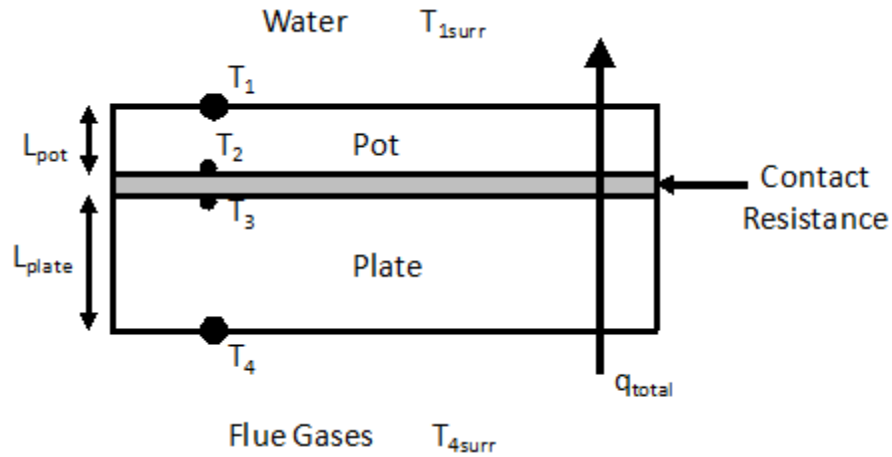
$$\frac{\text{Energy}_{\text{combustion}}}{\text{Energy}_{\text{fuel}}} \cdot 100 = 2 \quad \text{Total percentage of energy lost due to combustion inefficiency}$$

$$\frac{\text{Energy}_{\text{balance}}}{\text{Energy}_{\text{fuel}}} \cdot 100 = 4.964 \quad \text{Total percentage of heat released from the fuel which is unaccounted for}$$

$$\eta_{\text{thermal}} := \frac{Q_{\text{rad_gain}} + Q_{\text{conv_gain}}}{\text{Energy}_{\text{fuel}}} \cdot 100 = 20.651$$

Thermal Efficiency

Appendix K – Heat Plate Time-to-Boil Calculation using MathCAD



Estimating Total Thermal Resistance of Pot of Water on Top of Stove

$d_{pot} := 8.5in$

Pot diameter

$h_{side} := 0in$

Estimated vertical distance from pot bottom where hot gases flow

$A_{side_pot} := \pi \cdot d_{pot} \cdot h_{side}$

$A_{side_pot} = 0$

Area along side of pot where hot gases flow

$A_{bottom_pot} := \frac{\pi \cdot d_{pot}^2}{4}$

$A_{bottom_pot} = 0.037m^2$

Area of pot bottom

$T_{4surr} := 819K$

Surrounding flue gas temperature inside stove

$T_{1surr} := 325.5K$

Surrounding water temperature inside pot

$q_{total} = \frac{T_{4surr} - T_{1surr}}{R_{total}}$

Definition of Heat Transfer in terms of overall temperature difference and total thermal resistance.

$R_{total} = R_{conv} + R_{cond_pot} + R_{cond_plate} + R_{contact}$

Total thermal resistance defined in terms of convective resistance, conductive resistance, and contact resistance.

$$R_{\text{conv}} = \frac{1}{h \cdot A_{\text{bottom_pot}}} \quad \text{Thermal resistance due to convection of hot gases}$$

$$R_{\text{cond_pot}} = \frac{L_{\text{pot}}}{k_{\text{pot}} \cdot A_{\text{bottom_pot}}} \quad \text{Thermal resistance due to conduction through pot bottom}$$

$$R_{\text{cond_plate}} = \frac{L_{\text{plate}}}{k_{\text{plate}} \cdot A_{\text{plate}}} \quad \text{Thermal resistance due to conduction through plate}$$

$$R_{\text{contact}} := 0.02 \frac{\text{m}^2 \cdot \text{K}}{\text{W}} \quad \text{Contact resistance between bottom of pot and plate (estimated through experimentation).}$$

$$d_{\text{plate}} := 8.5 \text{in} \quad \text{Plate diameter}$$

$$A_{\text{plate}} := \frac{\pi \cdot d_{\text{plate}}^2}{4} \quad A_{\text{plate}} = 0.037 \text{m}^2 \quad \text{Area of heat exchanger plate}$$

$$k_{\text{castiron}} := 21.2 \frac{\text{W}}{\text{m} \cdot \text{K}} \quad \text{Thermal conductivity of plate material}$$

$$k_{\text{stainless}} := 16 \frac{\text{W}}{\text{m} \cdot \text{K}} \quad \text{Thermal conductivity of pot material}$$

$$L_{\text{pot}} := .011 \text{in} \quad \text{thickness of pot}$$

$$L_{\text{plate}} := .125 \text{in} \quad \text{thickness of plate}$$

$$h := 36.06 \frac{\text{W}}{\text{m}^2 \cdot \text{K}} \quad \text{h value from plane wall calculations} \quad R_{\text{conv}} := \frac{1}{h} = 0.028 \cdot \frac{\text{m}^2 \cdot \text{K}}{\text{W}}$$

$$R_{\text{cond_pot}} := \frac{L_{\text{pot}}}{k_{\text{stainless}}} = 1.746 \times 10^{-5} \cdot \frac{\text{m}^2 \cdot \text{K}}{\text{W}}$$

$$R_{\text{cond_plate}} := \frac{L_{\text{plate}}}{k_{\text{castiron}}} = 1.498 \times 10^{-4} \cdot \frac{\text{m}^2 \cdot \text{K}}{\text{W}}$$

$$R_{\text{total}} := R_{\text{conv}} + R_{\text{cond_pot}} + R_{\text{cond_plate}} + R_{\text{contact}} = 0.048 \cdot \frac{\text{m}^2 \cdot \text{K}}{\text{W}}$$

Relative Thermal Resistances as a Percentage of the Total Resistance

$$\frac{R_{\text{cond_pot}}}{R_{\text{total}}} \cdot 100 = 0.036$$

$$\frac{R_{\text{cond_plate}}}{R_{\text{total}}} \cdot 100 = 0.313$$

$$\frac{R_{\text{contact}}}{R_{\text{total}}} \cdot 100 = 41.755$$

$$\frac{R_{\text{conv}}}{R_{\text{total}}} = 0.579$$

Heat transfer which is "absorbed" by the additional contact thermal resistance of the plate/pot interface

$m_i := 5.002\text{kg}$ mass of water at beginning of test

$m_f := 4.968\text{kg}$ mass of water at end of test

$T_f := 363\text{K}$ Final water temp at end of test

$T_i := 288\text{K}$ Initial water temp at beginning of test

$h_{fg} := 2.283 \cdot 10^6 \frac{\text{J}}{\text{kg}}$ Enthalpy of evaporation of water at 363K

$C_p := 4180 \frac{\text{J}}{\text{kg} \cdot \text{K}}$ Specific heat of water at constant pressure

$t := 35\text{min}$ time required to boil 5L of water

$$U_{\text{water}} := m_i \cdot C_p \cdot (T_f - T_i) + (m_i - m_f) \cdot h_{fg}$$

$$U_{\text{water}} = 1.646 \times 10^6 \text{ J}$$

Total Internal Energy required to bring 5L of water to a boil in 35 minutes.

$$Q_{\text{total_nom}} := \frac{U_{\text{water}}}{t} = 783.69 \text{ W}$$

Total rate of Heat Transfer from stove to a 5L pot of water, without heat exchanger plate.

$$q_{\text{total_nom}} := \frac{Q_{\text{total_nom}}}{A_{\text{bottom_pot}}} = 2.141 \times 10^4 \cdot \frac{\text{W}}{\text{m}^2}$$

Total rate of Heat Transfer per unit area from stove to a 5L pot of water, without heat exchanger plate.

$$q_{\text{adjust}} := 3.665 \cdot 10^3 \frac{\text{W}}{\text{m}^2}$$

Adjusted heat transfer rate which corrects for the case if there is zero contact resistance.

$$q_{\text{total_plate}} := \frac{(T_{4\text{surr}} - T_{1\text{surr}})}{R_{\text{total}}} = 1.03 \times 10^4 \cdot \frac{\text{W}}{\text{m}^2}$$

Total rate of heat transfer to pot sitting on top of a flat, unfinned, plate with a prescribed contact resistance.

$$q_{\text{absorb}} := q_{\text{total_nom}} - q_{\text{total_plate}}$$

$$q_{\text{absorb_adj}} := q_{\text{total_nom}} - q_{\text{total_plate}} - q_{\text{adjust}}$$

$$q_{\text{absorb}} = 1.11 \times 10^4 \cdot \frac{\text{W}}{\text{m}^2}$$

heat transfer which is "absorbed" by contact resistance

$$q_{\text{absorb_adj}} = 7.439 \times 10^3 \cdot \frac{\text{W}}{\text{m}^2}$$

heat transfer which is "absorbed" by contact resistance, adjusted with correction factor.

Calculate intermediate temperatures

$$q_{\text{total_plate}} = \frac{(T_4 - T_{1\text{surr}})}{R_{\text{cond_pot}} + R_{\text{cond_plate}} + R_{\text{contact}}}$$

Definition of heat transfer written to solve for T_4

$$T_4 := q_{\text{total_plate}} \cdot (R_{\text{cond_pot}} + R_{\text{cond_plate}} + R_{\text{contact}}) + T_{1\text{surr}}$$

$$T_4 = 533.282 \text{ K}$$

Bottom plate temperature

$$q_{\text{total_plate}} = \frac{(T_3 - T_{1\text{surr}})}{R_{\text{cond_pot}} + R_{\text{contact}}}$$

Definition of heat transfer written to solve for T_3

$$T_3 := q_{\text{total_plate}} \cdot (R_{\text{cond_pot}} + R_{\text{contact}}) + T_{1\text{surr}}$$

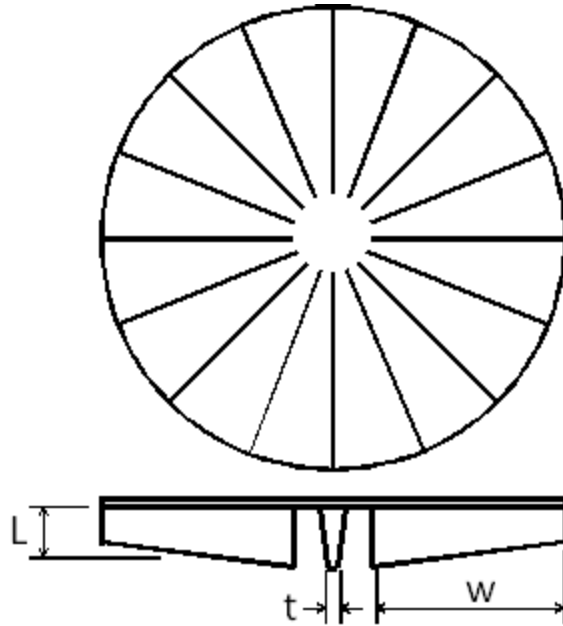
$$T_3 = 531.739 \text{ K}$$

Top plate temperature

$$T_{\text{plate}} := \frac{T_3 + T_4}{2} = 532.511 \text{ K}$$

Average plate temperature

Heat transfer gains from extended fins on the bottom of pot



Individual fin efficiency calculation

The dimensions shown below simplify the fins shown above by assuming rectangular cross-section

$w := 69.6\text{mm}$ fin width (this is the active width of the fin which would change depending on the diameter of the pot which is placed on top of the plate).

$L_{\text{fin}} := 23.3\text{mm}$ Fin length

$t_{\text{tip}} := 1.4\text{mm}$ fin tip thickness $t_{\text{base}} := 3.2\text{mm}$ fin base thickness

$t_{\text{ave}} := \frac{t_{\text{tip}} + t_{\text{base}}}{2}$ $t_{\text{ave}} = 2.3 \times 10^{-3} \text{ m}$ average fin thickness

$\epsilon_{\text{max}} := \frac{L_{\text{fin}}^2}{t_{\text{ave}}} = 20.261$ maximum fin effectiveness value

$P := 2 \cdot w + 2 \cdot t_{\text{ave}}$ $P = 0.144 \text{ m}$ Perimeter of each individual fin

$$A_c := w \cdot t_{ave} \quad A_c = 1.601 \times 10^{-4} \text{ m}^2 \quad \text{Average cross-sectional area of fin}$$

$$L_c := L_{fin} + \frac{t_{ave}}{2} = 0.024 \text{ m} \quad \text{Fin length corrected by assuming adiabatic tip conditions instead of accounting for convective losses along the length.}$$

$$m_s := \sqrt{\frac{h \cdot P}{k_{castiron} \cdot A_c}} \quad m_s = 39.089 \frac{1}{\text{m}} \quad \text{simplifying expression for the above variables}$$

$$\eta_f := \frac{\tanh(m_s \cdot L_c)}{m_s \cdot L_c} \quad \eta_f = 0.777 \quad \text{individual fin efficiency}$$

$$A_p := L_c \cdot t_{ave} \quad \text{corrected fin profile area}$$

$$L_c^{\frac{3}{2}} \cdot \left(\frac{h}{k_{castiron} \cdot A_p} \right)^{\frac{1}{2}} = 0.665 \quad \text{verification with Figure 3.18 in text}$$

$$\theta_b := T_{4surr} - T_4 \quad \theta_b = 285.718 \text{ K}$$

$$A_f := 2 \cdot L_{fin} \cdot w + 2 \cdot t_{ave} \cdot L_{fin} \quad A_f = 3.351 \times 10^{-3} \text{ m}^2 \quad \text{Total surface area of each individual fin}$$

$$q_{fin} := \eta_f \cdot h \cdot A_f \cdot \theta_b = 26.814 \text{ W} \quad \text{heat transfer rate of an individual fin}$$

$$\varepsilon_{fin} := \frac{q_{fin}}{h \cdot t_{base} \cdot w \cdot \theta_b} = 11.685 \quad \text{effectiveness of an individual fin (must satisfy } \varepsilon_{fin} > 2)$$

Overall fin array efficiency calculation and resulting heat flux from finned plate surface

$$N_{\text{fin}} := 44$$

Total number of fins placed on plate

$$\eta_o = \frac{q_t}{h \cdot A_t \cdot \theta_b} = \frac{q_t}{q_{\text{max}}} \quad \text{Overall fin array efficiency}$$

$$A_b := \frac{\pi \cdot d_{\text{plate}}^2}{4} - w \cdot t_{\text{base}} \cdot N_{\text{fin}} \quad A_b = 0.027 \text{ m}^2$$

Prime surface area: Exposed portion of the base plate area which is not occupied by fins.

$$A_t := N_{\text{fin}} \cdot A_f + A_b \quad A_t = 0.174 \text{ m}^2$$

Total exposed surface area associated with both the fin array and prime surface.

$$\eta_o := 1 - \frac{N_{\text{fin}} \cdot A_f}{A_t} \cdot (1 - \eta_f) \quad \eta_o = 0.811$$

Overall fin array efficiency

$$q_{\text{finned}} := \frac{\eta_o \cdot h \cdot A_t \cdot \theta_b}{A_{\text{bottom_pot}}}$$

$$q_{\text{finned}} = 3.977 \times 10^4 \cdot \frac{\text{W}}{\text{m}^2}$$

Rate of heat transfer from finned plate surface

$$q_{\text{total_finned}} := q_{\text{finned}} - q_{\text{absorb}} = 2.867 \times 10^4 \cdot \frac{\text{W}}{\text{m}^2}$$

Total rate of heat transfer to pot sitting on finned heat exchanger plate, accounting for contact resistance.

$$\text{Improvement} := \frac{q_{\text{total_finned}} - q_{\text{total_nom}}}{q_{\text{total_nom}}} \cdot 100 = 33.922$$

Percent improvement over pot without finned plate.

$$t_{\text{boil_finned}} := \frac{U_{\text{water}}}{q_{\text{total_finned}} \cdot A_{\text{bottom_pot}}} = 26.135 \cdot \text{min}$$

Expected TTb from finned plate, without accounting for internal energy required to bring plate up to temperature.

$$\rho_{\text{castiron}} := 6.95 \frac{\text{gm}}{\text{cm}^3} = 6.95 \times 10^3 \frac{\text{kg}}{\text{m}^3}$$

average density of plate material

$$C_{p_castiron} := 506 \frac{\text{J}}{\text{kg}\cdot\text{K}}$$

average specific heat capacity of plate material

$$v_{\text{baseplate}} := A_{\text{plate}} \cdot L_{\text{plate}} = 1.162 \times 10^{-4} \cdot \text{m}^3 \quad \text{total volume of the baseplate}$$

$$v_{\text{fins}} := t_{\text{ave}} \cdot L_{\text{fin}} \cdot w \cdot N_{\text{fin}} = 1.641 \times 10^{-4} \cdot \text{m}^3 \quad \text{total collective volume of all fins}$$

$$m_{\text{plate}} := (v_{\text{fins}} + v_{\text{baseplate}}) \cdot \rho_{\text{castiron}} = 1.948 \text{ kg} \quad \text{total mass of baseplate}$$

$$U_{\text{plate}} := m_{\text{plate}} \cdot C_{p_castiron} \cdot (T_{\text{plate}} - T_i) = 2.411 \times 10^5 \text{ J}$$

$$t_{\text{boil_finned_castiron}} := \frac{U_{\text{water}} + U_{\text{plate}}}{q_{\text{total_finned}} \cdot A_{\text{bottom_pot}}} = 29.963 \cdot \text{min}$$

Expected TTB from a finned plate, accounting for internal energy required to bring plate up to temperature.

$$Bi := \frac{h \cdot \frac{t_{\text{ave}}}{2}}{k_{\text{castiron}}} = 1.956 \times 10^{-3}$$

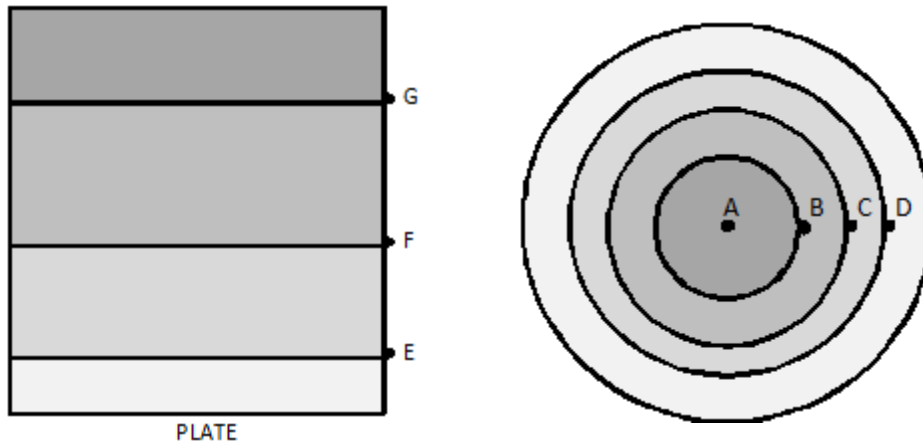
Biot number. If $Bi \ll 1$, then the error associated with using the lumped capacitance method is small. This assumes there is almost zero temperature gradient inside the fin perpendicular to its surface.

$$u = \left(\frac{L_{\text{fin_opt}}}{\frac{t_{\text{ave}}}{2}} \right) \cdot \sqrt{Bi} \quad \text{definition of optimal dimensionless volume provided by Razelos}$$

$$u_{n0} := 1.4192 \quad \text{Optimal dimensionless volume for a rectangular profile, longitudinal fin (Razelos).}$$

$$L_{\text{fin_opt_n0}} := \frac{u_{n0} \cdot \frac{t_{\text{ave}}}{2}}{\sqrt{Bi}} = 36.902 \cdot \text{mm} \quad \text{Optimal fin length}$$

Appendix L – Contact Resistance Experiment Calculations using MathCAD



Partition plate and cylinder into their respective areas:

$$r_b := 1.5\text{in} \quad r_c := 2.75\text{in} \quad r_d := 4\text{in} \quad r_{\text{out}} := 4.75\text{in}$$

$$h_e := 1\text{in} \quad h_f := 3\text{in} \quad h_g := 5\text{in} \quad h_{\text{cyl}} := 6.625\text{in}$$

$$A_{ab} := \pi \cdot r_b^2 = 4.56 \times 10^{-3} \text{m}^2 \quad A_{bc} := \pi r_c^2 - A_{ab} = 0.011 \text{m}^2$$

$$A_{cd} := \pi r_d^2 - A_{bc} - A_{ab} = 0.017 \text{m}^2$$

$$A_{\text{dout}} := \pi r_{\text{out}}^2 - A_{cd} - A_{bc} - A_{ab} = 0.013 \text{m}^2 \quad A_{\text{plate}} := \pi r_{\text{out}}^2 = 0.046 \text{m}^2$$

$$A_{\text{plate}_e} := 2 \cdot \pi \cdot r_{\text{out}} \cdot h_e = 0.019 \text{m}^2 \quad A_{ef} := 2 \cdot \pi \cdot r_{\text{out}} \cdot h_f - A_{\text{plate}_e} = 0.039 \text{m}^2$$

$$A_{fg} := 2 \cdot \pi \cdot r_{\text{out}} \cdot h_g - A_{ef} - A_{\text{plate}_e} = 0.039 \text{m}^2$$

$$A_{g_{\text{topcyl}}} := 2 \cdot \pi \cdot r_{\text{out}} \cdot h_{\text{cyl}} - A_{\text{plate}_e} - A_{ef} - A_{fg} = 0.031 \text{m}^2$$

$$A_{\text{cyl}} := 2 \cdot \pi \cdot r_{\text{out}} \cdot h_{\text{cyl}} = 0.128 \text{m}^2$$

Calculate the total mass of all respective areas represented above:

$$C_{p_{\text{steel}}} := 475 \frac{\text{J}}{\text{kg} \cdot \text{K}}$$

$$m_{\text{plate}} := 2.223 \text{kg}$$

$$m_{\text{cyl}} := .742 \text{kg}$$

$$m_{ab} := m_{plate} \cdot \frac{A_{ab}}{A_{plate}} = 0.222 \text{ kg}$$

$$m_{bc} := m_{plate} \cdot \frac{A_{bc}}{A_{plate}} = 0.523 \text{ kg}$$

$$m_{cd} := m_{plate} \cdot \frac{A_{cd}}{A_{plate}} = 0.831 \text{ kg}$$

$$m_{dout} := m_{plate} \cdot \frac{A_{dout}}{A_{plate}} = 0.647 \text{ kg}$$

$$m_{plate_e} := m_{cyl} \cdot \frac{A_{plate_e}}{A_{cyl}} = 0.112 \text{ kg}$$

$$m_{ef} := m_{cyl} \cdot \frac{A_{ef}}{A_{cyl}} = 0.224 \text{ kg}$$

$$m_{fg} := m_{cyl} \cdot \frac{A_{fg}}{A_{cyl}} = 0.224 \text{ kg}$$

$$m_{g_topcyl} := m_{cyl} \cdot \frac{A_{g_topcyl}}{A_{cyl}} = 0.182 \text{ kg}$$

$$m_{ab} + m_{bc} + m_{cd} + m_{dout} = 2.223 \text{ kg}$$

mass verification for plate

$$m_{plate_e} + m_{ef} + m_{fg} + m_{g_topcyl} = 0.742 \text{ kg}$$

mass verification for cylinder

Delta Temperature Values:

$$T_a := 11.9 \text{ K}$$

$$T_b := 11.7 \text{ K}$$

$$T_c := 10.8 \text{ K}$$

$$T_d := 10.3 \text{ K}$$

$$T_e := 10.6 \text{ K}$$

$$T_f := 11.1 \text{ K}$$

$$T_g := 10.4 \text{ K}$$

$$T_{water} := 20.2 \text{ K}$$

$$T_{top_cyl} := \frac{T_g}{2} = 5.2 \text{ K}$$

$$T_{outer_plate} := \frac{T_d + T_e}{2} = 10.45 \text{ K}$$

$$T_{ab} := \frac{T_a + T_b}{2} = 11.8 \text{ K}$$

$$T_{bc} := \frac{T_b + T_c}{2} = 11.25 \text{ K}$$

$$T_{cd} := \frac{T_c + T_d}{2} = 10.55 \text{ K}$$

$$T_{dout} := \frac{T_{outer_plate} + T_d}{2} = 10.375 \text{ K}$$

$$T_{plate_e} := \frac{T_{outer_plate} + T_e}{2} = 10.525 \text{ K}$$

$$T_{ef} := \frac{T_e + T_f}{2} = 10.85 \text{ K}$$

$$T_{fg} := \frac{T_f + T_g}{2} = 10.75 \text{ K}$$

$$T_{g_topcyl} := \frac{T_g + T_{top_cyl}}{2} = 7.8 \text{ K}$$

Internal Energy Absorbed by bucket:

$$U_{\text{plate}} := C_{p_steel} \cdot (m_{ab} \cdot T_{ab} + m_{bc} \cdot T_{bc} + m_{cd} \cdot T_{cd} + m_{dout} \cdot T_{dout})$$

$$U_{\text{plate}} = 1.139 \times 10^4 \text{ J}$$

$$U_{\text{cyl}} := C_{p_steel} \cdot (m_{\text{plate_e}} \cdot T_{\text{plate_e}} + m_{ef} \cdot T_{ef} + m_{fg} \cdot T_{fg} + m_{g_topcyl} \cdot T_{g_topcyl})$$

$$U_{\text{cyl}} = 3.532 \times 10^3 \text{ J}$$

$$U_{\text{bucket}} := U_{\text{plate}} + U_{\text{cyl}} = 1.492 \times 10^4 \text{ J}$$

Internal Energy Absorbed by water only:

$m_i := 5.0\text{kg}$ mass of water at beginning of test

$m_f := 5.0\text{kg}$ mass of water at end of test

$T_{\text{water}} = 20.2\text{K}$ Temperature change of water

$C_{p_water} := 4180 \frac{\text{J}}{\text{kg} \cdot \text{K}}$ Specific heat of water at constant pressure

$h_{fg} := 2.283 \cdot 10^6 \frac{\text{J}}{\text{kg}}$ Enthalpy of evaporation of water at 363K

$$U_{\text{water}} := m_i \cdot C_{p_water} \cdot (T_{\text{water}}) + (m_i - m_f) \cdot h_{fg}$$

$U_{\text{water}} = 4.222 \times 10^5 \text{ J}$ Total Internal Energy required to raise the temperature of the water by the amount indicated.

Internal Energy absorbed by pot:

$C_{p_stainless} := 477 \frac{\text{J}}{\text{kg} \cdot \text{K}}$

$m_{\text{pot}} := .597\text{kg}$

$$U_{\text{pot}} := m_{\text{pot}} \cdot C_{p_stainless} \cdot T_{\text{water}} = 5.752 \times 10^3 \text{ J}$$

Total Heat Transfer absorbed by apparatus:

$t_{\text{diff}} := 656\text{s}$ time difference within time frame of interest

$$Q_{\text{total}} := \frac{U_{\text{pot}} + U_{\text{water}} + U_{\text{bucket}}}{t_{\text{diff}}}$$

$Q_{\text{total}} = 675.086 \text{ W}$

Total heat transfer rate into assembly

$$d_{\text{pot}} := 8.5\text{in}$$

diameter of pot which is in contact with plate

$$A_{\text{bottom_pot}} := \frac{\pi \cdot d_{\text{pot}}^2}{4} - 2.125\text{in}^2 = 0.035\text{m}^2$$

Area of pot bottom, corrected for thermocouple slot

$$q_{\text{total}} := \frac{Q_{\text{total}}}{A_{\text{bottom_pot}}} = 1.916 \times 10^4 \cdot \frac{\text{W}}{\text{m}^2}$$

Total heat transfer rate into assembly per unit area.

Calculate Contact Resistance:

$$q_{\text{total}} = \frac{T_{\text{burner_ave}} - T_{\text{water_ave}}}{R_{\text{total}}}$$

heat transfer rate written in terms of the overall temperature difference and overall resistance assuming steady-state, plane wall conduction.

$$T_{\text{burner_ave}} := 700\text{K}$$

estimated average burner temperature

$$T_{\text{water_ave}} := 343\text{K}$$

estimated average water temperature during specified time frame

$$R_{\text{total}} = R_{\text{cond_plate}} + R_{\text{contact}} + R_{\text{cond_pot}}$$

Total resistance of the entire assembly

$$k_{\text{steel_hot}} := 47.5 \frac{\text{W}}{\text{m}\cdot\text{K}}$$

Thermal conductivity of plate material at average temp of 620K

$$k_{\text{stainless}} := 16 \frac{\text{W}}{\text{m}\cdot\text{K}}$$

Thermal conductivity of pot material

$$L_{\text{pot}} := .011\text{in}$$

thickness of pot

$$L_{\text{plate}} := .25\text{in}$$

thickness of plate on bottom of bucket

$$R_{\text{cond_pot}} := \frac{L_{\text{pot}}}{k_{\text{stainless}}} = 1.746 \times 10^{-5} \cdot \frac{\text{m}^2\text{K}}{\text{W}}$$

Conductive resistance of pot

$$R_{\text{cond_plate}} := \frac{L_{\text{plate}}}{k_{\text{steel_hot}}} = 1.337 \times 10^{-4} \cdot \frac{\text{m}^2\text{K}}{\text{W}}$$

Conductive resistance of bottom plate on bucket

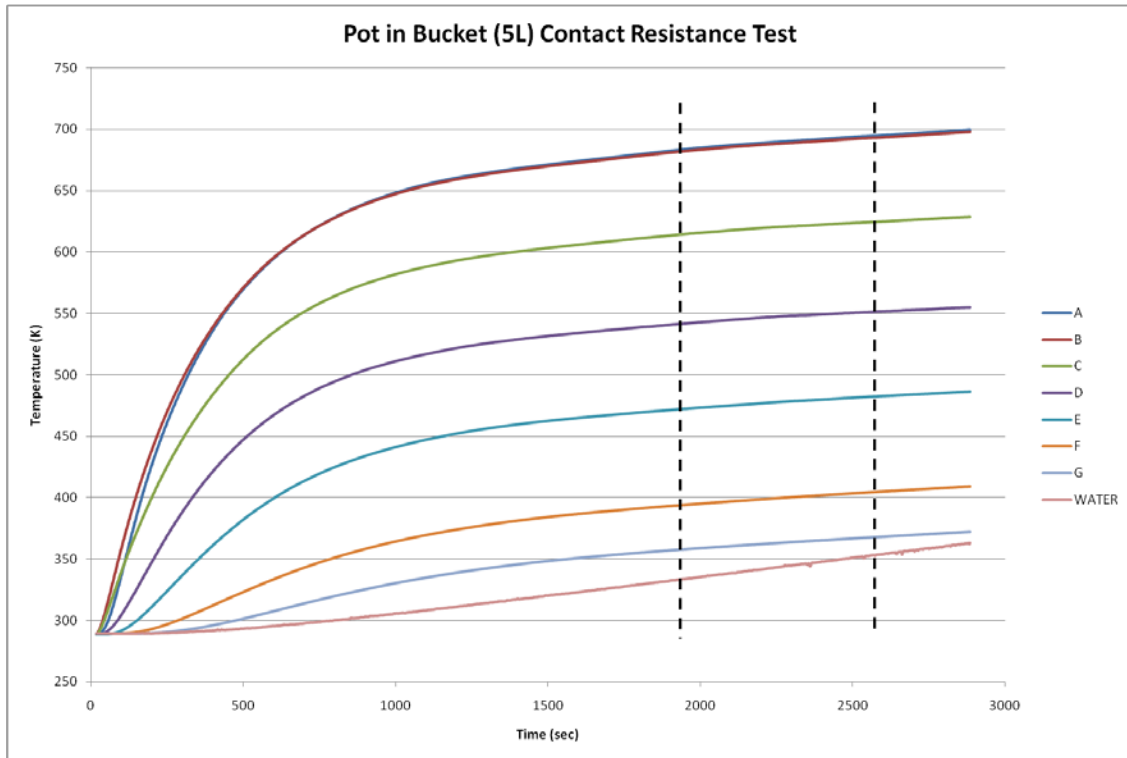
$$R_{\text{contact}} := \frac{T_{\text{burner_ave}} - T_{\text{water_ave}}}{q_{\text{total}}} - R_{\text{cond_pot}} - R_{\text{cond_plate}}$$

$$R_{\text{contact}} = 0.0185 \cdot \frac{\text{m}^2\text{K}}{\text{W}}$$

Total estimated contact resistance between pot and plate

Appendix M – Contact Resistance Experiment Results using Microsoft Excel

FINISHING VALUES - 5L Pot in Bucket									
	Time (sec)	A Temp (K)	B Temp (K)	C Temp (K)	D Temp (K)	E Temp (K)	F Temp (K)	G Temp (K)	Pot Temp (K)
Final Values	2886	699.47942	697.7294	628.72834	554.88347	486.41367	409.2875	372.47443	363.1617914
Steady State Max.	2575	694.6356	692.94807	624.66578	551.32091	482.35111	404.75618	367.97436	353.2866407
Steady State Min.	1919	682.69792	681.2604	613.85312	541.07076	471.78845	393.66226	357.59921	333.0988327
DELTA VALUES - 5L Pot in Bucket									
Total	2868.0	410.8	408.8	339.9	266.1	197.4	119.9	82.9	73.6
Steady State	656.0	11.9	11.7	10.8	10.3	10.6	11.1	10.4	20.2



FINISHING VALUES - 5L Bucket Only									
	Time (sec)	A Temp (K)	B Temp (K)	C Temp (K)	D Temp (K)	E Temp (K)	F Temp (K)	G Temp (K)	Pot Temp (K)
	2047	370.4431525	372.1306783	373.818204	363.9430533	361.9430228	362.2242771	352.192874	363.06804
Steady State Max.	1784.0	365.0	369.1	370.7	355.9	351.8	352.0	342.9	353.0
Steady State Min.	1246.0	347.5	353.4	355.3	337.4	332.1	332.2	325.7	333.1
Beginning Max.									
DELTA VALUES - 5L Bucket Only									
Total	2030.0	80.7	82.0	83.4	74.4	72.5	72.8	63.1	73.5
Steady State	538.0	17.5	15.7	15.3	18.5	19.7	19.8	17.2	19.9

